

SEPARATION OF VOCl_3 FROM TiCl_4
USING SOYA OIL

JARED H CRANE



Doctor of Philosophy
Department of Chemistry
University College London

2014

I, Jared H Crane, confirm that the work presented in this thesis is my own. Where information has been derived from other sources, I confirm that this has been indicated in the thesis.

This thesis is dedicated to my family, new and old. The support of everyone over the years has allowed me to reach this point and I am eternally grateful for that

ABSTRACT

This thesis investigated the reactivity of the metal chlorides TiCl_4 , VOCl_3 and VCl_4 with different organic ligands. The chosen ligands were based around the chemical structure of soya oil due to its relevance to the industrial chlorine process used to manufacture TiO_2 . This thesis primarily used nuclear magnetic resonance (NMR) spectroscopy to characterise the reactions of the metal chlorides with soya oil and component parts, namely the glycerol and the alkene.

This thesis goes on to investigate the coordination chemistry of the metal chlorides with ligands including diester groups. The chemical properties of the metal chlorides are known to be similar and hence hard to separate, the reactions studied provide a mechanism for their separation using diesters. It will be shown that TiCl_4 coordinates with the ligands without the loss of any chlorine atoms and without disrupting the ligand. The VOCl_3 reacted with the ligands, releasing a chlorine atom to produce a VOCl_2 adduct. The difference in reactivity provides a removal mechanism. In the industrial process TiCl_4 is present in very high concentrations and the coordination of TiCl_4 can be seen as reversible and in equilibrium. Whereas, the VOCl_3 converts VOCl_3 into VOCl_2 , VOCl_2 has a higher boiling point and can therefore be removed by distillation.

ACKNOWLEDGMENTS

I would like to thank the following people for their help and support throughout the last 4 years during the completion of this thesis:

Professors Claire Carmalt and Ivan Parkin for supervising me throughout the last 4 years. It is their regular discussions which has allowed this thesis to develop from an industrial question into an academic research project.

Huntsman Pigments, in particular Steve Sutcliffe, Andrew Brown and Neil Richmond for their assistance in all the industrial areas within this investigation.

Dr Abil Aliev for all the NMR analysis work, his insight into the spectroscopy was invaluable throughout this thesis.

Ben Blackburn, Dr Caroline Knapp and Dr Peter Marchand for all their help working through synthetic routes, growing crystals and analysing them.

Dr Rachael Hazael for her love and support and help proof reading this piece of work on numerous occasions.

CONTENTS

1	INTRODUCTION	14
1.1	Overview	14
1.2	Titanium Dioxide	15
1.3	Titanium Dioxide Pigment	17
1.4	Titanium Tetrachloride	26
1.5	Vanadium Oxychloride	31
1.6	Vanadium Tetrachloride	34
1.7	Separation of Vanadium Oxychloride and Titanium Tetrachloride	35
2	INITIAL NMR BASED ANALYSIS OF SOYA OIL	38
2.1	NMR	38
2.2	Oil Analysis	40
2.3	Experimental	46
2.4	Results	48
2.5	Conclusions	55
3	REACTIONS OF $TiCl_4$ WITH DIESTERS	57
3.1	Introduction	57
3.2	Results	63
3.3	Titanium complexes	63
3.3.1	Synthesis of tetrachloro(diethyl malonate)-titanium(IV) [1]	63
3.3.2	Synthesis of tetrachloro(bis isopropyl malonate)-titanium(IV) [2]	66
3.3.3	Synthesis of tetrachloro(di-tBu malonate)-titanium(IV)	74
3.3.4	Synthesis of tetrachloro(di-Benzyl malonate)-titanium(IV) [3]	74
3.3.5	Synthesis of tetrachloro(diethyl succinate)-titanium(IV) [4]	81
3.3.6	Synthesis of tris titanium tetrachloro di-glyceroltribenzoate [5]	83
3.3.7	Synthesis of tetrachloro(acac)-titanium(IV) [6]	91
3.4	Conclusion	93

3.5	Experimental	95
3.5.1	Synthesis of tetrachloro(diethyl malonate)-titanium(IV) [1]	95
3.5.2	Synthesis of tetrachloro(bis isopropyl malonate)-titanium(IV) [2]	96
3.5.3	Synthesis of bis t-Bu Malonate-titanium(IV) chloride	96
3.5.4	Synthesis of tetrachloro(dibenzyl malonate)-titanium(IV) [3]	97
3.5.5	Synthesis of tetrachloro(diethyl succinate)-titanium(IV) [4]	97
3.5.6	Synthesis of glycerol tribenzoate TiCl_4 [5]	98
3.5.7	Synthesis of tetrachloro(acac)-titanium(IV) [6]	98
4	REACTIONS OF VANADIUM CHLORIDES WITH DIESTERS	100
4.1	Vanadium Oxychloride complexes	100
4.1.1	Reaction of VOCl_3 with diethyl malonate [7]	101
4.1.2	Reaction of VOCl_3 with bis-isopropyl malonate [8]	105
4.1.3	Reaction of VOCl_3 with di-ethyl succinate [9]	107
4.1.4	Reaction of VOCl_3 with glycerol tribenzoate [10]	112
4.1.5	The reaction of VOCl_3 acacH [11]	114
4.2	Vanadium Tetrachloride complexes	118
4.2.1	Reaction of VCl_4 with di-ethyl malonate [12]	119
4.2.2	Reaction of VCl_4 with di-ethyl succinate [13]	121
4.2.3	Reaction of VCl_4 with glycerol tribenzoate	124
4.2.4	Reaction of VCl_4 with acacH [14]	125
4.3	Conclusion	129
4.4	Experimental	130
4.4.1	Reaction of VOCl_3 with ethyl malonate [7]	131
4.4.2	Reaction of VOCl_3 with bis-isopropyl malonate [8]	131
4.4.3	Reaction of VOCl_3 with di-ethyl succinate [9]	132
4.4.4	Reaction of VOCl_3 with glycerol tribenzoate [10]	132
4.4.5	Reaction of VOCl_3 with acacH [11]	133
4.4.6	Reaction of VCl_4 with di-ethyl malonate [12]	133
4.4.7	Reaction of VCl_4 with di-ethyl succinate [13]	134
4.4.8	Reaction of VCl_4 with glycerol tribenzoate	135

4.4.9	Reaction of VCl_4 with acacH[14]	135
5	DESIGN OF UV-VIS FLOW CELL	136
6	CONCLUSIONS	146
	BIBLIOGRAPHY	150

LIST OF FIGURES

Figure 1	Unit cell of rutile TiO ₂ on the left and anatase TiO ₂ on the right.	16
Figure 2	Photo of the spiral heat exchange	18
Figure 3	Simplified Schematic of the TiO ₂ production plant showing the steps in creating pure TiO ₂ pigment	22
Figure 4	Structure of monomeric TiCl ₄ compared to polymeric ZrCl ₄	26
Figure 5	Structure of [TiCl ₄ (C ₄ H ₈ S) ₂]	27
Figure 6	Crystal structure of 2,7-bis(1,1-dimethylethylfluorene)-1,8-trichlorotitanium phenoxide) showing an alkoxide synthesised from TiCl ₄	29
Figure 7	Reaction scheme for the polymerisation of ethene to polyethene via the Cossee mechanism.	30
Figure 8	Scheme to show the bonding of a metal centre to an alkene through the Dewar-Chatt-Duncanson model	31
Figure 9	Structure to show VOCl ₃ bound to a neutral N-donor ligand	32
Figure 10	Structure to show VOCl ₃ bound to a neutral N-donor ligand with a bridging oxygen	33
Figure 11	NMR of Soya Oil	41
Figure 12	Chemical Structure Soya Oil	41
Figure 13	NMR of Soya Oil	43
Figure 14	COSY spectrum to show proton-proton coupling in soya oil.	47
Figure 15	NMR of soya oil with metal chlorides	50
Figure 16	NMR of linseed oil with metal chlorides	50
Figure 17	Molecular structure of octadecene	51
Figure 18	Molecular structure of tristearin	51

Figure 19	Molecular structure of trimyristin	52
Figure 20	NMR of trimyristin with metal chlorides	53
Figure 21	NMR of octene with metal chlorides	54
Figure 22	NMR of octene with metal chlorides after 48 hours	54
Figure 23	Structure of $[\text{CH}_2(\text{COOCH}_2\text{CH}_3)_2\text{TiCl}_4]$	58
Figure 24	Figure to show TiCl_4 bound to acac	58
Figure 25	TiCl_4 bonded to 3,3-dimethyl-2 4- pentanedione	59
Figure 26	Scheme to show the addition of acacH to TiCl_4 in differing solvents	59
Figure 27	Structure of malonate where R = ethyl, benzyl, isopropyl and t- Bu.	61
Figure 28	Structure of glycerol tribenzoate.	61
Figure 29	Structure of acacH.	61
Figure 30	Representation of the structure of soya oil	62
Figure 31	Figure to show crystal structure of tetrachloro(diethyl malonate)-titanium(IV) [1] .	63
Figure 32	Scheme to show the reaction of TiCl_4 with the malonate ligands	66
Figure 33	Crystal structure of tetrachloro(bis isopropyl malonate)-titanium(IV) [2a]	67
Figure 34	Figure to show crystal structure of trichloro-O-(bis isopropyl malonate)-titanium(IV) dimer [2b]	71
Figure 35	NMR spectra to show iso-propyl malonate coordinated to TiCl_4 and then dissociated, both are compared to the starting material shown at the bottom	73
Figure 36	Figure to show crystal structure of [3]	76
Figure 37	Chemical structure of diethyl succinate	78
Figure 38	^1H NMR of diethyl succinate shown in blue compared to tetrachloro(diethyl succinate)-titanium(IV)[4] shown in red	79
Figure 39	Crystal structure of tetrachloro(diethyl succinate)-titanium(IV)[4]	80
Figure 40	Structure of <i>cis</i> - $\text{C}_2\text{H}_2(\text{CO}_2\text{CH}_2\text{CH}_3)_2$	82
Figure 41	Structure of [<i>Cis</i> - $\text{C}_2\text{H}_2(\text{CO}_2\text{CH}_2\text{CH}_3)_2\text{TiCl}_4$]	82

Figure 42	Structure of glycerol tribenzoate.	84
Figure 43	^1H NMR spectra of glycerol tribenzoate (red) and compound [5] (blue). The top spectra shows the entire range where peaks are present with labels to show where the protons are on the molecule. The bottom two spectra show areas B and P zoomed in to show coordination shifts.	85
Figure 44	Crystal structure of [5]. Two dichloromethane molecules were observed in the unit cell but have been removed for clarity	86
Figure 45	Chemical structure of compound 5 shown as a simple chemical structure to aid understanding of bonding positions	88
Figure 46	Scheme to show the different reported reactions of TiCl_4 and acacH with compound [6] shown on the final row	92
Figure 47	Crystal structure of [7], one malonate ligand is shown for clarity, O17 and O18 are part of a malonate as are O13,O14,O9 and O10.	102
Figure 48	Diagram to show the possible structure of complex [8]	106
Figure 49	Crystal structure of [9]	108
Figure 50	Crystal structure of [11]	115
Figure 51	Diagram to show the possible structure of the intermediate complex [12]	120
Figure 52	Diagram to show positions of protons ABC for reference in the NMR study	122
Figure 53	COSY NMR of compound[13]	122
Figure 54	^1H NMR of compound[13] shown before and after exposure to air and compared to the starting material	123
Figure 55	Crystal structure of [12]	126
Figure 56	Schematic of the original design of UV-vis flow cell	137
Figure 57	UV-vis cell as received from Mettler Toledo	137
Figure 58	UV-vis spectra of TiCl_4 and VOCl_3	139

Figure 59	UV-vis spectra of TiCl_4 and VOCl_3 and VCl_4 recorded using the UV-vis flow cell	141
Figure 60	Diagram to show the mechanism of a Soxhlet extractor. The solid of which the product is to be extracted from is placed in the Soxhlet at position (3). The solvent is evaporated from position (1) through (2), to (3) where it dissolves the product, the siphon (4) is then filled and once full deposits back into the round bottomed flask (1)	142
Figure 61	Photo to show the UV-vis flow cell set up with the Soxhlet extractor attached.	143
Figure 62	Diagram to show the mechanism of the adapted Soxhlet extractor. (1) The TiCl_4 is evaporated, (2) the hot gaseous mixture passes through the UV-vis cell, (3) the TiCl_4 is condensed, (4) the TiCl_4 collects in the Soxhlet, (5) the siphon activates when the Soxhlet is full releasing the liquid back into the reaction flask	145

LIST OF TABLES

Table 1	Table to show the boiling points of metal chlorides with the key vanadium compounds highlighted in red due to their boiling points being so similar to TiCl_4 at atmospheric pressure	25
Table 2	^1H NMR positions of the different protons in soya oil, integrals calculated based on the previously mentioned literature values.	42
Table 3	Table to show the amount of different proton environments for different acid chains	44
Table 4	NMR results for soya oil.	44

Table 5	Selected bond lengths Å and angles (°) for tetrachloro(diethyl malonate)-titanium(IV) [1] taken from ¹	64
Table 6	Selected bond lengths Å and angles (°) for bis isopropyl malonate)-titanium(IV)[2a]	68
Table 7	Selected bond lengths Å and angles (°) for bis isopropyl malonate)-titanium(IV) [2b]	72
Table 8	Selected bond lengths Å and angles (°) for compound [3]	77
Table 9	Selected bond lengths Å and angles (°) for tetrachloro(diethylsuccinate)-titanium(IV)[4] .	79
Table 10	Bond angle data comparing Kokkonen's structure to the structure obtained through this work	83
Table 11	Selected bond lengths Å and angles (°) for compound [5]	89
Table 12	Selected bond lengths Å and angles (°) for compound [7]	103
Table 13	Selected bond lengths Å and angles (°) for compound [9]	109
Table 14	Selected bond lengths Å and angles (°) for compound [11]	116
Table 15	Table to compare properties of TiCl ₄ and VCl ₄	119
Table 16	Selected bond lengths (Å) and angles (°) for compound [14]	127

INTRODUCTION

1.1 OVERVIEW

This project was designed to understand a common industrial process, namely the removal of vanadium oxide from titanium dioxide. To remove the vanadium the entire metal oxide mixture is chlorinated, this leaves the titanium as TiCl_4 and the vanadium as VOCl_3 . These metal chlorides are liquids at room temperature and can be distilled to be purified. However, their boiling points are so similar that a chemical reaction is required to alter the properties. Oils are commonly used to react with the vanadium chloride and change its boiling point.² The detailed mechanism for this removal is not well understood and it is this process that this thesis focuses on. In addition the work explores new coordination and reaction chemistry of both titanium and vanadium halides.

Initially this project focused on investigating the problems with the distillation process, involving reactions of TiCl_4 with soya oil. Soya oil is a naturally occurring oil from the soya bean and it is made up of a glycerol, which in turn is made up of ester, and long fatty acid chains containing alkenes. Nuclear magnetic resonance (NMR) spectroscopy was used to characterise soya oil and compare it to other oils to give an understanding of this oil, and to develop

a standard method to compare different batches of soya oil utilised in the industrial process.

The project was then expanded to study the interactions of metal chlorides with the esters and alkenes at a molecular level. This involved the synthesis of novel compounds and the growth of single crystals to provide accurate analysis of the compounds formed so that the mechanism of the vanadium removal can be further understood.

1.2 TITANIUM DIOXIDE

TiO₂ is the naturally occurring oxide of titanium, it is abundant and found as three minerals; rutile, anatase and brookite. Rutile is the most common natural form and it adopts a primitive tetragonal unit cell as shown in Figure 1.³ The anatase unit cell packs in such a way that it adopts a pseudo octahedral structure, also shown in Figure 1. Brookite is an orthorhombic mineral with a larger cell volume than anatase or rutile. TiO₂ has unique electronic properties⁴ and this has led to many applications such as photocatalysis. TiO₂ has been shown to be used as a photocatalyst due to its intrinsic band gap at 3.18 eV⁵ (for anatase) being so close to the visible region.⁶

TiO₂ is a nonstoichiometric semiconductor that has outstanding photoelectrochemical properties, as shown by Fujishima and Honda.⁷ After irradiation of the electrode with UV light, oxygen was produced from the breakdown of water, which

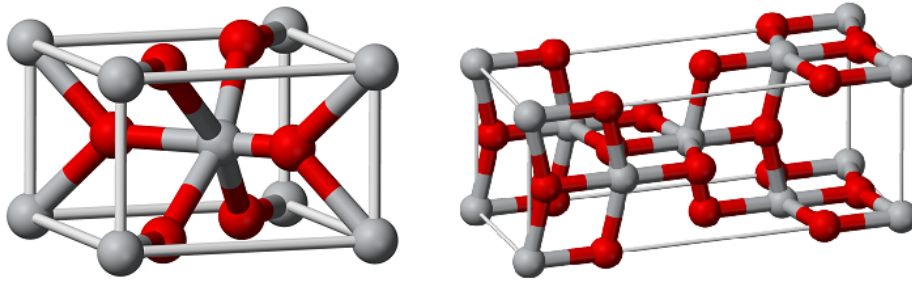


Figure 1: Unit cell of rutile TiO_2 on the left and anatase TiO_2 on the right.³

essentially used TiO_2 to split water, demonstrating that it can be used to convert solar energy into chemical energy.

These initial promising results have led to a vast amount of research in this area. Over 50,000 papers have been published on TiO_2 in the last 10 years and over 7,000 on its use as a photocatalyst.^{8,9,10} These have ranged from water splitting,¹¹ self-cleaning windows¹² and as nanoparticles in antimicrobial applications.¹³

TiO_2 as a photocatalyst can exhibit photoinduced hydrophilicity, which is used for self cleaning applications (Pilkington-NSG activ). It works by the wetting of a surface through the hydrophilicity and then the formation of electron/hole pairs for dirt degradation.^{14,15}

The band gap for TiO_2 is in the UV range, at 3.0 eV for rutile and 3.2 eV for anatase. There has been a push to decrease the band gap so that light is absorbed in the visible to create a visible light photocatalyst. Nitrogen doping of TiO_2 is the most common way to shift the band gap.^{16,17} This is because the nitrogen valence electrons

lie higher than the oxygen valence electrons therefore reducing the gap to the titanium states in the conduction band.

Recently advances have been made to develop TiO_2 for electronic materials such as transparent conducting oxides (TCO).¹⁵ TCO's are used for liquid crystal displays, touch screens, electrical contacts, solar control coatings (Pilkington-NSC K-glass) and photovoltaic devices. TiO_2 is a semiconductor that exhibits *n*-type and *p*-type conductivity at low and high oxygen partial pressures respectively. To improve the intrinsic conductivity of TiO_2 , to enable it to be a TCO the defect nature of the system needs to be modified by doping. Both Nb and Ta have been used to dope anatase TiO_2 by replacing some of the Ti^{4+} sites with Nb^{5+} resulting in charge compensation by electrons in the conduction band.^{18 19}

1.3 TITANIUM DIOXIDE PIGMENT

This project was sponsored by Huntsman Pigments a division of Huntsman. Huntsman are an American multinational chemical company, Huntsman Pigments is a branch of the firm predominantly operating from the United Kingdom. They produce TiO_2 pigment for several applications including paint and plastics. Their biggest manufacturing plant is in Teesside and from this plant they produce 150,000 tonnes of pigment each year. The plant is run on a continuous process,²⁰ this means that the plant runs 24 hrs a day and ideally 365 days a year, the plant is only stopped when there is a problem. The success of a continuous process is

determined by the amount of time the process is not running, this is referred to as 'downtime'. This project was funded in order to reduce downtime on the plant by studying the chemistry of the metal chloride separation to provide new information and ideally novel solutions to problems encountered resulting in downtime.



Figure 2: Photo of the spiral heat exchange from Huntsman Pigments's plant showing the carbonaceous build up on the equipment caused by the soya oil. The heat exchanger reduces the temperature of the pure TiCl_4 and the sticky carbonaceous build up reduces the efficiency. This build up is caused by impurities. Reducing these impurities therefore reduces downtime. For scale this heat exchange has a diameter of 2.5 metres

Huntsman Pigments refine TiO_2 ore (which contains compounds such as iron, vanadium and aluminium oxides) into pure TiO_2 . The purification involves chlorination of the metal oxide mixture and then removal of non titanium metal chlorides, such as VOCl_3 , FeCl_3 and AlCl_3 . This project has been commissioned due to serious issues concerning the plant at different points during the

continuous process due to the removal of VOCl_3 from TiCl_4 . The separation of VOCl_3 involves the addition of soya oil,²¹ the breakdown of this oil during the process is thought to lead to carbonaceous deposits which have to be removed, resulting in downtime. Carbon deposits build up on different pieces of equipment throughout the plant (see Figure 2). These deposits reduce the efficiency of the cooling mechanism as it has to be cleaned out which is time consuming and due to the downtime occurs at a great cost.

More TiO_2 pigment is produced than any other pigment and this is mainly due to the paint industry. It is used because of its high refractive index ($n = 2.6$)²² and brightness. Refractive index is a measure of the speed of light within the associated medium, this value is higher than the refractive index of diamond ($n = 2.4$).²³ This high value means that a thin coating of TiO_2 pigment can create an opaque surface. Due to the industrial growth seen in Asia the demand for paint and related products has greatly increased. This industry has not been hit by the recent economic downturn seen in western economies. In fact the high demand is causing more problems because obtaining high grade feedstock is becoming increasingly difficult.

The production of TiO_2 pigment is a global business worth billions of pounds. Its uses include but are not limited to food colouring with the E number E171²⁴ and toothpaste.²⁵ This pigment has also been used for its IR reflective qualities in roof

ceramics.^{26,27} Another key factor is its low toxicity,²⁸ TiO_2 is stable due to its high melting point (at over 1500 °C) and low reactivity.

TiO_2 is produced by two methods, the chlorine process which this thesis looks into in detail and the sulphate process.²⁹ In the sulphate process, there are three main stages described below.

(1) The ore, usually an ilmenite, is dissolved in sulphuric acid to form a mixture of sulphates. Ilmenite, formally FeTiO_3 , is a highly abundant mineral and the ilmenite used for the sulphate process is usually a low vanadium ilmenite where around 80 % of the ilmenite is TiO_2 .³⁰ Iron is removed from the solution so that the colour of the final product is not spoiled.

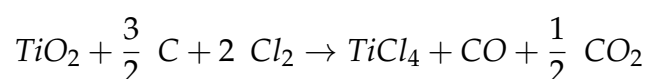
(2) The titanyl sulphate is then hydrolysed in solution to give insoluble, hydrated titanium dioxide. The titanium bonds to the sulphuric acid displacing a hydrogen atom and forming a titanium-oxide bond.

(3) The final stage involves heating the solid in a calciner to evaporate the water and decompose the sulphuric acid in the solid. It also turns the solid into seed crystals which can be milled to the size required. These crystals can be coated with another substance, such as aluminium oxide,³¹ to make the titanium dioxide mix more easily with liquids or extend the lifetime of the paint manufactured from them.

The chlorine process produces a purer product, where the particle sizes can be controlled more precisely. Due to the large quantities of acid necessary for the sulphate process, the chlorine process has cheaper start up costs and is more environmentally friendly.³² This is the technique employed by Huntsman Pigments at Teesside and of specific relevance to this project.

The chlorine process can be simplified into three steps from the TiO₂ ore to the TiO₂ pigment:

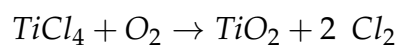
- Step (1) CHLORINATION:



- Step (2) PURIFICATION:

Distillation of TiCl₄

- Step (3) OXIDATION:



A simplistic schematic of the plant is shown in Figure 3 describing the processes involved in the production of TiO₂ via the chlorine process. The plant is complicated but the majority of the processes involve the separation of other metal chlorides from titanium tetrachloride (tetra). Titanium tetrachloride will be

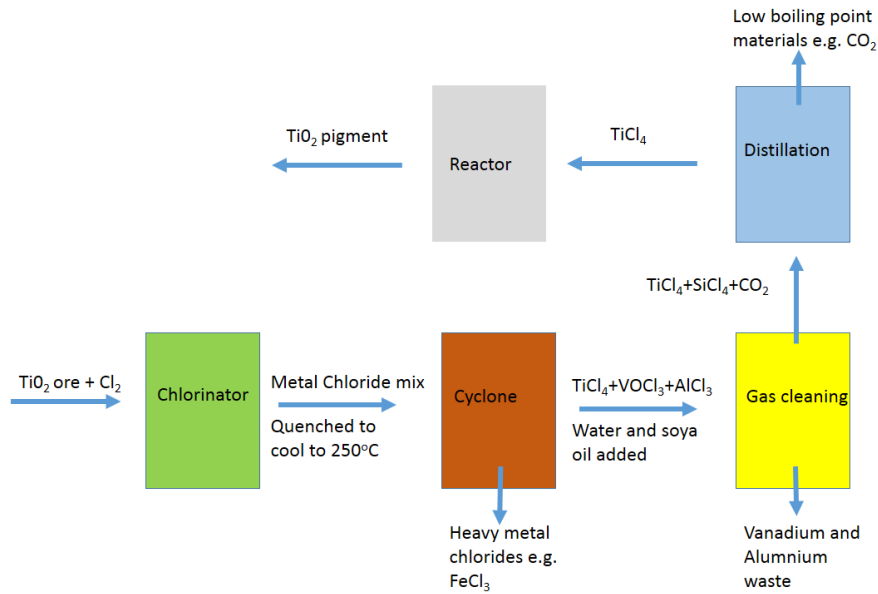


Figure 3: Simplified Schematic of the TiO₂ production plant showing the steps in creating pure TiO₂ pigment

referred to as tetra when discussed in reference to the industrial plant.

Step (1): The plant runs from left to right and the chlorination step is where the TiO₂ ore is fed in along with chlorine gas and coke. This ore which is mined globally including Australia, India and South Africa is approximately 95 % TiO₂³³ but also contains contaminants of approximately 0.3 % VO₂, 2.5 % Fe₂O₃, 0.5 % Al₂O₃ and various other metal oxides. The carbon coke reduces the metal down from its oxide form, which then reacts with the chlorine to form the metal chlorides. This occurs at around 1000 °C, to separate the metal chlorides with a higher boiling point, the temperature of the mixture is reduced by quenching before reaching the cyclone. At this point tetra from a colder tank are added to reduce the temperature. An industrial cyclone is a large cylinder which separates solids from liquids using high speed gas.

The cyclone plays a key part in the process as this is the only point in which solid material is removed from the tetra. The mixture enters the cyclone at between 150-250 °C and metal chlorides with high boiling points, such as FeCl₃, are removed. The mixture should now only contain TiCl₄, AlCl₃ and VOCl₃. Before reaching the gas cleaning distillation set up, a water based reagent is added which converts the AlCl₃ to a solid oxychloride. It is not known how this reaction proceeds but it has been shown to work at the plant and is thought to involve the formation of solid aluminium species such as Al₂O₃. The mixture then enters gas cleaning at a temperature of 220 °C.

Step (2): The gas cleaning section is the point at which the majority of this project is focused, as this where which the vanadium compounds are removed. The gaseous tetra mix rises up the column and mixes with with soya oil at a lower temperature. The oil is added to remove the vanadium chlorides from the tetra, this technique has been used for many years by many companies but the process is not yet fully understood. Pure tetra should leave the gas cleaning tank at the top and the aluminium and vanadium should be removed by the soya oil and the water and be left in the gas cleaning tank. The aluminium and vanadium is left at the bottom because it has reacted with the soya oil and water, it is this that the project investigates further. This tank facilitates the separation of the tetra leaving the titanium tetra chloride at the top which is recycled through gas cleaning to increase the yield. A solid mixture is left at the bottom of the tank and is made up of tetra and solids, which are used to quench the mixture in the

chlorinator. It achieves this by 1) reducing the temperature and 2) removing the soya oil in its solid form by the cyclone.

Step (3): After gas cleaning the tetra should be relatively pure and the final distillation step is to remove any other impurities that may have reached this point of the process and to release gases after primary condensation. The tetra is further cooled to 50 °C then heated to 350 °C and finally oxidised to produce the TiO₂ pigment at the reactor. The second part of the plant should remain clean but it is here where several problems have been observed, e.g. carbon deposits forming on the spiral coil. This suggests that the oil is not completely removed by the cyclone. Furthermore, if vanadium reaches the oxidiser in an amount greater than 5 ppm the pigment is stained yellow, which is recycled at a high cost to the company.

The tetra produced in the chlorination step is actually a metal chloride mix made up of compounds containing titanium, iron, aluminium, vanadium, niobium, silicon, zirconium, and tin. The boiling point of all the metal chlorides involved, which forms the basis for the distillation, are presented in Table 1.

The boiling points for iron, niobium, zirconium and hafnium chlorides are high enough (>250°C) to be removed by distillation and are removed by the cyclone. The boiling points of silicon and tin chlorides are low enough (<120°C) to be taken off as a gas when the TiCl₄ is a liquid. However, the aluminium and vanadium chlorides cause the majority of the problems due to the similarity

Compound	Boiling Point ° C
ZrCl ₄	331
HfCl ₄	317
NbCl ₅	254
FeCl ₃	316
VCl ₄	148
TiCl ₄	136
VOCl ₃	127
AlCl ₃	120
SnCl ₄	114
SiCl ₄	58

Table 1: Table to show the boiling points of metal chlorides with the key vanadium compounds highlighted in red due to their boiling points being so similar to TiCl₄ at atmospheric pressure

of their boiling points to TiCl₄ (shown in red in Table 1). In the past aluminium and vanadium chlorides were both removed by the addition of soya oil. Recently water has been introduced into the system to remove AlCl₃ before contact with the oil. It is thought that the water reacts with AlCl₃ and converts it to AlOCl which has a much higher boiling point and can therefore be removed by the cyclone. In this case the water would act as a hydrolysing agent. The vanadium removal mechanism is not yet known, however, vanadium solid species have been extracted from the cyclone suggesting the formation of VOCl or VO₂, both of which have considerably higher boiling points than TiCl₄. This suggests that the vanadium is reduced during the removal and therefore determining the reducing agent should allow an understanding of this mechanism.

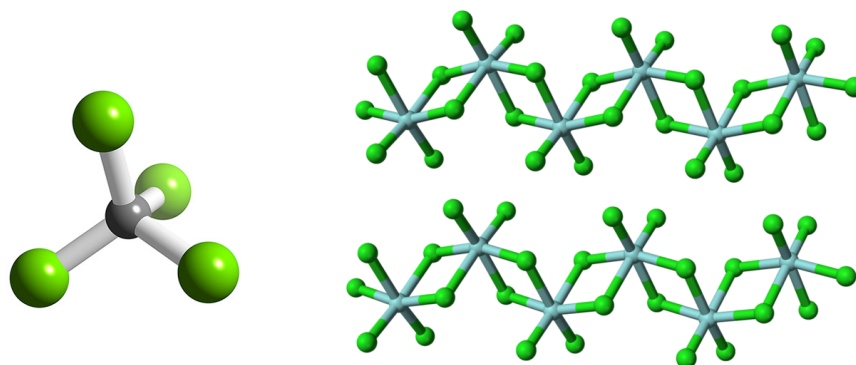
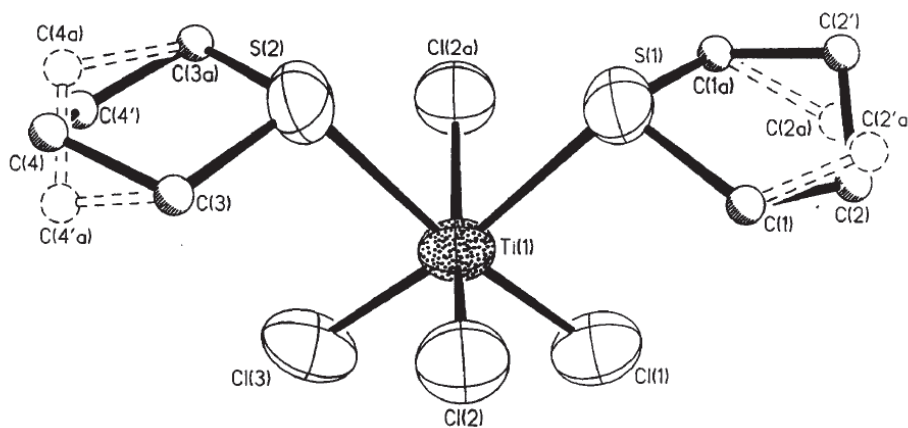


Figure 4: Structure of monomeric TiCl_4 compared to polymeric ZrCl_4

1.4 TITANIUM TETRACHLORIDE

TiCl_4 adopts a monomeric tetrahedral structure in the vapour phase, shown in Figure 4. It is one of only two transition metal chlorides that are liquid at room temperature, the other being VCl_4 . This is due to the monomeric structure which has been confirmed computationally.^{34,35} Heavier group 4 metal chlorides, such as ZrCl_4 and HfCl_4 , are solids at room temperature due to octahedrally coordinated polymeric bonding around the metal centre,³⁶ as shown in Figure 4 forming a monoclinic structure.

TiCl_4 is highly hygroscopic and can be completely hydrolysed in moist air as shown in equation 1. Incomplete hydrolysis of TiCl_4 produces oxychlorides such as TiOCl_2 . TiCl_4 therefore must always be handled in an inert environment since the smallest amount of moisture results in the formation of hydrochloric gas, the gas being easy to observe as the titanium oxide particles in the fumes make the gas white in colour. Hydrochloric gas can be a major problem as it is toxic and causes serious damage to the respiratory system if inhaled.

Figure 5: Structure of $[\text{TiCl}_4(\text{C}_4\text{H}_8\text{S})_2]$ ³⁹

TiCl_4 is a strong Lewis acid.³⁷ Lewis acids were first described by Lewis and the definition was based around the redistribution of the reactant's valence electrons.³⁸ TiCl_4 is therefore a Lewis acid and is an example of a hard acid. A hard acid is formed when the bond between the Ti and the Cl is strong and short. Early transition metals generally form hard acids. Soft acids would be larger in size and show polarisability across the molecule. Hard acids react more with hard bases, and soft acids react strongly with soft bases according to Pearson's rule. This means TiCl_4 reacts readily with bases especially with hard bases, a reaction with a hard base would be extremely vigorous. Water acts as a base and thus the reaction is very violent which is an indication of its high reactivity.

Complexes with diethyl malonate, which is a simple bidentate ligand have been formed with the two oxygen bonds from the metal centre in the *cis* positions.⁴⁰ There are numerous examples of trans

complexes in the literature⁴¹ where the ligands bind from opposite sides of the Ti centre.

TiCl₄ is so reactive that its reactivity is not constrained to hard bases, it can also form compounds with soft Lewis bases. Compounds with organo sulphur compounds have been formed around a single TiCl₄ molecule in the *cis*-conformation, for example [TiCl₄(C₄H₈S)₂],³⁹ as shown in Figure 5.

TiCl₃ and TiCl₂ are also stable and are solids at room temperature and contain bridging Cl atoms. They have a low magnetic moment even with their unpaired electron, this suggests a large degree of Ti-Ti bonding creating an antiferromagnetic effect.^{42,43} TiCl₃ is also a strong Lewis acid and it is believed to be the reactive intermediate in olefin polymerisation.⁴⁴

TiCl₄ is readily utilised as a precursor to titanium alkoxides.⁴⁵ Alkoxides from TiCl₄ have been shown to be useful in forming bidentate ligands with multiple Lewis acid centres as shown in Figure 6.⁴⁶ Multidentate Lewis acids are very important as they are more selective and can bond in more ways to Lewis bases than is possible with traditional Lewis acids.⁴⁷

TiCl₄ is widely used as a precursor to TiO₂ thin films,^{48,49} which can be used to coat surfaces and this coating will allow the application of the properties of TiO₂ onto a surface. Due to the colour of TiO₂ the films are transparent so can be used to coat glass without effecting the optical transparency. It is not only

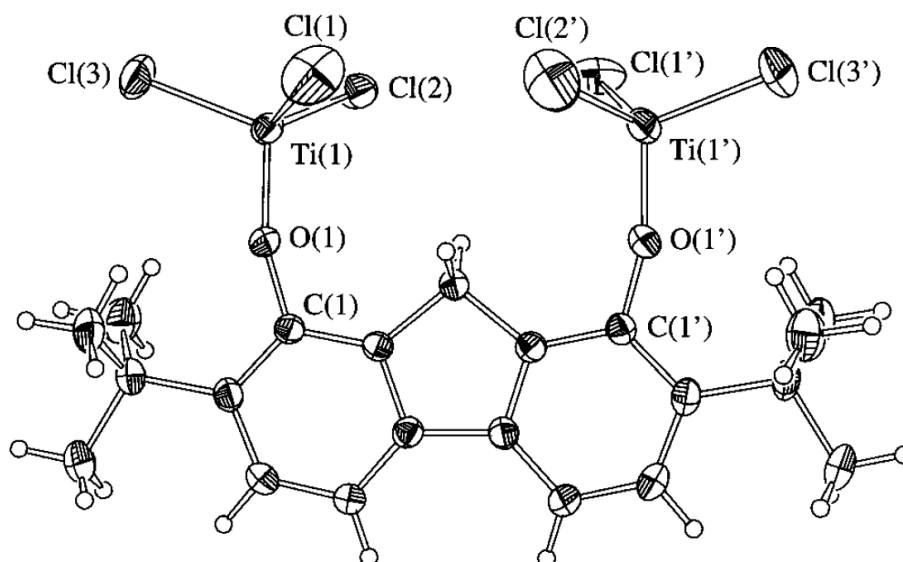


Figure 6: Crystal structure of 2,7-bis(1,1-dimethylethylfluorene)-1,8-trichlorotitanium phenoxide) showing an alkoxide synthesised from TiCl_4

used to form TiO_2 films, other thin films such as TiN can be synthesised easily by the reaction of TiCl_4 with NH_3 .⁵⁰

The Kroll process³³ is used globally to manufacture tonnes of titanium metal each year by the reaction of TiCl_4 and magnesium at $1000\text{ }^\circ\text{C}$. For this process the TiCl_4 must be very pure due to the need for very pure titanium metal. The Kroll process was developed by W.Kroll in 1940 as a way of preparing ductile high grade titanium metal.⁵¹ The demand for titanium metal is high due to demand in the construction industry, therefore this project idealising the conditions for the purification of TiCl_4 is highly valuable.

TiCl_4 has been shown to be used as a polymerisation catalyst. Karl Ziegler first observed the ability of TiCl_4 to catalyse ethylene⁵² by being reduced to TiCl_3 which acts as a heterogeneous catalyst.

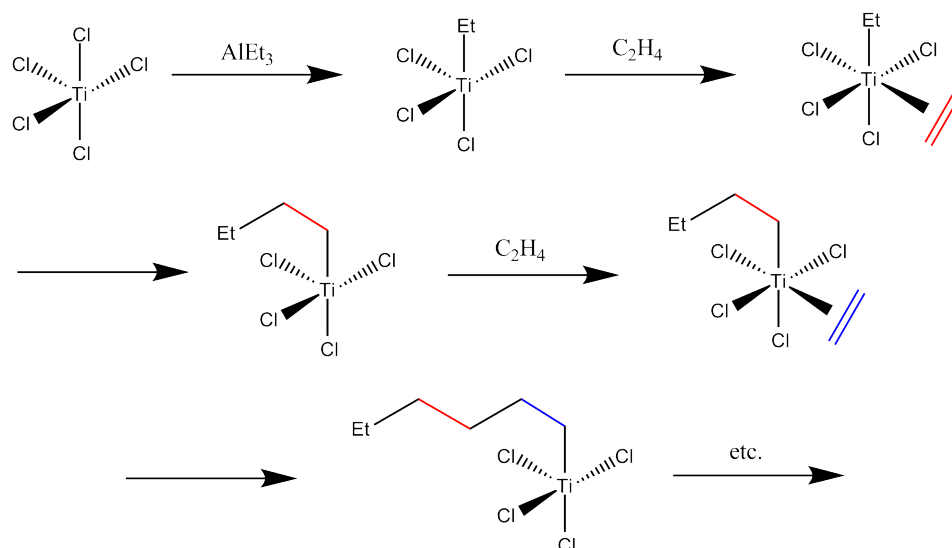


Figure 7: Reaction scheme for the polymerisation of ethene to polyethene via the Cossee mechanism.

Giulla Natta developed this for propylene and the Ziegler-Natta catalyst⁵³ was developed. It is capable of reducing the temperature of polymerisation down $300\text{ }^\circ\text{C}$ to $110\text{ }^\circ\text{C}$ making a large energy saving. The mechanism that has been widely accepted is the Cossee mechanism⁵⁴ which proceeds via a two step mechanism; (1) the ethene complexes to the metal centre; (2) migratory insertion of the monomer into the metal carbon bond forming the polymer chain.⁵⁵ This is shown in Figure 7 for the polymerisation of ethene to form polyethene. A major advantage of this method for more complexed polymers is the formation of isotactic polymers.⁵⁶ This is where functional groups on the alkene are added on the same face of the chain, which is controlled by steric effects.

The bonding of the titanium centre to the alkene is a key part of the Ziegler Natta catalysis, it is also believed to be very important in the reaction with soya oil. The bonding of alkenes to metal centres occurs by the Dewar-Chat-Duncanson model, which is shown in

Figure 8.⁵⁷ This shows how the alkene bonds through a simple σ -donation of the alkene π -bond to an empty metal d-orbital with back donation from a filled metal d-orbital to the empty alkene π^* orbital. This is well known for transition metals on the right hand side of the periodic table which back-bond readily. This can occur for titanium although not for titanium (IV) as it is d^0 . However, in the Ziegler-Natta catalytic mechanism titanium is believed to be Ti^{3+} when bonding to the ethene so π -backbonding could occur.

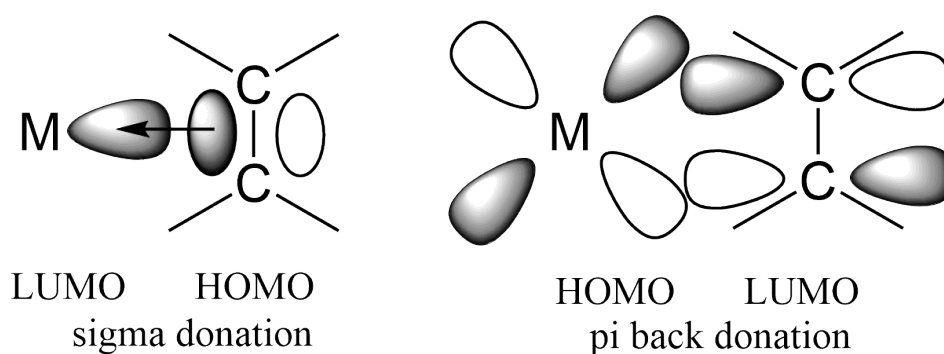


Figure 8: Scheme to show the bonding of a metal centre to an alkene through the Dewar-Chatt-Duncanson model

1.5 VANADIUM OXYCHLORIDE

$VOCl_3$ is a highly moisture sensitive liquid and it is one of the very few oxychlorides that is a liquid at room temperature (293 K) and as low as 196 K.⁵⁸ Most metal oxychlorides form dimers or larger molecules with bridging oxygen and chlorine atoms. However, $VOCl_3$ is tetrahedral in respect to geometry with the electronic configuration d^0 . It is produced by the chlorination of vanadium oxide at 600 °C, as shown in equation 2.



VOCl_3 is also a strong Lewis acid and has been used as a Ziegler- Natta catalyst,⁵⁹ a $\text{VOCl}_3\text{-R}_3\text{Al}$ catalyst was used and it lowered the molecular weight density of the polymer.⁶⁰ It has also been shown to polymerise larger monomers such as styrene.³¹

The Lewis acidity of VOCl_3 has been utilised to form complexes with N-donor ligands.⁶¹ This was the first work to extensively show how VOCl_3 reacted with neutral donor ligands. Beard *et al*⁶¹ looked into N-donor and P=O donor ligands and showed that compounds could be formed with a wide ranging series of ligands to give structures such as 2,2'-bipyridyl vanadyl trichloride as shown in Figure 9. The single crystal X-ray for these adducts has not been reported. This paper reports a crystal structure for a dimeric vanadium species with a bridging oxygen atom as shown in Figure 10.

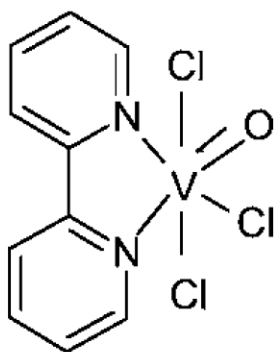


Figure 9: Structure to show VOCl_3 bound to a neutral Nitrogen-donor bipy ligand⁶¹

VOCl_3 has also been used as a precursor to make vanadium oxide films⁶². Thin films of VO_2 are desirable to utilise the metal-to-semiconductor phase transition of the material at 68 °C.⁶³ This property has been exploited in the manufacture of intelligent

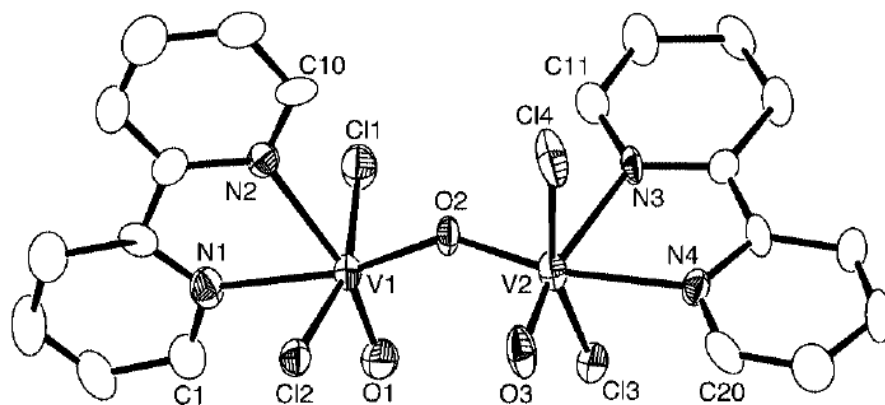


Figure 10: Structure to show VOCl_3 bound to a neutral N-donor ligand with a bridging oxygen⁶¹

glass, data storage and optical switches.⁶⁴ It is the result of a structural change from monoclinic below 68 °C and a tetragonal phase above such temperature. Thin films have been produced by chemical vapour deposition using VOCl_3 and water as starting precursors.⁶⁵

The redox chemistry of vanadium is particularly interesting as compounds can easily be synthesised from V^{2+} through to V^{5+} . Each vanadium oxidation state has a strong characteristic colour, therefore any compounds made from vanadium carry a characteristic colour which can be a useful analytical tool. Compounds with V^{2+} tend to be violet, V^{3+} green, V^{4+} blue and V^{5+} yellow.⁶⁶ The redox ability of vanadium is so strong that vanadium batteries have been invented that utilise the ease of charge transfer from V^{2+} to V^{3+} .⁶⁷

Vanadium is in fact most stable in the V^{4+} state and this can be observed by the vanadyl (VO^{2+}) ion which is a very stable

ion.⁶⁸ Vanadium (V) oxide is used as a catalyst in the production of sulphuric acid, the vanadium can oxidise SO_2 to SO_3 by reducing to V_2O_4 . This illustrates the stability of vanadium in different oxidation states, the cycle is completed by reacting V_2O_4 with O_2 to reform V_2O_5 .⁶⁹

1.6 VANADIUM TETRACHLORIDE

VOCl_3 is the most common vanadium species found in the gas phase in the plant, however, it is worth noting the possible presence of VCl_4 . As stated above vanadium is most stable in the V^{4+} oxidation state even though this gives a paramagnetic liquid of VCl_4 , which is very rare, VCl_4 is prepared by the chlorination of vanadium metal. In the plant, VOCl_3 is formed as it is reported that VOCl_3 forms from vanadium oxide and VCl_4 is synthesised from vanadium metal.⁷⁰ VCl_4 is not thermodynamically stable it breaks down to VCl_3 and Cl_2 gas over time at room temperature.⁷¹

The formation of inorganic complexes from VCl_4 is not well known from the literature. In the early 1970's⁷² and 1980's^{73 74 75} there were several studies carried out, although no recent work. However, recently VCl_4 has been used in organic synthesis^{76 77} and as a CVD precursor.^{78 79} The structure of VCl_4 is considered the same as TiCl_4 as concluded by Pothoczki et al.⁸⁰ They conclude that whilst they can be distinguished it is reasonable to consider the structure the same for all purposes.

Cavell *et al*⁷² worked on reactions of metal chlorides including TiCl_4 and VCl_4 with difluorodithiophosphinic acid. The metal chlorides were used to react with the free hydrogen of the acid to give HCl. Therefore the information regarding the chemistry of the metal chlorides is vague apart from highlighting their high reactivity which is known. Fernandez *et al* showed benzofuroxane could coordinate to VCl_4 and TiCl_4 ^{73,74} using the NO oxygen atom without breaking down any of the metal-chlorine bonds. Arquero *et al*⁷⁵ report the complexation of Schiff Bases to TiCl_4 and VCl_4 showing bidentate ligands completing the desired octahedral structure of the metal chlorides.

All these studies show that simple coordination and complexed structures which have been observed for TiCl_4 and VOCl_3 have not been synthesised for VCl_4 . VCl_4 was considered alongside TiCl_4 throughout this thesis showing how similar their chemical properties were. The lack of further work is probably due to the highly moisture sensitive nature of VCl_4 and the comparative ease of working with VCl_3 and VOCl_3 .

1.7 SEPARATION OF VANADIUM OXYCHLORIDE AND TITANIUM TETRACHLORIDE

In the previous two sections TiCl_4 and VOCl_3 have been described, from this it is clear that they have very similar properties. Their boiling points are separated by under 10°C and they are both considered Lewis acids. These properties along with their reactivity with many simple compounds results in the separation

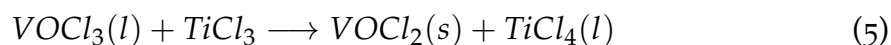
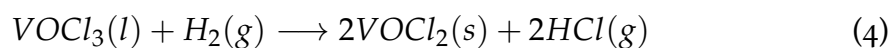
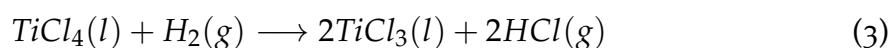
of TiCl_4 and VOCl_3 being extremely difficult and it is this that the project focuses on.

In the literature there are a few examples of a group directly comparing TiCl_4 , VCl_4 and VOCl_3 . Cuadrado *et al*^{81,82} compared the three metal chlorides by their reactivity to tetraalkyldiphosphine disulphides. They observed that TiCl_4 and VCl_4 formed hexacoordinate complexes with the metal chloride remaining intact and the bidentate ligand filling the coordination sphere. When VOCl_3 reacted with the ligands it led to the reduction of the vanadium to give a pentacoordinated species. Both of these studies showed a difference in the reactivity between TiCl_4 and VOCl_3 when compared to neutral ligands. However the characterisation used in the study was limited with no proton NMR or single crystal XRD carried out.

The separation of VOCl_3 from TiCl_4 is an area of research that has been studied for years, however, most of the information is held in patents.^{2,83,84} Boyd² reported the use of white mineral oil to remove VOCl_3 from TiCl_4 , which was demonstrated through distillation experiments but no attempts were made to understand how the mineral oil interacted.

Some research has been carried out academically, however, it is for radically different methods involving absorption by molecular sieves,⁸⁵ use of hydrogen⁸⁶ or it is related to the sulphate process.⁸⁷ Lynch investigated the addition of H_2 to reduce both the titanium and vanadium chlorides, as shown in

equations 3 and 4. The key reaction is shown in equation 5, however attempts to repeat this reaction during this project failed. The two compounds did not react and hence the TiCl_3 and VOCl_3 remained unreacted. This was monitored observationally as the VOCl_3 liquid is orange and should become more transparent if it is converted to TiCl_4 . If the reaction had occurred the solid would have gone from violet TiCl_3 to yellow/brown VOCl_2



The following investigates using NMR as a characterisation technique for observing the overall reaction of the different metal chlorides, before further chapters involve breaking down the oil to simpler esters where the chemistry was simplified to study through isolating complexes. Chapter 2 describes initial work to understand the system further before the thesis continues to delve deeper into the reason of differing reactivity between the metal chlorides.

INITIAL NMR BASED ANALYSIS OF SOYA OIL

2.1 NMR

Proton Nuclear Magnetic Resonance (NMR) spectroscopy provides structural information because the magnetic field measured at the nucleus is not the same as the applied magnetic field. This is caused by the electrons around the nuclei shielding the nucleus. It is this that allows the determination of the environment of the nucleus by observing the resultant chemical shift. Functional groups, such as esters or alkenes, shield the nuclei more than other groups such as alkyl groups, due to their greater electron density, thus causing a larger chemical shift. Another major factor in an NMR spectrum is spin-spin coupling, this is where the proton in question is close enough to one or more other protons and interacts with their spin. If the proton then couples to one other proton it forms a doublet, if it couples to two it forms a triplet and so on. More complex spin arrangements can be seen, such as a doublet of quartets when the proton is coupled to one proton in one environment and they are both coupled to three protons in a separate environment.

NMR has been used in many different ways over the last 50 years as a structure determination technique.⁸⁸ The primary use

has been in organic chemistry as ^1H and ^{13}C NMR are the most sensitive to subtle changes in chemistry at low concentrations. The chemical shift is dependant on the functional group adjacent to the carbon that the proton is bound to. The coupling also gives structural information about the environment of the nearby protons. These two pieces of information can be combined to give an accurate structure of a simple molecule.

NMR has been used to investigate the reaction of TiCl_4 , VOCl_3 and VCl_4 with soya oil. As mentioned in the introduction it is known that soya oil reacts with a mixture of vanadium chlorides and titanium chloride to remove the vanadium content to ppm levels. The mechanism for this removal is not known and this NMR study looks into the interaction of the soya oil with different metal chlorides.

NMR has been used extensively to look at metal coordination to molecules, for example Kondo et al⁸⁹ observed that the protons on the d-biotin methyl ester were downshifted upon the addition of magnesium or silver ions. This work looks at the change in position of the NMR peaks upon the addition of the metal chloride. If there is a break down of the functional groups this method will clearly illustrate this.

Soya oil was shown in industry to remove vanadium from a metal chloride mix, it is therefore expected that the most intense reaction would be with the vanadium chlorides. It is anticipated

that NMR will describe how the oil preferentially reacts with the vanadium chlorides.

2.2 OIL ANALYSIS

To study the interaction of soya oil with the various metal chlorides an understanding of the chemical structure of soya is needed. This section describes the analysis of soya oil using NMR to provide an accurate starting point as the current literature studies are not sufficient.

NMR has been used to record a ^1H spectrum of soya oil and observe the proton environments within soya oil. The spectra were recorded on a Bruker 600 MHz NMR machine using deuterated chloroform as the solvent. The NMR spectrum of soya oil is shown in Figure 11. In soya oil there are 10 different proton environments all relating to different proton shifts in the NMR, as shown in Figure 12. The shift is dependent on the proximity of the functional group to the oxygen atoms and the alkenes to the hydrogen atoms. This is due to the high electron density in these functional groups which deshield the proton. The protons that will be shifted the most will be the ones bonded to the carbon which is situated next to the oxygen or the double bond. Figure 12 labels these protons as **A**, **B** and **G**. Protons **C**, **F** and **H** will also be shifted to some extent. Whereas protons **E**, **D**, **J** and **I** will not be shifted to the same extent. Therefore it is possible to monitor the different proton environments in the oil.

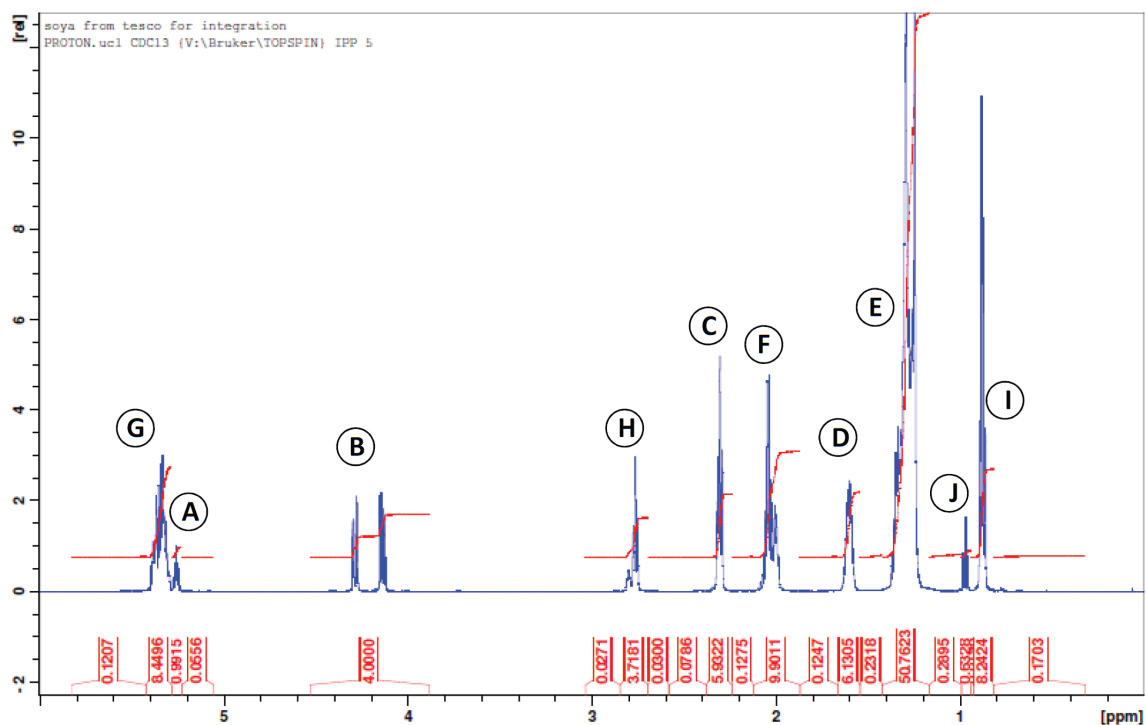


Figure 11: Spectrum to show the ^1H NMR of Soya Oil with the peaks labeled A-J relating to the 10 different environments)

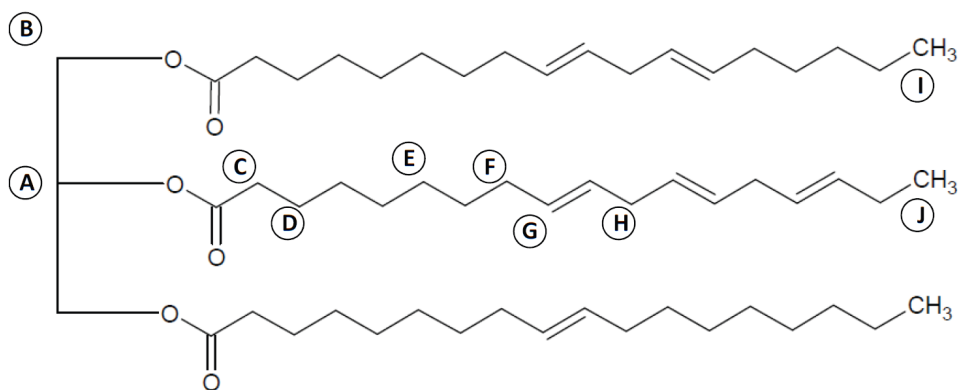


Figure 12: Schematic to show different proton environments in the soya oil, for reference the top chain is linoleic acid, the middle is α -linolenic acid and the bottom chain is oleic acid. Palmatic and stearic acid chains are not shown and they would consist of the environments A, B, C, D and E as they do not contain any alkene groups.)

NMR Shift / ppm	Calculated literature integrals	Proton Label	Analysis
0.85	8.32	I	Small shift due to the fact it is a terminal alkane group
0.95	0.68	J	Shifted slightly compared to I values due to proximity of alkene in α -linolenic acid
1.3	49.5	E	Describes the alkane chain content, shifted slightly due to being in the middle of a chain
1.6	6	D	Shifted due to the effect of the carbonyl, weak due to distance from the carbonyl.
2.0	10.14	F	Shifted due to the alkene, the integral describes the alkene component of the mixture
2.3	6	C	Shifted due to the effect of the carbonyl group, stronger as it is closer to the group
2.8	4.14	H	Shifted by the alkene, describes the poly unsaturated content as it is between two alkene bonds.
4.2	4.0	B	Strongly shifted as the carbon the protons are bonded to is directly bonded to an oxygen atom.
5.3	1	A	Relates to the glycerol end and is shifted strongly due to 3 oxygen atoms nearby.
5.4	8.9	G	The G environment directly describes the amount of alkene content as the G protons are directly connected to the alkene bond.

Table 2: ^1H NMR positions of the different protons in soya oil, integrals calculated based on the previously mentioned literature values.

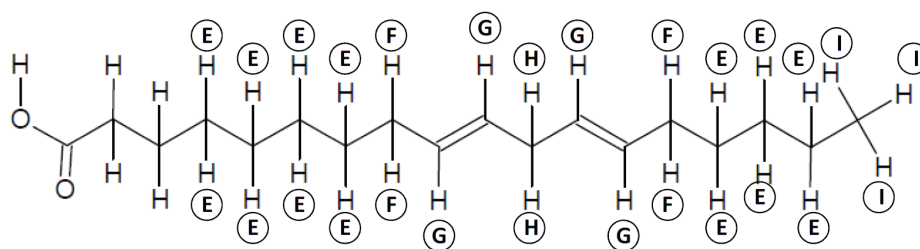


Figure 13: Diagram to show the different proton environments on a linoleic acid chain and the number of each of the appropriate environments associated with the chain.

From the literature values the composition of soya oil is; 7.5% alpha-linolenic acid, 54% linoleic acid, 22% oleic acid, 4.1% stearic acid, and 11% palmitic acid. It is possible to use this composition to calculate the predicted integrals of the NMR peaks. This can be achieved by taking a triglyceride molecule and analyzing the integrals it would provide. It can be seen that whichever of the acids are attached to the glycerol, the integral for peaks **A**, **B**, **C** and **D** should remain the same. Therefore, the NMR integrals can be scaled to these peaks. Thus NMR peaks have been standardized to the **B** peak as it is the clearest.

Calculating the predicted integrals for the other peaks is complex due to the different acids that could be connected. Each acid has therefore been described in relation to their differing proton environment. The data in Table 3 describe the number of each proton environment associated with each acid chain excluding the ester/ glycerol end.

This is shown schematically in Figure 13. By taking the data contained within Table 3 along with the % of each component, the

Linoleic acid:	14 E	4F	4G	2H	3I
α -Linolenic acid:	8 E	4F	6G	4H	3J
Oleic acid:	20 E	4F	2G	0H	3I
Palmitic acid:	24 E				3I
Stearic acid:	28 E				3I

Table 3: Table to show the amount of different proton environments for different acid chains

size of the integrals have been calculated as followed; **E**: 49.3, **F**: 10.2, **G**: 9.3, **H**: 4.2, **I**: 8.3, **J**: 0.7. This data is tabulated in Table 2 which also describes why the peaks are shifted.

Fatty acid	Soya oil 2008	Soya oil 2011	Soya oil from Tesco	Literature values
α -linolenic	7.4	7.5	7.2	7.5
Linoleic	49	52	49	54
Oleic	20	19	24	22
Saturated	23	21	20	15

Table 4: ^1H NMR analysis of different soya oils shown as percentages.

Using the method described above several types of soya oil were analysed. Three oils were tested; two used on the plant in recent years and one food grade sourced commercially. It is simple to compare the numbers and see what has increased and decreased as this would give an approximation of the oil composition. It is more complicated to provide a new composition for the oil.

This was achieved by studying the equations relating to the differing acid contents and the relative integrals. From looking at Table 3 it can be seen that the **J** integral can only be present due

to α -linolenic acid chain. Therefore, this gives a numerical value for the α -linolenic acid content which is divided by 3 to be relevant for a single proton as there are 3J protons in every chain. For the 2011 soya oil this gives a value for α -linolenic acid of 0.227, therefore the sample has 7.5% α -linolenic acid.

There are two chains which contain the H environment and these are linoleic acid and α -linolenic acid. A value for α -linolenic acid has already been established so this can be taken away from the integral value for H. This leaves a value for the 2011 soya oil of 1.55 units of linoleic acid.

The same calculation can be carried out for the G environment and this gives an oleic acid content of 0.633 units.

The calculation for the palmitic and stearic acid content is not as simple as they both contain only the E environment so it is not possible to distinguish between them, however, the value for the two together can be obtained. This was calculated and gave a value of 0.642. These values were all transformed into percentages and the results for all three oils are shown in Table 4.

The soya oil now fully analysed could be used to compare different batches and act as a method of quality control. The soya oil was then reacted with the metal chlorides; TiCl_4 , VOCl_3 and VCl_4 and the reactions were observed using ^1H NMR.

2.3 EXPERIMENTAL

A 1% stock solution of metal chlorides in deuterated chloroform was made up. One drop of this solution was added to a clean NMR tube filled with 0.3 ml deuterated chloroform. One drop of the desired oil was added to the NMR tube and the sample was analysed in a Bruker 600 MHz NMR machine. The spectra were integrated and the peak positions determined. Samples of the pure oils were run as standards in deuterated chloroform.

The spectrum of soya oil was analysed using more complex two dimensional NMR techniques. A cosy spectra is shown in Figure 14 to show how the peaks were determined. Each proton environment was defined as described in the previous chapter. Soya oil contains two main functional groups, the alkene and the carboxylic acid. The peak observed at 5.4 ppm corresponds to the alkene and the peak at 4.2 ppm to the glycerol, a disguised glycerol peak can be picked out at 5.3 ppm. It is the two peaks at 5.4 and 4.2 ppm that will be monitored.

Using the same technique, the NMR experiments were carried out with linseed oil, octene and trimyristin. Trimyristin was isolated from Nutmeg⁹⁰ by grinding nutmeg purchased from Sainsbury and then washing with diethyl ether which the trimyristin was dissolved in. This was dried *in vacuo* and left an orange powder. A mixture of 2-octene and 3-octene were synthesised by the dehydration of 3-octanol. This was carried out

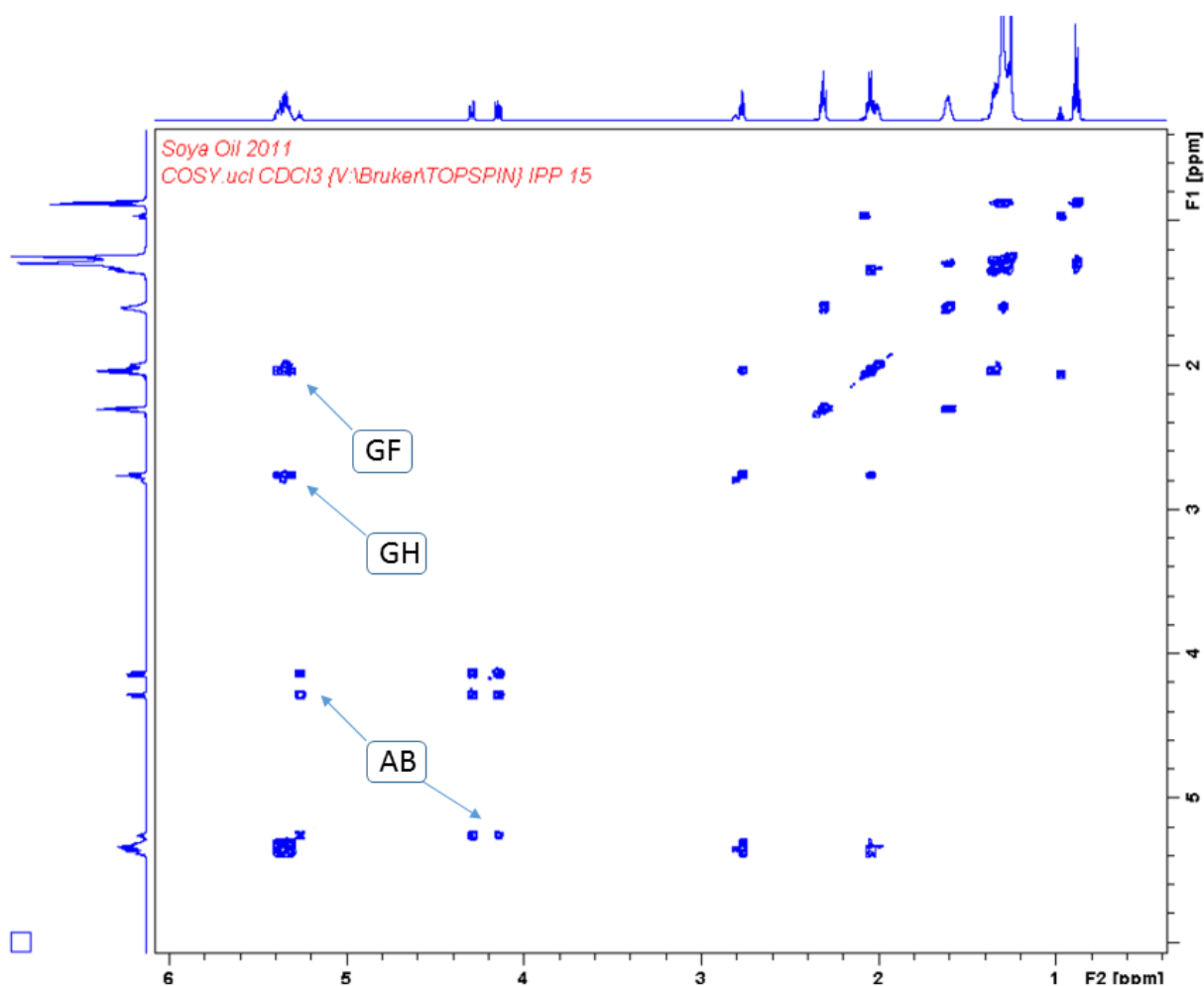


Figure 14: COSY spectrum to show proton-proton coupling in soya oil. The spectrum shows that peaks A and B (AB) are coupled to each other and represent the glycerol part of the oil. Peaks G,F and H are also coupled together (GF and GH) showing the long chain of the oil around the alkene bond.

by reacting 3-octanol with concentrated sulphuric acid and heated to 170 °C and then separated using distillation.

2.4 RESULTS

The reaction of soya oil with TiCl_4 , VOCl_3 and VCl_4 was monitored via ^1H NMR spectroscopy. The resulting spectra are shown together in Figure 15 in order to compare the reactivity. Distinct differences in the ^1H NMR spectra of the three samples following the addition of the metal chlorides to soya oil were observed as indicated in Figure 15.

The first observation from these experiments was the broad nature of the peaks in the spectrum for VCl_4 and soya oil. This is due to VCl_4 being paramagnetic. This paramagnetism results in a broadening of the peaks and NMR studies containing paramagnetic materials are less common but have been carried out.^{91,92} The data analysis suggests that the alkene peak has been reduced from two peaks to one but this could be due to peak broadening. This spectra indicates that the peaks are still present and shifted slightly down field. These results suggest that the VCl_4 does not react to any large extent with the soya oil during the experiment.

The ^1H spectrum of the TiCl_4 /oil mixture however displays a major change from the soya oil standard, with both the alkene peak (shown at 5.5 ppm) and glycerol peaks (4.2 and 5.4 ppm) no longer being observed. Therefore both the functional groups seem to have

been broken down by the metal chloride, converting the alkene to an alkane and splitting the oil up at the point of the glycerol. During this experiment there was no evidence of an alkyl chloride having been formed. This spectra was recorded after only 10 minutes which clearly displays how quickly TiCl_4 reacts with oil. Figure ?? shows the possible ways in which the soya oil molecules could be broken down and possible interactions with metal chlorides.

The ^1H NMR spectrum of VOCl_3 and soya oil displays results somewhere between those observed for VCl_4/oil and TiCl_4/oil . A shift of the alkene peak downfield by 0.2 ppm occurred from what was observed in neat soya oil. A reduction of the glycerol peak at 4 ppm was evident as shown in Figure 15. This suggests that while the vanadium coordinated slightly with the alkene it reacts strongly with the glycerol end of the oil.

These results are in contrast to the original hypotheses, as it appears that TiCl_4 actually reacts quicker with soya oil than with vanadium chlorides. Therefore, further analysis was necessary to look into how the soya oil does remove the vanadium contamination in the industrial process.

Various oils have been used in the industry therefore another oil was analysed, linseed oil. Therefore, the same test was carried out using linseed oil. The spectra from these runs are shown in Figure 16. It is clear to see that these spectra are very similar to those from the reaction of the metal halides with soya oil. Similar peaks for the ester and the glycerol functional groups were observed

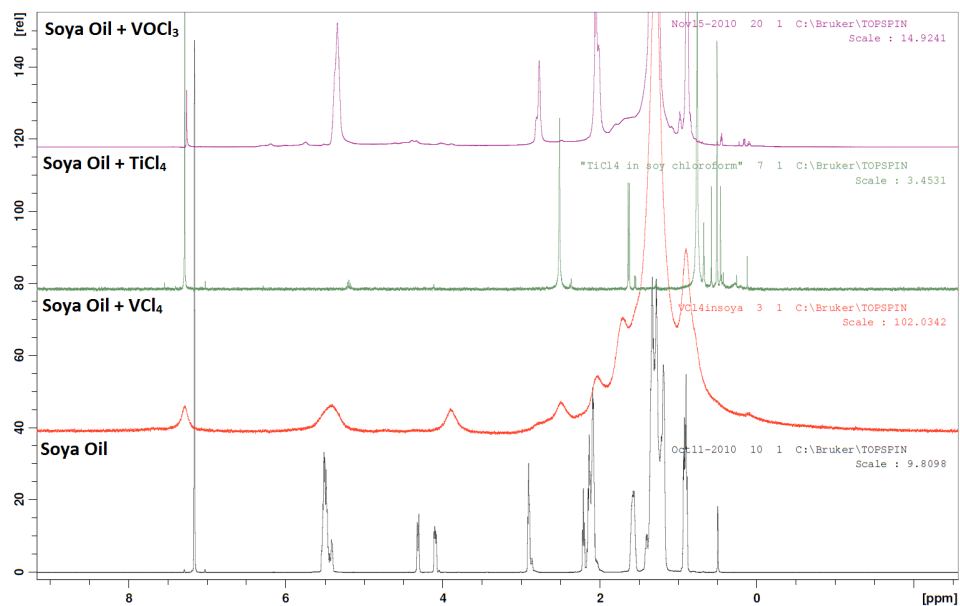


Figure 15: Spectra to show from bottom to top; pure soya oil, soya oil and VCl₄, soya oil with TiCl₄, soya oil and VOCl₃

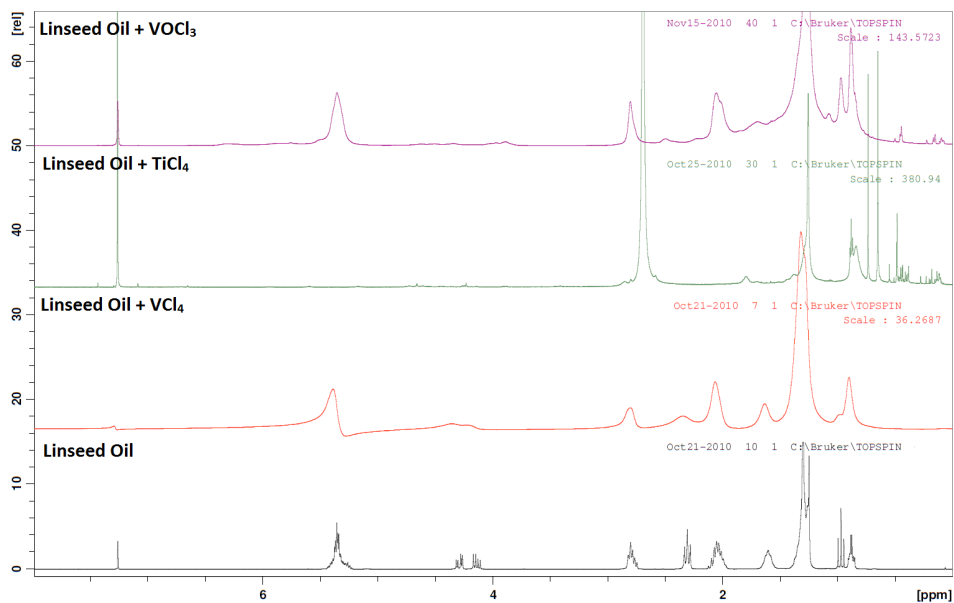


Figure 16: Spectra to show from bottom to top; pure linseed oil, oil and VCl₄, linseed oil with TiCl₄, linseed oil and VOCl₃

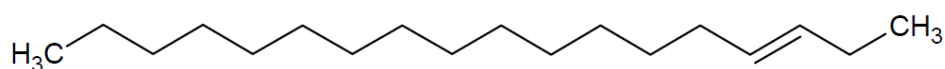


Figure 17: Molecular structure of octadecene

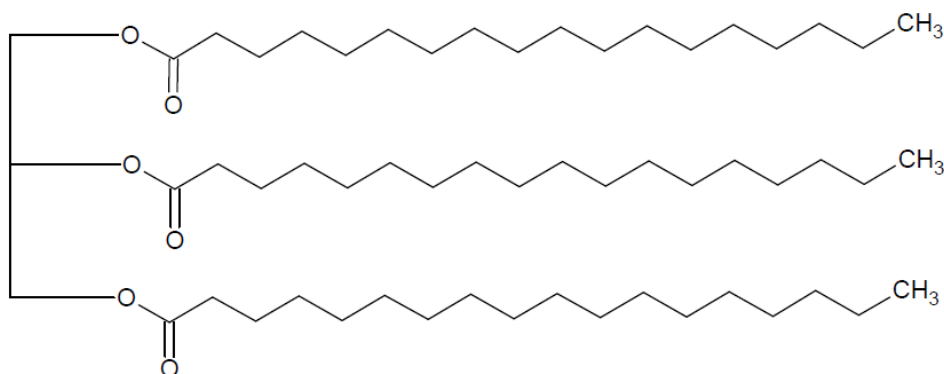


Figure 18: Molecular structure of tristearin

with small differences due to a greater alkene content. The reactivity of the linseed oil with the metal chlorides is the same as the soya oil which is not surprising as the functional groups are the same. Both oils show the same reactivity, with the TiCl_4 once again being the most reactive and the VOCl_3 preferentially reacting with the glycerol.

The two functional groups on the oil are the point of interest therefore, the next logical step was to break down the oil into the constituent parts. This involved performing the same NMR experiments with oils containing a long chained alkene and a fully saturated oil. The ideal molecules for this analysis are octadecene with non terminal alkenes and tristearin. Both of these molecules are shown in Figures 17 and 18.

In this research neither of these two molecules were actually used due to difficulties sourcing tristearin and a non terminal

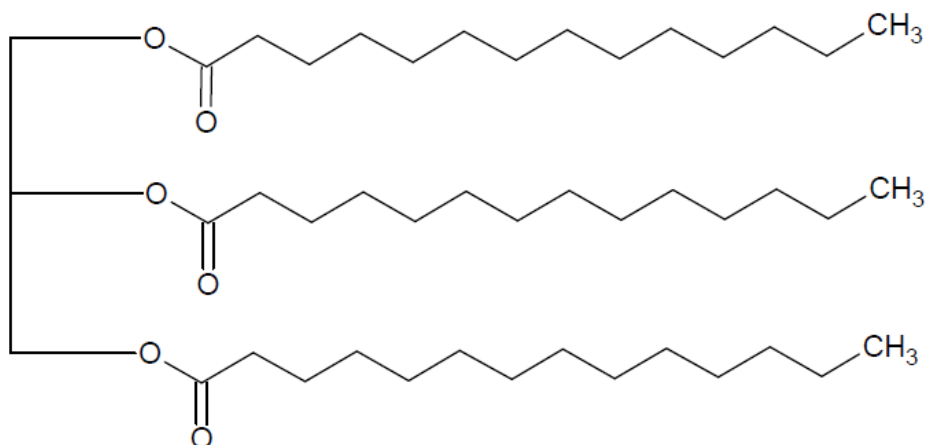


Figure 19: Molecular structure of trimyristrin

alkene. A simple technique⁹⁰ was used to isolate a C₁₄ analogue from nutmeg. This compound is called trimyristin and can be easily extracted and purified from nutmeg within hours. The chemical structure for this is shown in Figure 19 and it can be seen that it is similar to tristearin.

Instead of octadecene, a similar hydrocarbon was synthesised through a dehydration reaction of 3-octanol to produce a mixture of oct-2-ene and oct-3-ene. It was believed that it was more important in terms of the chemistry for the alkene to be non terminal than it was for the long chain to be present. This is because the terminal alkenes are very reactive and polymerise easily, the length of the chain has little effect on the direct chemistry around the bond.

The ¹H NMR spectra for trimyristin with the different metal chlorides is shown in Figure 20. The ¹H spectrum for just trimyristin shows the glycerol peaks at 4.2 ppm and 5.3 ppm as before but the alkene peak is not observed due to the lack of

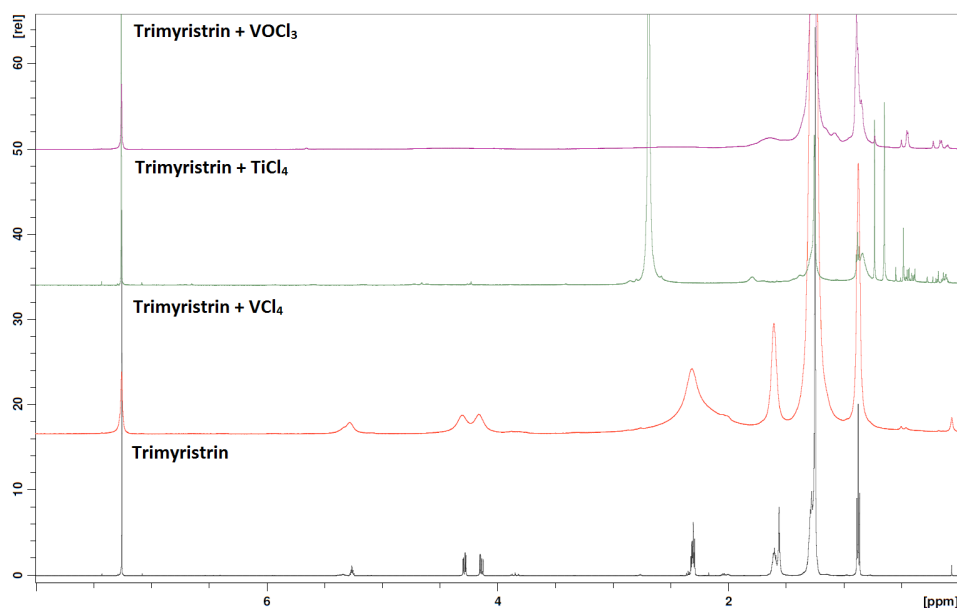


Figure 20: Spectra to show from bottom to top; trimyristin, trimyristin and VCl_4 , trimyristin with $TiCl_4$, trimyristin and $VOCl_3$

alkene groups in the oil. The trends previously observed with relation to the glycerol peaks are substantiated with reactions occurring for $TiCl_4$ and $VOCl_3$ but no interaction with VCl_4 . Hence the glycerol signals are only present in the 1H NMR spectrum of VCl_4 /oil. The previous experiments with soya oil indicated that the $TiCl_4$ and $VOCl_3$ reacted with the ester end of the oil and it is shown that they have now reacted with the ester, due to the reduction of the peaks at 4.2 and 5.3 ppm. As before the VCl_4 has not reacted and it is only a broadening of the peaks at 4.2 and 5.3 ppm which can be observed.

The 1H NMR spectra for octene with the different metal chlorides is shown in Figure 21. Apart from the broadening observed on the addition of VCl_4 the spectra all show no change in peak positions or intensities. This showed that after ten minutes at room temperature none of the metal chlorides react with the

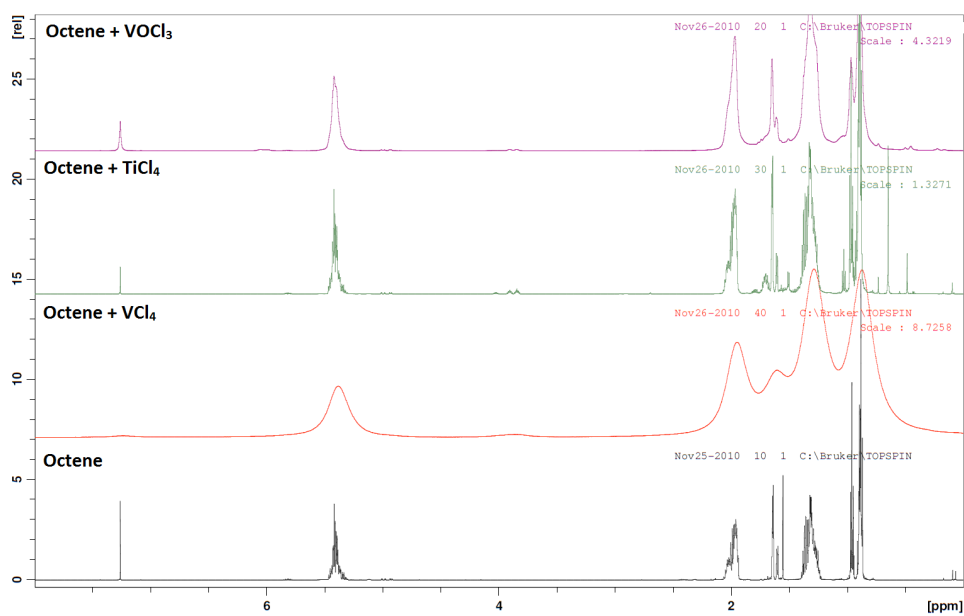


Figure 21: Spectra to show from bottom to top; octene, octene and VCl_4 , octene with TiCl_4 , octene and VOCl_3

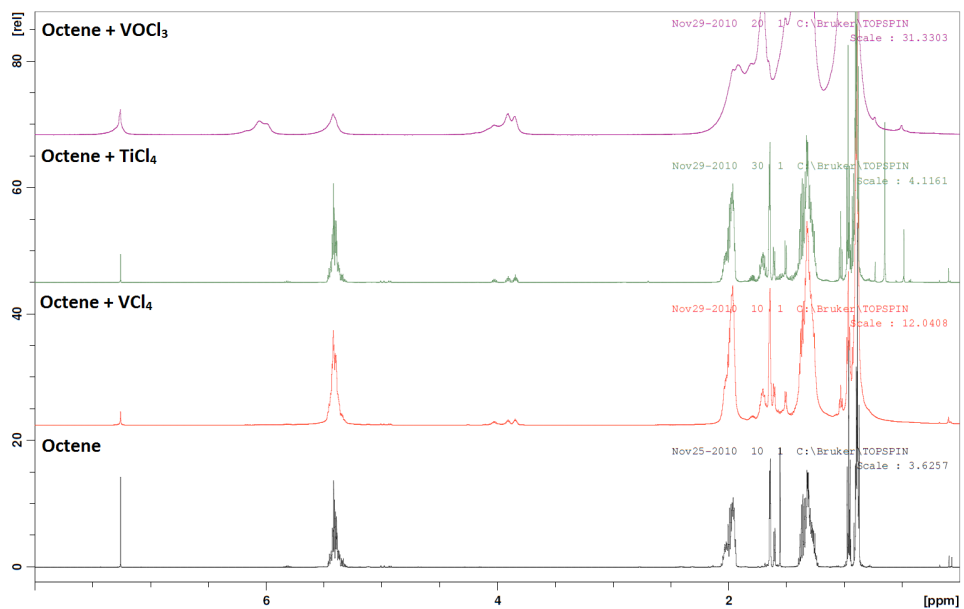


Figure 22: Octene spectra recorded after 48 hours showing from bottom to top; octene, octene and VCl_4 , octene with TiCl_4 , octene and VOCl_3

alkene. The VOCl_3 sample was left in the NMR tube with the octene for 48 hours. After 48 hours the solution looked much darker in colour so the spectrum was re-recorded. The spectra showed a decrease in the alkene peak at 5.4 ppm therefore this practice was carried out for all of the metal chlorides. The ^1H NMR spectra for octene with the different metal chlorides after 48 hours is shown in Figure 22. This shows a clear alkene peak at 5.3 ppm in the starting material at the bottom, it also shows the lack of reaction with the metal chlorides with the only differences in the other spectra being due to broadening.

After 48 hours the ^1H NMR spectra for the metal halides with octene had changed, a peak at approximately 4 ppm was observed. This peak corresponds to a hydrogen atom bonded to the same carbon as a chlorine atom. Protons which share a carbon centre with a Cl atom have been observed between 3 and 4 ppm.⁹³ The VOCl_3 shows the largest peak in this region and the largest reduction in the alkene peak at 5.3 ppm. This is the first example where the ^1H NMR study indicated a preference for reaction with a vanadium chloride compound rather than titanium tetrachloride.

2.5 CONCLUSIONS

The ^1H NMR reactions of the metal chlorides with the various oils show that the TiCl_4 reacts quicker with the oil than the vanadium chlorides. VCl_4 however, does not react with the oil very much at all so if this was present in abundance the process would not succeed in removing it. Huntsman pigments believe that the amount of VCl_4

in the system has always been low and it is VOCl_3 which dictates the vanadium content.

Both TiCl_4 and VOCl_3 showed the same reactivity with the glycerol/ester and the oil throughout this study. Therefore it is believed that this part of the oil cannot be responsible for the separation. The alkene, however, over a period of 48 hrs reacted preferentially with the VOCl_3 . In industry the entire process occurs at higher temperatures so what takes 48 hours at room temperature may proceed much faster at around $140\text{ }^\circ\text{C}$.

The work represented in this chapter acted as a starting point to study the industrial process using chemical techniques in the chloride process to make TiO_2 . To investigate the chemistry further this project steps away from industry and focuses on the reactivity of TiCl_4 and VOCl_3 with alkenes and diesters. This chapter has shown that there is different reactivity with these two groups and understanding this is one key to understanding the industrial process. In the next chapter the reactions will be studied by the formation of inorganic coordination compounds which can be analysed using NMR and single crystal X-ray analysis.

REACTIONS OF TiCl_4 WITH DIESTERS

3.1 INTRODUCTION

Chapter 2 discussed the breaking down of soya oil into its constituent parts; octene and trimyristin. To further elucidate this chemistry a molecular approach was taken in an attempt to investigate the reactivity of TiCl_4 and VOCl_3 with alkenes and diesters. The results could provide information about the reactivity of the oil with these metal chlorides, since it will allow an understanding of how the functional groups in the oils react with the metal. Taking a molecular approach allows for characterisation *via* NMR and single crystal X-ray analysis. This chapter investigates the bonding of TiCl_4 with diesters.

Complexes of TiCl_4 with diesters have been synthesised before, both Sobota *el al*⁹⁴ and Kakkonen *el al*¹ synthesised TiCl_4 coordinated to diethyl malonate. The structure is depicted in Figure 23 and reveals that the titanium centre is bonded to both the ester oxygens adopting a distorted octahedral geometry.

Kakkonen *el al*¹ investigated further malonates by adding R - groups to the middle carbon atom of the diester. They observed no difference in the coordination compared to the diethyl malonate.

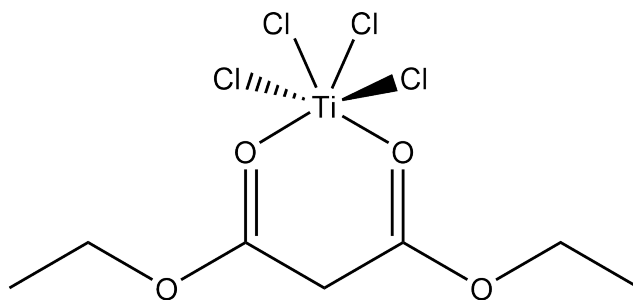


Figure 23: Structure of $[\text{CH}_2(\text{CO})\text{CH}_2\text{CH}_3)_2\text{TiCl}_4]^1$

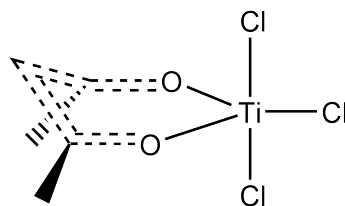


Figure 24: Figure to show TiCl_4 bound to acac⁹⁵

This area has not been well studied in the literature apart from these two papers.

A more frequently studied system in coordination compounds is that of acetylacetonate (AcacH). AcacH is a diketone which is known to form delocalised systems by the loss of a hydrogen atom. This has been reported to have been observed by Gopinthan *et al*⁹⁵ but no crystal structure of the molecule (shown in Figure 24) was reported. The structure involved the loss of a Cl atom from the titanium and this was explained by the stabilisation of the titanium centre through delocalisation. This will be further investigated during this chapter as this structure does not fill the coordination sphere to enable the titanium to be octahedral.

A further study by Maier *et al*⁹⁶ reported the reaction of TiCl_4 with 3,3-dimethyl-2,4-pentanedione. In this system there is no free H atom to be lost between the ketones therefore a delocalised

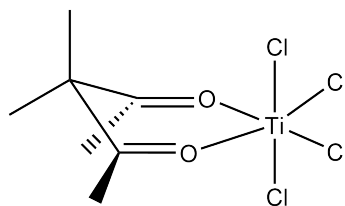


Figure 25: TiCl_4 bonded to 3,3-dimethyl-2,4-pentanedione⁹⁶

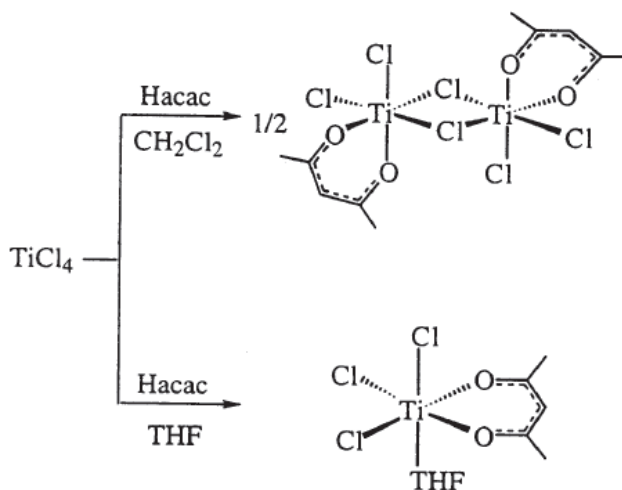


Figure 26: Scheme to show the addition of acacH to TiCl_4 in differing solvents

system cannot be formed. The TiCl_4 does not lose a Cl atom as the titanium charge cannot be stabilised by the ketones, as shown in Figure 25, and the ligand coordinates to the titanium centre. Maier *et al*, however, went further and reported the reaction of TiCl_4 with acacH to leave a structure where a chlorine atom is not lost.⁹⁷ This reaction was carried out at -20°C and is in opposition to the previous study by Gopinathan.

This report has therefore shown a difference of a opinion in the literature. A further study by Shao *et al*⁹⁸ reported the possibility of a dimeric titanium species, they demonstrated control over the formation of the monomer by the addition of THF, as shown in Figure 26. When THF is added it fills the coordination

sphere of the TiCl_4 allowing a chlorine atom to be lost and the acac to bind in its preferred way. When dichloromethane is used as the solvent it can not coordinate to the titanium centre and the coordination sphere is completed by bridging chlorine atoms. These different reports have demonstrated the sensitivity of reaction ratios in the addition of acacH to TiCl_4 . When an excess of acacH is added two acac ligands bind to the titanium centre with the loss of two chlorine atoms,⁹⁹ this fills the coordination sphere and charge compensates the titanium. This is the most stable TiCl_4 acac product but requires a 2:1 excess of the acacH ligand. When the two starting materials are used in molar concentrations it has been shown there are three possible structures from the literature: (1) The acacH bound without the delocalisation and no loss of chlorine. (2) The complex dimerisation and the loss of a chlorine atom and acac delocalisation with a loss of chlorine. (3) The formation of a Cl bridged dimer. This chapter will assess which of these products is most likely.

The literature regarding the reactivity of vanadium chloride compounds with these diketones is not as expansive. It was studied by two groups in India around 30 years ago.⁹⁵ From reading these papers many results were assumed and no crystal structures were solved. They reported that the acacH and other diketones formed monomeric species with the loss of a chlorine atom. They also reported a monomeric species when reacted with a keto-ester. These results provided a reason to study these systems as reactions clearly took place but the results cannot be confirmed.

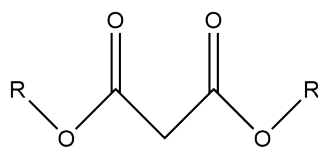


Figure 27: Structure of malonate where R = ethyl, benzyl, isopropyl and t-Bu.

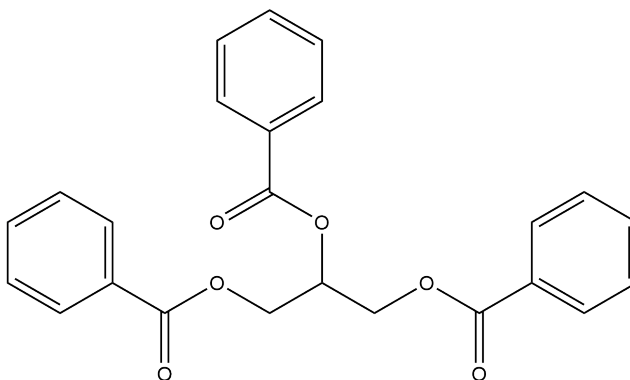


Figure 28: Structure of glycerol tribenzoate.

The literature suggests that the acac ligand delocalises causing the loss of a chlorine atom from the titanium or vanadium metal centre. When the titanium complex loses a chlorine it dimerises to fill its coordination sphere, whereas the vanadium complex is stable as a monomer. When the TiCl_4 reacts with the diester it does not lose a chlorine and is stable as a monomer, this could be due to the ester oxygen donating electron density to stabilise the α carbon. The reactivity of a diester has not been studied with VOCl_3 and this will be investigated later in this thesis.

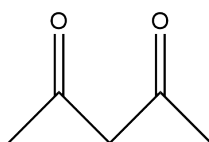


Figure 29: Structure of acacH.

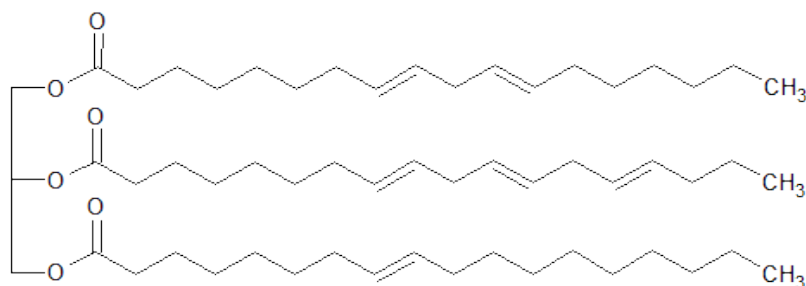


Figure 30: Representation of the structure of soya oil

This chapter looks into how titanium tetrachloride reacts with esters and ketones. The majority of the work involves a malonate ligand with differing R groups, as shown in Figure 27.

This study was derived from the structure of soya oil which is shown in Figure 30. The ligands in this thesis focus on the glycerol end of the soya oil. Soya oil is a very oily material and it is very difficult to isolate parts of the oil for a coordination study. The oil can be broken down as shown in the last chapter into the glycerol and the alkene ends. The glycerol is a triester, so the starting point of this work was to look at simple esters and their coordination with TiCl_4 .

Also included in this work are reactions with glycerol tribenzoate, as shown in Figure 28. Glycerol tribenzoate was used because it represents a closer link to the glycerol end of soya oil without having the fatty acid chains which make coordination complexes harder to form. It further strengthens the link from the ester towards the oil and gives an accurate representation of the soya oil in a manageable form for a coordination study.

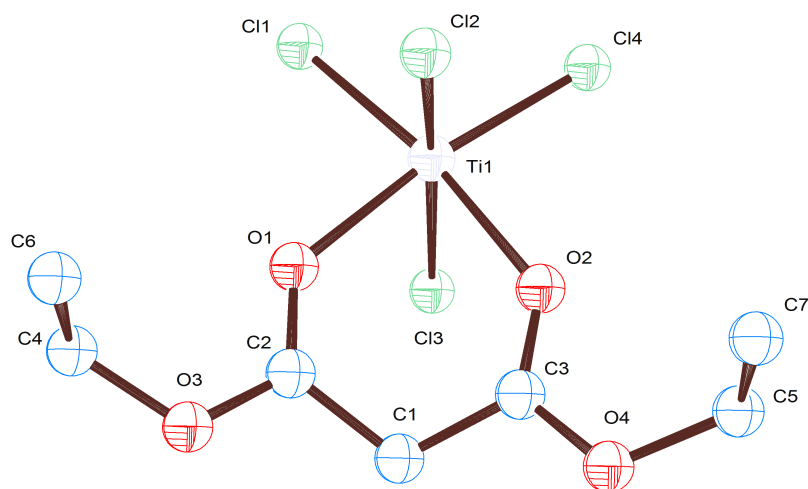


Figure 31: Figure to show crystal structure of tetrachloro(diethyl malonate)-titanium(IV) [**1**]¹

The final ligand investigated is the commonly used acac ligands shown in Figure 29. This is a commonly used organic ligand and can provide an interesting difference between a diester and a diketone. The ester oxygen is the difference between the two functional groups and may act to stabilise the ketone through delocalisation, if the double bond nature of the ketone is lost.

3.2 RESULTS

3.3 TITANIUM COMPLEXES

3.3.1 Synthesis of tetrachloro(diethyl malonate)-titanium(IV) [**1**]

The reaction of TiCl_4 and diethyl malonate has been previously synthesised and characterised to give compound [**1**]¹⁹⁴. The

Table 5: Selected bond lengths Å and angles (°) for tetrachloro(diethyl malonate)-titanium(IV) [**1**] taken from¹

C(3)-O(2)-Ti(1)	133.4(3)	Cl(1)-Ti(1)-Cl(3)	95.1(1)
C(2)-O(1)-Ti(1)	132.6(3)	O(1)-Ti(1)-Cl(2)	84.3(1)
O(1)-Ti(1)-O(2)	79.6(1)	Cl(3)-Ti(1)-Cl(2)	165.5(1)
O(1)-Ti(1)-Cl(3)	84.4(1)	Cl(1)-Ti(1)-Cl(2)	94.4(1)
O(1)-Ti(1)-Cl(4)	91.7(1)	C(3)-C(1)-C(2)	113.3(3)
Cl(1)-Ti(1)-Cl(4)	97.7(1)	O(1)-C(2)-C(1)	124.7(3)
O(1)-Ti(1)-Cl(1)	170.6(1)	O(2)-C(3)-C(1)	124.4(4)
Cl(3)-Ti(1)	2.304(2)	Cl(1)-Ti(1)	2.223(2)
Cl(4)-Ti(1)	2.225(2)	Cl(2)-Ti(1)	2.27(2)
O(2)-Ti(1)	2.109(3)	C(2)-O(1)	1.229(5)
O(1)-Ti(1)	2.136(3)	C(3)-C(1)	1.498(6)
C(2)-O(2)	1.305(5)(4)	C(1)-C(2)	1.493(6)

synthesis provided a way to ensure the reaction conditions stipulated by Sobota *et al*⁹⁴ were repeatable. The reaction progressed as described and a yellow product was isolated which could be characterised by NMR and elemental analysis. Recrystallisation of the yellow solid by layering dichloromethane with hexane afforded yellow crystals. While these crystals were suitable for single X-ray analysis it was not carried out as the structure was already known, however, the unit cell was checked and found to match the previous structure shown in Figure 31. Selected bond lengths and angles for this structure are shown in Table 5 for later comparison.

The ¹H NMR of [1] showed δ shifts of 0.8 ppm for CH₂ of the ethyl group and 0.3 ppm for the CH₃. This is a clear indication that the TiCl₄ has coordinated to the malonate, which has in turn allowed the other oxygen to donate electron density to the α -carbon causing the shifts from the original positions. The ¹³C {¹H} NMR showed the terminal CH₂ next to the CH₃ has shifted downfield towards zero by 7 ppm. This is because the electron density from the ester has shifted towards the central CH₂ and towards the C=O, this is also observed as the peaks have shifted upfield by 3 ppm. The elemental analysis confirmed the result as expected.

The synthetic route to form the complex was optimised from the literature by using a greater excess of TiCl₄. By using an excess the chemistry was not altered, but it ensured all of the malonate reacted. This was useful as an excess of malonate was problematic as it is a viscous liquid which resulted in difficult crystallisation and

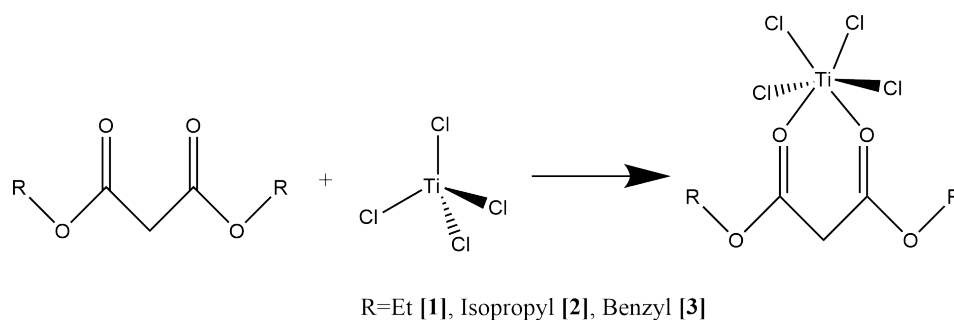
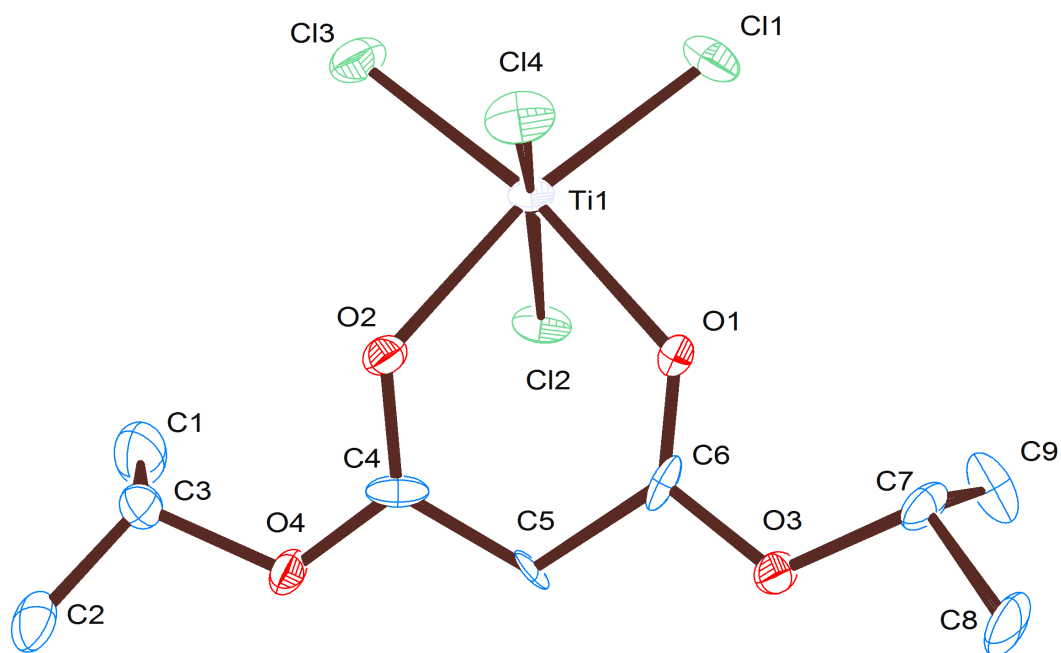


Figure 32: Scheme to show the reaction of TiCl_4 with the malonate ligands purification. The excess TiCl_4 was easily removed by washing with hexane.

3.3.2 Synthesis of tetrachloro(bis isopropyl malonate)-titanium(IV) [2]

After the optimisation of conditions described above for compound [1] bis-isopropyl malonate was used as a starting material. The reaction scheme is shown in Figure 32. An excess of TiCl_4 was reacted with bis-isopropyl malonate to give compound [2]. This provided a way to study the effect of changing the R-groups on the chemistry and to synthesise novel compounds. The synthesis proceeded in the same way as the diethyl malonate, a yellow precipitate was formed and crystals were grown again using a dichloromethane/hexane layering technique.

The ^1H NMR of [2] showed the same shifts as the diethyl malonate, therefore it was clear that the TiCl_4 had coordinated to the malonate without breaking it down. The $-\text{CH}_2$ peak in the malonate next to the oxygen shifted from 5.05 ppm to 5.46 ppm. The other $-\text{CH}_2$ peak between the two ketones shifted from 3.25 ppm to 3.96 ppm. The third peak for the $-\text{CH}_3$ protons shifts from



Crystal system	triclinic
Space group	$P1$
	$a = 6.6655(15) \text{ \AA}$ $\alpha = 90.000^\circ$
	$b = 12.954(3) \text{ \AA}$ $\beta = 89.968(4)^\circ$
	$c = 18.983(5) \text{ \AA}$ $\gamma = 90.000^\circ$

Figure 33: Crystal structure of tetrachloro(bis isopropyl malonate)-titanium(IV) [2a]

Table 6: Selected bond lengths Å and angles (°) for bis isopropyl malonate)-titanium(IV)[2a]

Cl(3)-Ti(1)	2.2217(11)	Cl(1)-Ti(1)	2.2350(9)
Cl(4)-Ti(1)	2.2555(9)	Cl(2)-Ti(1)	2.3423(10)
O(2)-Ti(1)	2.089(2)	C(6)-O(1)	1.176(5)
O(1)-Ti(1)	2.123(3)	C(4)-C(5)	1.449(6)
C(4)-O(2)	1.272(4)	C(5)-C(6)	1.511(6)
<hr/>			
C(4)-O(2)-Ti(1)	129.5(3)	Cl(1)-Ti(1)-Cl(3)	98.51(3)
C(6)-O(1)-Ti(1)	130.9(3)	O(1)-Ti(1)-Cl(2)	82.98(8)
O(1)-Ti(1)-O(2)	79.34(10)	Cl(3)-Ti(1)-Cl(2)	94.00(3)
O(1)-Ti(1)-Cl(3)	170.30(8)	Cl(1)-Ti(1)-Cl(2)	92.90(3)
O(1)-Ti(1)-Cl(4)	84.72(8)	C(6)-C(5)-C(4)	114.0(3)
Cl(1)-Ti(1)-Cl(4)	97.12(3)	O(1)-C(6)-C(5)	127.8(3)
O(1)-Ti(1)-Cl(1)	90.86(7)	O(2)-C(4)-C(5)	125.5(4)

1.20 to 1.47 ppm. These are all clear indications of coordination which were backed up by single crystal X-ray analysis.

The crystal structure of [2] shown in Figure 33 looks similar to that of the diethyl malonate complex previously reported. It shows the titanium forming coordinative bonds with both the ketone and oxygen atoms to give a six coordinate Ti centre. A distorted octahedral geometry is adopted with the bond angles between the two oxygen atoms bonded to the titanium being $79.34(10)^\circ$. This is smaller than the expected octahedral angle of 90° , which can be explained by the chelating nature of the ligand and the relative electronegativity of the 6 atoms surrounding the Ti centre. The chlorine atoms are more electronegative so repel each other strongly to give Cl-Ti-Cl angles of $98.51(3)^\circ$ at the extreme. Selected bond lengths and angles are shown in Table 6.

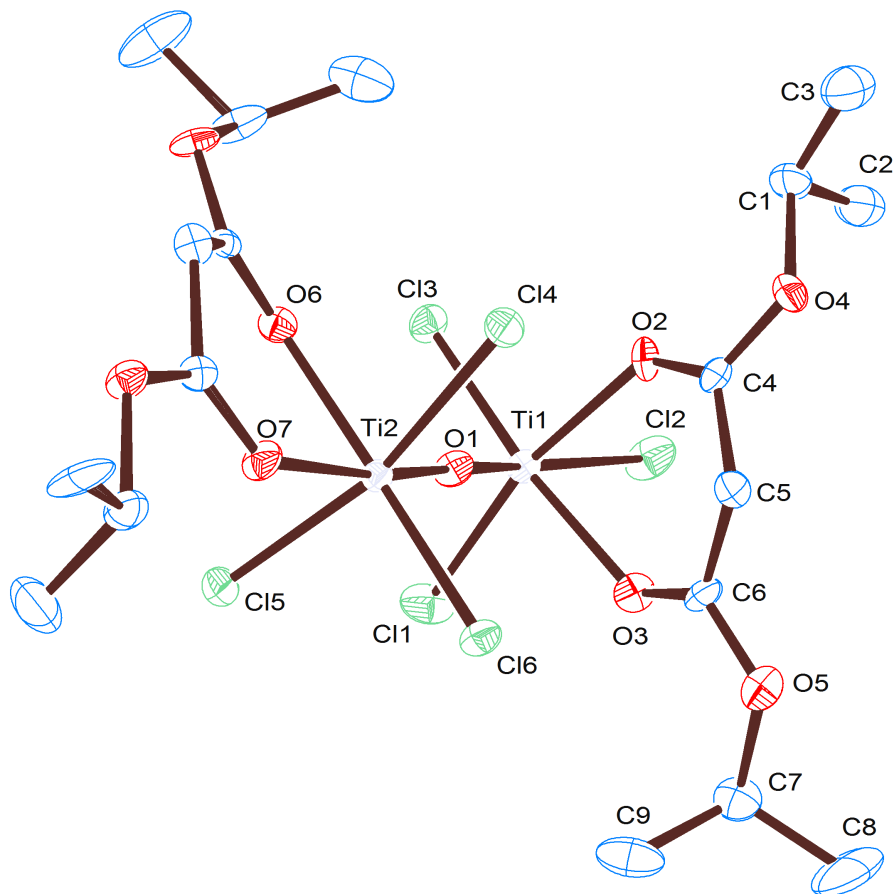
The O-Ti-O angle which makes up a hexagon with 3 carbon atoms, 2 oxygen atoms and 1 titanium atom is $79.34(10)^\circ$. This angle is much smaller than the 120° which would be expected for a flat hexagon. Although to some extent this can be explained by puckering in the ring, it is considerably lower than expected. It is lower than another reported O-Ti-O angle of 84° ,¹⁰⁰ this is again due to the strong electronegativity of the Cl atoms.

The titanium-oxygen bond length is $2.089(2) \text{ \AA}$ which is longer than reported Ti-O bond lengths, such as in $[\text{TiCl}_2((\text{OSi}(\text{SiMe}_3)_2)_2)]$.¹⁰¹ The bond length is similar to that observed in $[\text{TiCl}_4(\text{THF})_2]$ at 2.15 \AA , as in this complex the THF

was acting solely as a coordinating solvent forming a dative bond. This further confirms that TiCl_4 is coordinating to the ester groups and not forming Ti-O covalent bonds.

The bond angles and lengths observed for compound **2** are very similar to those recorded for compound **1**¹. This suggests that the change of R-group from ethyl to isopropyl has had little effect on the structure. This is not surprising as the isopropyl group differs mainly in steric bulk and even this is by a relatively small amount. There is little steric hinderence around the structure so larger R-groups such as benzyl will be used to investigate this further.

When the product of the reaction of bis isopropyl malonate with TiCl_4 was crystallised, two types of crystals were observed, block type [**2a**] and plate type [**2b**]. The other structure solved for the compound is shown in Figure 34 and selected bond angles and distances are shown in Table 7. This structure shows a bridging oxygen between the two titanium centres with a loss of a Cl atom. This was likely due to hydrolysis of the product during the reaction as a result of a small amount of air entering the vessel. The bridging oxygen stabilised the system and similar bridged compounds have been reported before¹⁰⁰ as it is easier to crystallise when large stabilising ligands are removed. The bond angles and distances are similar to those in compounds [**1**] and [**2a**] with the new Ti-O-Ti bond angle being 177° which is as expected. The dimer demonstrates how air/moisture sensitive this system is and how any form of oxygen can stabilise the product.



Crystal System	monoclinic
Space group	$P2_1/c$
unit cell dimensions	$a = 18.335(16) \text{ \AA}$ $\alpha = 90.000^\circ$ $b = 12.436(12) \text{ \AA}$ $\beta = 102.474(14)^\circ$ $c = 13.683(11) \text{ \AA}$ $\gamma = 90.000^\circ$

Figure 34: Figure to show crystal structure of trichloro-O-(bis isopropyl malonate)-titanium(IV) dimer [**2b**]

Table 7: Selected bond lengths Å and angles (°) for bis isopropyl malonate)-titanium(IV) [2b]

Ti(2)-O(1)-Ti(1)	177.2(5)	O(3)-Ti(1)-Cl(1)	87.3(2)
C(4)-O(2)-Ti(1)	131.6(7)	Cl(3)-Ti(1)-Cl(1)	100.27(13)
C(6)-O(3)-Ti(1)	132.6(7)	O(1)-Ti(1)-Cl(2)	162.7(3)
O(1)-Ti(1)-O(2)	83.4(3)	O(2)-Ti(1)-Cl(2)	81.6(2)
O(1)-Ti(1)-O(3)	84.1(3)	O(3)-Ti(1)-Cl(2)	84.7(2)
O(2)-Ti(1)-O(3)	79.9(3)	Cl(3)-Ti(1)-Cl(2)	94.37(12)
O(1)-Ti(1)-Cl(3)	95.0(2)	Cl(1)-Ti(1)-Cl(2)	96.20(15)
O(2)-Ti(1)-Cl(3)	92.5(2)	C(6)-C(5)-C(4)	113.8(9)
O(3)-Ti(1)-Cl(3)	172.4(2)	O(3)-C(6)-C(5)	124.3(9)
O(1)-Ti(1)-Cl(1)	96.4(3)	O(2)-C(4)-C(5)	125.9(9)
O(2)-Ti(1)-Cl(1)	167.2(2)		
<hr/>			
O(1)-Ti(2)	1.740(7)	Cl(1)-Ti(1)	2.230(3)
O(1)-Ti(1)	1.865(7)	Cl(2)-Ti(1)	2.308(4)
O(2)-Ti(1)	2.128(7)	Cl(3)-Ti(1)	2.224(3)
O(3)-Ti(1)	2.135(8)	Cl(4)-Ti(2)	2.374(3)
C(4)-O(2)	1.222(12)	C(4)-C(5)	1.502(14)
C(6)-O(3)	1.227(12)	C(5)-C(6)	1.501(14)

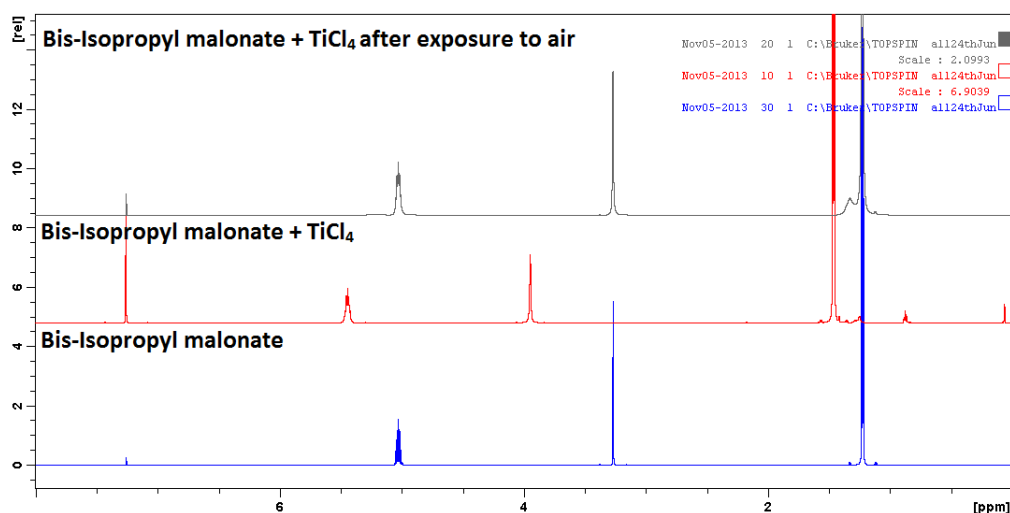


Figure 35: NMR spectra to show iso-propyl malonate coordinated to TiCl_4 and then dissociated, both are compared to the starting material shown at the bottom

Comparing the bond angles and lengths of the dimeric species with the monomeric species gives an idea of what stabilising effect the bridging oxygen has had on the system. The bridging oxygen has bond lengths to the titanium atoms of 1.865(7) Å and 1.740(7) Å, which are much closer to a typical Ti-O single covalent bond of 1.75 Å. The Ti-Cl bonds are the same as with the monomer with the longest Ti-Cl bond length of 2.308(4) Å observed for the chlorine closest to the malonate. This is due to the electron density around the malonate ester forcing the Cl atom out slightly from its usual position increasing the bond length. Titanium is known to be very oxophilic¹⁰² so it is this that forces the oxo-bridging. The evidence from looking at the bond distances, suggests that the bridging oxygen atom stabilises the dimer as the Ti-O bond distance is around 1.8 Å instead of the 2.25 Å observed for TiCl_4 .

After observing a reaction with air and complex [2a] forming [2b] further experiments were carried out to understand the

reactivity with air. A portion of the compound was then exposed to air, this yielded a white solid which was a mixture of bis-isopropyl malonate and TiO_2 , a residue of which was used to obtain ^1H NMR. The ^1H NMR showed a match to the NMR of bis-isopropyl malonate, the starting material. Therefore it is clear that the TiCl_4 can coordinate and disassociate with the malonate without breaking down any bonds in the ligands. In an air free environment, such as the industrial plant, this reaction could be reversible and the malonate could go on to react with other species such as VOCl_3 . The ^1H NMR of before and after air exposure are shown in Figure 35 in comparison to the starting ligand. The peaks clearly shift upfield when coordinated to TiCl_4 and then revert to their original position when dissociated.

3.3.3 *Synthesis of tetrachloro(di-tBu malonate)-titanium(IV)*

Di-tBu-malonate was reacted with an excess of TiCl_4 for 2 hrs. A similar yellow precipitate was observed as before and the precipitate was washed and dried. However, when deuterated chloroform was added to attempt to record NMR data it was found to be insoluble, this was also true for all easily available NMR solvents so NMR data could be collected. Crystals of this product could not be formed so further analysis was not continued.

3.3.4 *Synthesis of tetrachloro(di-Benzyl malonate)-titanium(IV) [3]*

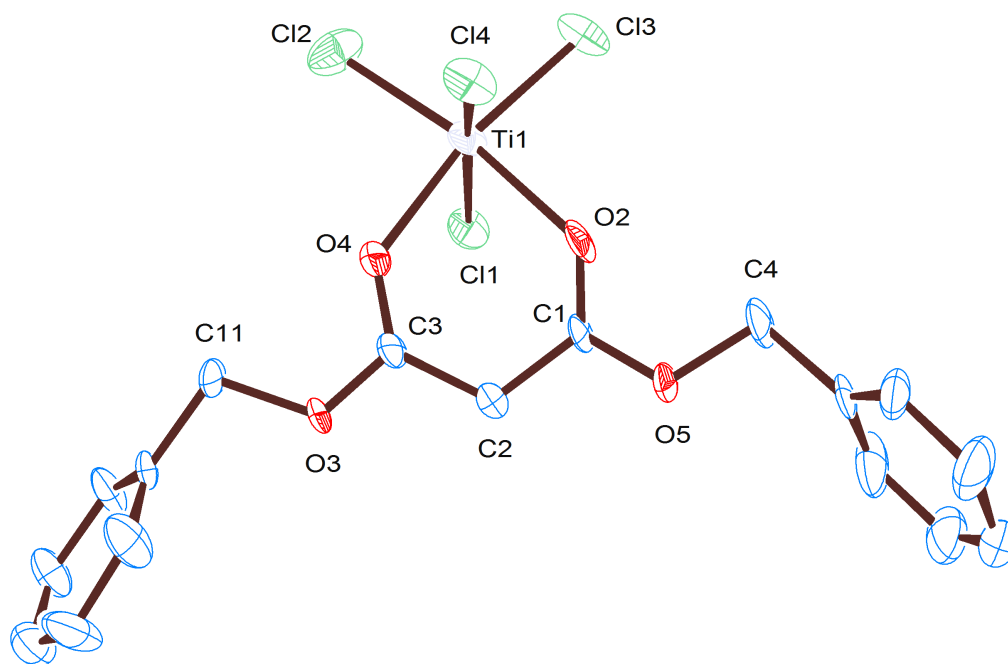
Dibenzyl malonate was reacted with an excess of TiCl_4 in anaerobic conditions. Benzyl provided a fourth mechanism to look at larger R groups after the inability to crystallise bis-tBu malonate.

As with the other reactions a yellow precipitate formed immediately. The reaction was left stirring for 2 hrs to ensure a full reaction, the product was then filtered and dried. The powder was analysed by NMR and then re-crystallised by dissolving in dichloromethane and layering with hexane. Yellow crystals of compound [3] were afforded over night and were analysed using single crystal X-ray diffraction.

The ^1H NMR of [3] showed clear shifts within the proton positions indicating coordination. The 3 main peaks relating to the ester bridging carbons, the carbons between the ester and benzene ring, and the benzene ring all shifted downfield. The largest shift was for the carbons between the ester groups which shifted by 0.5 ppm from 3.5 ppm to 4.0 ppm, it is closest to the titanium tetrachloride and adjacent to the affected ketone bond. The other CH_2 group was shifted by 0.3 ppm from 5.2 ppm to 5.5 ppm and even the benzyl peaks were shifted 0.1 ppm from 7.4 ppm to 7.5 ppm.

From the ^{13}C $\{^1\text{H}\}$ NMR it was not possible to make out the $\text{C}=\text{O}$ peak due to the peak height being in-discriminant amongst the noise. The other peaks in the spectrum do not shift from the neat dibenzyl malonate.

Crystals of compound [3] were analysed by single crystal X-ray diffraction, the results of which are shown in Figure 36 along with selected bond lengths and angles in Table 8. The structure of [3] was found to be similar to that of compounds [1] and [2] as a



Crystal System	monoclinic	
Space group	$P2_1$	
Unit cell dimensions	$a = 16.3215(4) \text{ \AA}$	$\alpha = 90.000^\circ$
	$b = 9.5645(2) \text{ \AA}$	$\beta = 90.069(2)^\circ$
	$c = 19.7379(4) \text{ \AA}$	$\gamma = 90.000^\circ$

Figure 36: Figure to show crystal structure of [3]

Table 8: Selected bond lengths Å and angles (°) for compound [3]

Ti1-Cl1	2.300(2)	O2-C1	1.237(12)
Ti1-Cl4	2.296(3)	O4-C3	1.231(11)
Ti1-Cl3	2.224(3)	C3-C2	1.489(12)
Ti-Cl2	2.211(3)	C1-C2	1.481(12)
Ti1-O2	2.119(7)	Ti1-O4	2.139(6)
<hr/>			
Cl4-Ti1-Cl1	165.39(13)	O2-C1-C2	125.2(8)
Cl3-Ti1-Cl1	95.18(11)	O4-C3-C2	121.6(8)
Cl2-Ti1-Cl1	94.93(10)	C3-O4-Ti1	132.2(6)
Cl2-Ti1-Cl3	99.54(13)	C1-O2-Ti1	133.9(5)
O2-Ti1-Cl1	84.0(2)	C1-C2-C3	115.3(9)
O2-Ti1-Cl4	84.8(2)	O2-Ti1-Cl2	170.8(2)
O2-Ti1-Cl3	89.64(19)	O2-Ti1-O4	79.7(3)

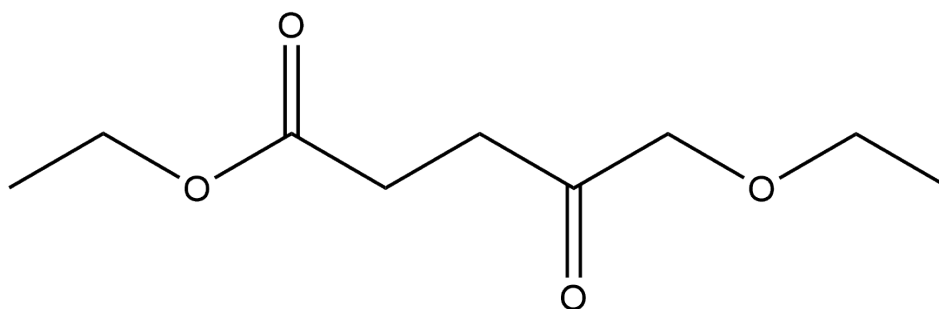


Figure 37: Chemical structure of diethyl succinate

monomeric species with one malonate bidentate ligand coordinated, was formed.

The bond lengths for the Ti-Cl bonds can be grouped into two pairs, one where the length is on average 2.30 Å and the other on average 2.22 Å. It is clear from Figure 36 that this is due to the proximity of the oxygen atoms. The chlorine atoms *trans* to the oxygen atoms lie closer to the titanium centre as there is less steric hinderance for the O atoms. It again shows a distorted octahedral geometry with the O-Ti-Cl angle for the *trans* position being 170.8(2)°. Comparing these bond lengths with the structures of the di-ethyl malonate and bis-isopropyl malonate it can be seen that two of the Cl bond lengths are consistent, however, the Cl atoms *trans* to the ketone show differing bond lengths. They range from 2.2217(11) Å to 2.3423(10) Å in the case of the bis-isopropyl malonate, whereas in compound [3] they are equal at 2.300(2) and 2.296(3) Å. The di-ethyl shows the bond lengths at 2.27(2) Å and 2.304(2) Å. This is due to the different R-groups and is related to the stacking effects of the other nearby structures.

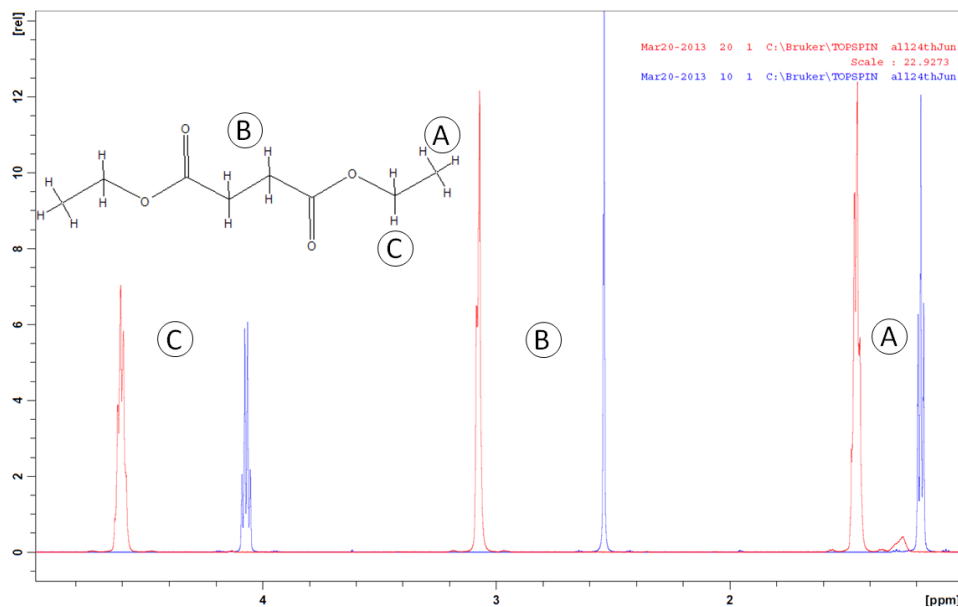
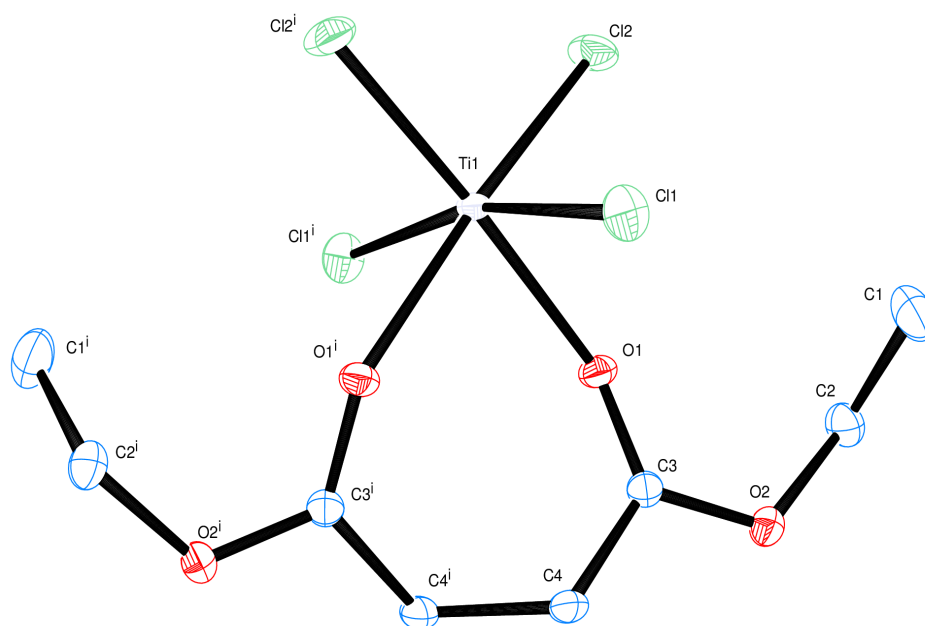


Figure 38: ^1H NMR of diethyl succinate shown in blue compared to tetrachloro(diethyl succinate)-titanium(IV)[4] shown in red

Table 9: Selected bond lengths Å and angles ($^\circ$) for tetrachloro(diethylsuccinate)-titanium(IV)[4]

Ti(1)-O(1)	2.1101(13)	C(3)-C(4)	1.498(2)
Ti(1)-Cl(2)	2.2379(8)	C(4)-C(4)1	1.540(3)
O(2)-C(3)	1.3109(17)		
O(1) ¹ -Ti(1)-O(1)	86.26(7)	O(1)-Ti(1)-Cl(1) ¹	86.39(4)
Cl(1)-Ti(1)-Cl(1)1	166.23(3)	Cl(2)-Ti(1)-Cl(1) ¹	93.12(3)
O(1)-Ti(1)-Cl(2)	88.39(5)	O(1)-Ti(1)-Cl(1)	83.57(4)
C(3)-O(1)-Ti(1)	136.55(10)	Cl(2)-Ti(1)-Cl(1)	95.99(3)
O(1)-Ti(1)-Cl(2) ¹	173.87(3)	O(1)-C(3)-C(4)	124.26(12)
Cl(2)-Ti(1)-Cl(2) ¹	97.10(4)	C(3)-C(4)-C(4) ¹	112.95(12)



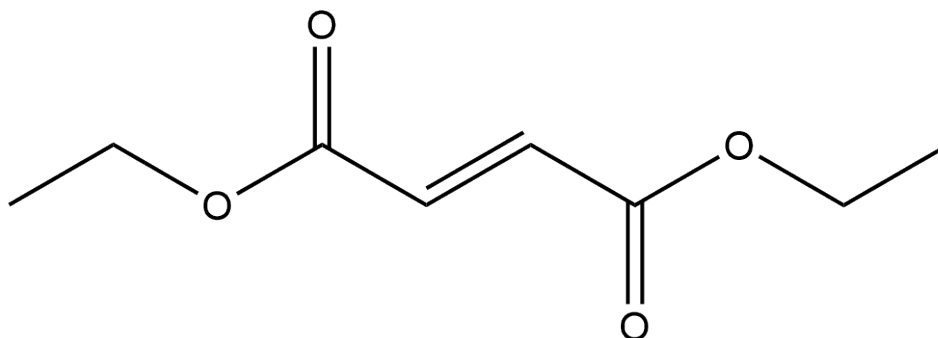
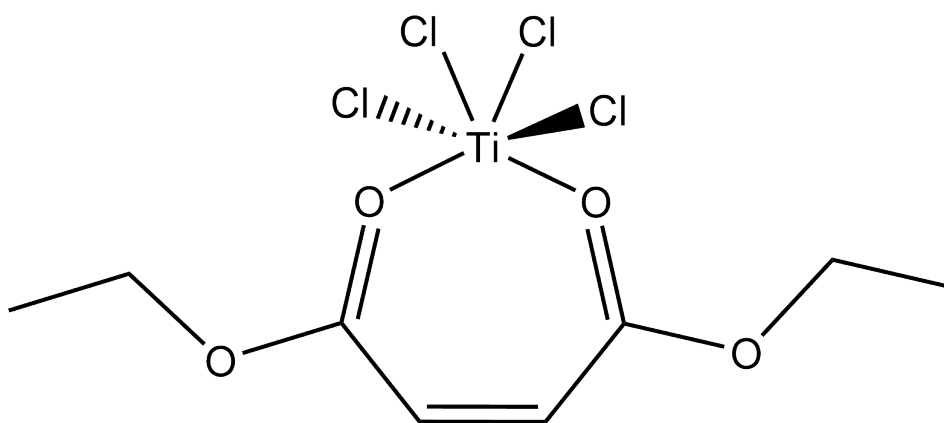
Crystal system	monoclinic
Space group	$C 2/c$
Unit cell dimensions	$a = 16.659(5) \text{ \AA}$ $\alpha = 90.000(5)^\circ$ $b = 8.542(5) \text{ \AA}$ $\beta = 98.836(5)^\circ$ $c = 10.371(5) \text{ \AA}$ $\gamma = 90.000(5)^\circ$

Figure 39: Crystal structure of tetrachloro(diethyl succinate)-titanium(IV)[4]

3.3.5 *Synthesis of tetrachloro(diethyl succinate)-titanium(IV) [4]*

To consider similar ligands with di-ester groups diethyl succinate was reacted with TiCl_4 . Diethyl succinate has 3 bridging carbons between the ester groups as opposed to the 2 bridging carbons of the malonate as shown in Figure 37. The reaction of the TiCl_4 with diethyl succinate proceeded in the same way as those with malonates forming a yellow solid product [4]. Compound [4] was analysed by elemental analysis and found to match the calculated results for the same predicted compound. Crystals suitable for single X-ray diffraction were grown from a solution of dichloromethane layered with hexane.

The ^1H NMR, shown in Figure 38, with peaks for [4] indicated in red are overlaid above the spectrum for pure diethyl succinate for comparison. The 3 peaks representing protons **A**, **B** and **C** were observed at 1.0 ppm, 2.55 ppm and 4.05 ppm. Protons **A** are furthest from the ester group so have the lowest chemical shift, they also have the lowest change in chemical shift as they are furthest from the titanium centre when coordinated. The shift on coordination is 0.27 ppm which for a terminal CH_3 is a large shift. Protons **C** correspond to the CH_2 group for a terminal CH_3 bonded to the ester oxygen, and hence this peak is shifted by 0.5 ppm upon coordination. Protons **B** corresponding to the two CH_2 groups which are bridging the two ester groups and are shifted by 0.5 ppm clearly indicating the coordination of TiCl_4 to the ligand.

Figure 40: Structure of *cis*-C₂H₂(CO₂CH₂CH₃)₂Figure 41: Structure of [*Cis* - C₂H₂(CO₂CH₂CH₃)₂TiCl₄]

The crystal structure for compound [4] is shown in Figure 39 along with the bond angles and distances shown in Table 9. A monomeric structure similar to compounds [1] and [2] was formed with the titanium centre bonded to the two ester groups and the four chlorine atoms. The main difference to compounds [1] and [2] which incorporates the malonate, is a greater O-Ti-O bond angle (86°), which is due to [4] having a 7 membered ring formed from coordination of the succinate ligand with 4 carbons, 2 oxygens and 1 titanium atom. The angle is still smaller than would be expected for a 7 membered ring due to the strong electronegativity of the chlorine atoms. This compound therefore likely to be strained and more unstable than the malonate structure.

Table 10: Bond angle data comparing Kokkonen's structure to the structure obtained through this work

	Kakkonen structure	Compound [4]
	angle [°]	angle [°]
O-Ti-O	81	86
Ti-O-C ₃	145	136
O-C ₃ -C ₄	126	124
C ₃ -C ₄ -C ₄ ⁱ	129	113

Kakkonen *et al*¹ synthesised a similar molecule that was derived from *cis*-C₂H₂(CO₂CH₂CH₃)₂ (shown in Figure 40) which had an alkene group bridging the two ester groups as shown in Figure 41. The internal angles of the structure reported by Kakkonen *et al* are shown in Table 10 and compared with the internal angles observed in compound [4]. A smaller O-Ti-O angle of 81° (compared to 86°) was observed. The alkene bond forces the C₃-C₄-C₄ⁱ angle out to 129° as expected and there is also an increase in the Ti-O-C angle. This is likely to be due to the ligand being more planar than the succinate in compound [4] and hence the alkene stabilises a more planar structure.

3.3.6 Synthesis of tris titanium tetrachloro di-glyceroltribenzoate [5]

Having synthesised many TiCl₄ diester complexes to show how TiCl₄ coordinated to the ligands it was important to relate this back to the industrial plant. The diester ligands represented the glycerol end of the oil in a simple fashion. Reactions of TiCl₄ with the oil directly yielded an insoluble black polymer like material of which analysis proved challenging at a molecular level. Glycerol benzoate was therefore used as it has the same glycerol group as the oil, but

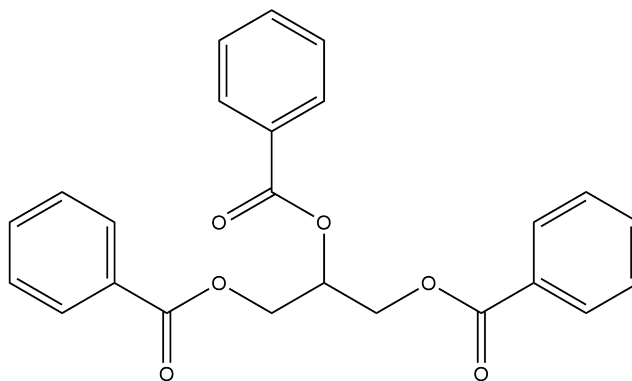


Figure 42: Structure of glycerol tribenzoate.

instead of long chained hydrocarbons it has three benzene groups, as shown in Figure 42.

Glycerol benzoate was reacted with excess TiCl_4 under Schlenk conditions in hexane. Since glycerol benzoate was poorly soluble in hexane, it was added as a solid, not dropwise as before. The reaction was not as fast as the reactions previously described involving malonates and succinate due to the solid nature of the starting material. However, after two hours a yellow product, compound [5] had formed, which was washed with hexane and dried *in vacuo*. Re-crystallisation was attempted by layering with hexane after dissolving in dichloromethane however, no crystals were observed. Crystals suitable for single crystal X-ray crystallography were grown by making a concentrated solution of [5] in dichloromethane and cooling to -10°C for 1 month.

The ^1H NMR spectrum for glycerol tribenzoate is very interesting before the addition of any metal chloride. The spectra for neat glycerol tribenzoate and compound [5] (TiCl_4 coordinated to glycerol tribenzoate) are shown in Figure 43. The figure shows

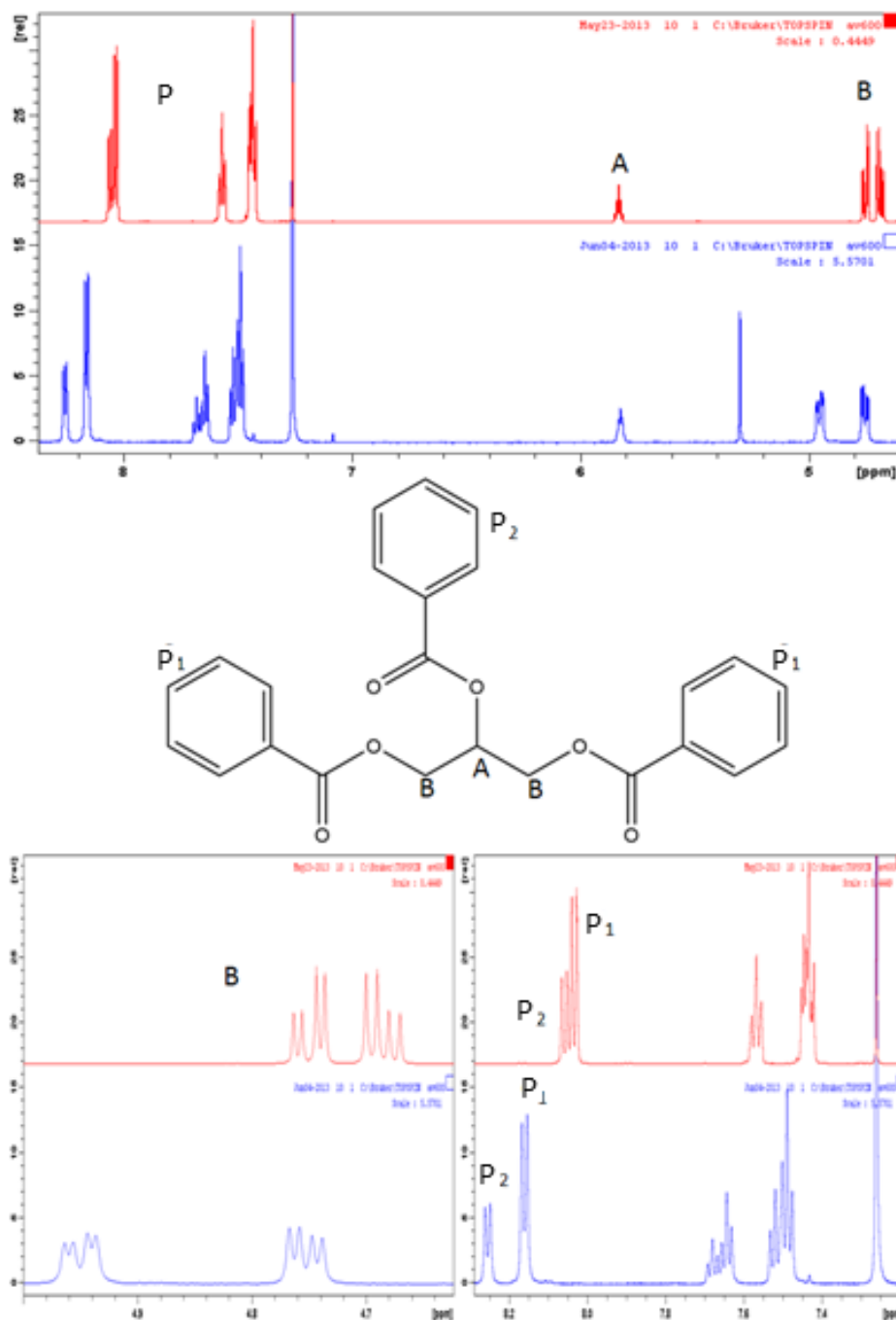
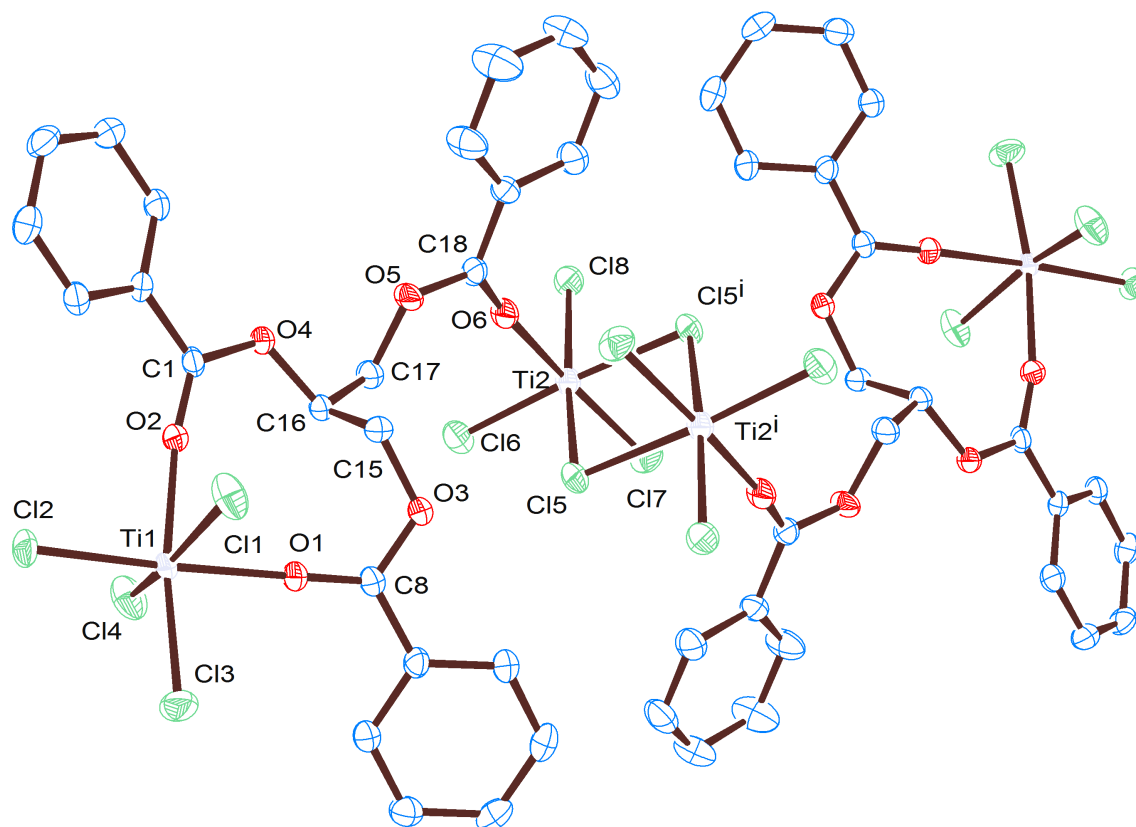


Figure 43: ^1H NMR spectra of glycerol tribenzoate (red) and compound [5] (blue). The top spectra shows the entire range where peaks are present with labels to show where the protons are on the molecule. The bottom two spectra show areas B and P zoomed in to show coordination shifts.



Crystal System	triclinic	
Space group	$P-1$	
Unit cell dimensions	$a = 9.9955(3) \text{ \AA}$	$\alpha = 71.868(2)^\circ$
	$b = 13.9772(3) \text{ \AA}$	$\beta = 76.307(2)^\circ$
	$c = 14.4644(4) \text{ \AA}$	$\gamma = 77.073(2)^\circ$

Figure 44: Crystal structure of [5]. Two dichloromethane molecules were observed in the unit cell but have been removed for clarity

the complexity of the spectra for neat glycerol tribenzoate in red. There are two sets of doublet of doublets at around 4.7 ppm, where eight peaks are observed because the two protons on carbon **B** are not equivalent and therefore couple to each other and to proton **A**. The protons around the benzene ring are also interesting as **C**₁ and **C**₂ are not equivalent due to the nature of the glycerol centre, this is shown clearly for the *ortho*-phenyl protons observed at 8.05 ppm (see in the bottom right spectra of Figure 43).

The ¹H NMR spectrum for compound [5] where glycerol tribenzoate is coordinated to TiCl₄ shows shifts for the protons on the benzene ring (**C**) and the CH₂ group (**B**) of the glycerol. One of the doublet of doublets shifts by 0.07 ppm downfield, the other doublet of doublet at 4.7 ppm shifts by 0.2 ppm. These different shifts show how the two hydrogens are in a different environment and by studying the crystal structure, the hydrogens are closer to the titanium centre causing a greater shift. The benzyl peaks also shift by between 0.05 ppm and 0.2 ppm depending on the proton and whether it is attached to **C**₁ and **C**₂ rings. Coordination to TiCl₄ increases the gap between the peaks for groups **C**₁ and **C**₂ for the meta and para protons which are now observed at 8.15 ppm and 8.25 ppm.

The ¹³C {¹H} NMR shows shifts for the various groups once coordination to TiCl₄ takes place. The C=O peaks shift upfield from 174 ppm to 168 ppm, which is due to the dative bond of the ketone to the titanium centre reducing the electron density around the carbon. The benzene peaks do not shift, however, the glycerol

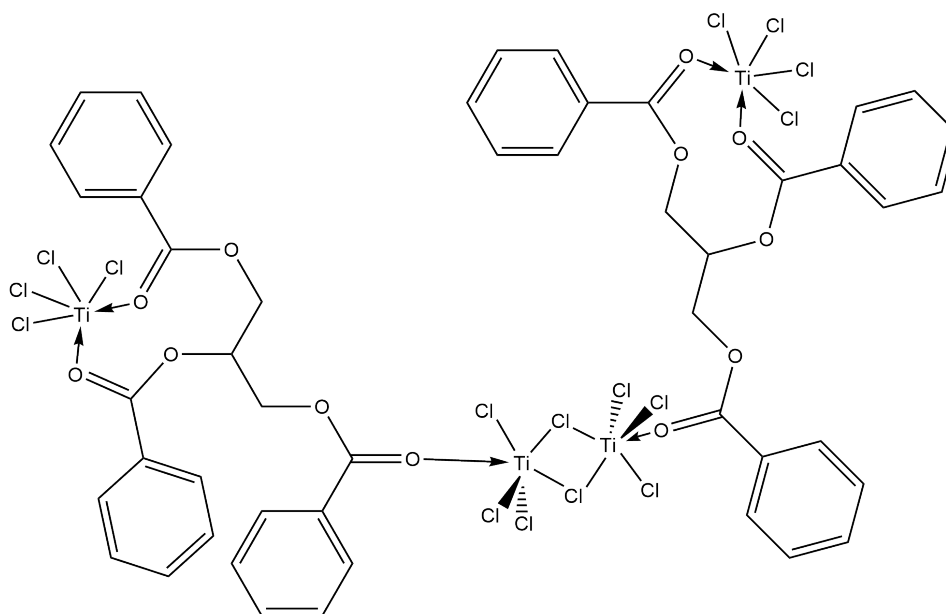


Figure 45: Chemical structure of compound **5** shown as a simple chemical structure to aid understanding of bonding positions

peaks corresponding to carbon **B** at 68 ppm and **A** at 76 ppm shift to 64 ppm for **B** and 72 ppm for **A**. Which is due to the ester oxygen donating electron density away from the central glycerol molecule towards the ketone on coordination to TiCl_4 .

Compound [**5**] was analysed by single crystal X-ray crystallography the results of which are shown in Figure 44 and selected bonds and angles given in Table 11. The chemical structure of compound [**5**] is shown again in Figure 45 for clarity as the structure is hard to visualise in Figure 44. The structure shows two environments for compound [**5**] for the TiCl_4 bound to the glycerol tribenzoate. The first observed environment is around $\text{Ti}(1)$ where the titanium is bonded to four chlorine atoms and also to two ketones of the glycerol tribenzoate ligand as observed for the malonate structures [**1-3**]. The bond distances and angles observed around this titanium centre which adopts a distorted

Table 11: Selected bond lengths Å and angles (°) for compound [5]

Ti1-Cl2	2.2235(8)	O6-C18	1.239(3)
Ti1-Cl3	2.2259(9)	O5-C18	1.311(3)
Ti1-Cl1	2.2938(8)	O5-C17	1.460(3)
Ti1-Cl4	2.2756(9)	C17-C16	1.506(4)
Ti1-O1	2.1010(19)	C16-C15	1.533(4)
Ti1-O2	2.123(2)	O3-C15	1.452(3)
Ti2-Cl8	2.2301(8)	O4-C16	1.453(3)
Ti2-Cl5	2.5000(8)	O4-C1	1.331(3)
Ti2-Cl7	2.2329(8)	O3-C8	1.329(3)
Ti2-Cl6	2.2186(9)	O1-C8	1.227(3)
Ti2-O6	2.020(2)	O2-C1	1.229(3)
<hr/>			
Cl3-Ti1-Cl2	94.63(3)	C15-C16-O4	108.5(2)
Cl1-Ti1-Cl2	93.61(3)	C17-C16-O4	106.3(2)
Cl1-Ti1-Cl3	96.02(4)	C15-C16-C17	112.7(2)
Cl4-Ti1-Cl1	162.38(4)	C16-C17-O5	106.6(2)
O1-Ti1-Cl2	177.38(6)	C18-O5-C17	119.4(2)
O1-Ti1-Cl3	87.97(6)	O6-C18-O5	121.1(3)
O1-Ti1-Cl1	85.85(6)	O6-Ti2-Cl8	88.69(6)
O1-Ti1-Cl4	84.49(6)	O6-Ti2-Cl5	82.68(6)
O2-Ti1-O1	83.60(8)	O6-Ti2-Cl7	171.72(7)
C8-O1-Ti1	170.7(2)	O6-Ti2-Cl6	90.13(6)
C1-O2-Ti1	164.30(19)	O6-Ti2-Cl5i	84.63(6)
O2-C1-O4	121.9(2)	Cl7-Ti2-Cl8	96.57(3)
O1-C8-O3	121.1(3)	Cl6-Ti2-Cl8	98.35(3)
C8-O3-C15	116.1(2)	Cl5-Ti2-Cl8	167.70(4)
C1-O4-C16	117.4(2)	Cl5i-Ti2-Cl8	92.11(3)
C16-C15-O3	109.7(2)	Cl5i-Ti2-Cl5	78.41(3)

octahedral coordination geometry are all similar to those observed for compound [3]. The bridging atoms between the two ketone groups are more difficult to compare with previous structures, the backbone is longer and the ester oxygen atoms form part of the backbone. The major difference this has caused to the geometry around the titanium centre is an increase in the O-Ti-O angle from $79.7(3)^\circ$ in [3] to $83.60(8)^\circ$ for [5]. This reduces the distortion for the octahedral geometry as the oxygen atoms are forced apart by the larger backbone which compensates for the stronger electronegativity of the Cl atoms.

Glycerol tribenzoate contains 3 ester groups as opposed to the 2 ester groups shown in the malonates. This thesis has shown that a diester binds strongly to TiCl_4 in an octahedral geometry. This third ester group complicates the structure. The titanium centre is oxophilic therefore each ketone group is going to be involved in the bonding to the titanium centre in some way. Ti(1) binds as seen for compound [1-4], however, Ti(2) binds in a different fashion. Instead of a second ketone group from another glycerol tribenzoate molecule binding to the Ti centre a dimeric species is formed. This dative interaction from two different ketones to different titanium centres results in a Cl bridged dimer which has been reported before. Gau *et al* took the simple reaction of 2-propanol of TiCl_4 to give a simple Ti_2Cl_8 dimer as shown in Figure 46.¹⁰³ The crystal data from this study matches the data observed for compound [5]. The bridging Ti-Cl bond of $2.5000(8) \text{ \AA}$ is longer than the terminal Ti-Cl bond distances observed of on average 2.25 \AA . These are a good match to the Gau structure which were between $2.48\text{-}2.41 \text{ \AA}$.

The Ti-O bond length is shorter than Gau's bond length reported at 1.700(5) Å, with the Ti-O bond length for [5] being 2.020(2)Å. This is different as we are comparing an alcohol bonding to that of a ketone, the alcohol forms a stronger bond possibly due to hydrogen bonding of the H atom. Gau reported a further step in the reaction which further stabilises the product by the O-H hydrogen bonding to one of the Cl atoms on the titanium.

3.3.7 Synthesis of tetrachloro(acac)-titanium(IV) [6]

The acac ligand derived from acacH is a commonly used inorganic ligand as it is facile to remove the hydrogen bound to the bridging carbon between the two ketones. A simple search on the Cambridge structural database shows over 5000 crystal structures published with the acac ligand present. Searching for acac coordinated to titanium centres produces 70 structures showing how commonly the system has been used compared to malonates. There are three reported structures of titanium acac complexes with two or more chlorines.^{104 105 99}

Cox *et al*¹⁰⁴ reported the reaction between TiCl₄ and acacH to give a structure where two acac groups have coordinated to the metal centre with the two remaining chlorine atoms appearing *trans* to each other. Ferguson *et al*⁹⁹ reported the *cis* structure in 2001 when reacting TiCl₄ and acacH, it was believed to be *cis* previously but not proven through crystallography until 2001. The *cis* structure with two acac groups was synthesised with a three fold excess of acacH. When molar equivalents of acacH and TiCl₄ are used, a dimer with two titanium centres with one acac group

Figure 46: Scheme to show the different reported reactions of TiCl_4 and acacH with compound [6] shown on the final row

Reagents		Reaction conditions	Structure
TiCl_4	Excess acacH	Room temperature and pressure in benzene	
TiCl_4	Excess acacH	20 minute reflux in toluene	
TiCl_4	acacH	Room temperature and pressure in THF	
TiCl_4	acacH	Room temperature and pressure in DCM	
Excess TiCl_4	acacH	Room temperature and pressure in DCM	

each results.¹⁰⁵ This experiment was repeated in this project to ensure the same product was observed when an excess of TiCl_4 was used to mimic the conditions in the plant. A summary of the reaction schemes for previous studies are shown in Figure 46.

An excess of TiCl_4 was reacted with acacH and stirred at room temperature for 2 hrs. An orange precipitate was formed immediately and this precipitate was washed and dried *in vacuo*. The ^1H NMR spectrum of the orange solid was recorded in deuterated chloroform and the product was crystallised by dissolving in dichloromethane and layering with hexane. This afforded red crystals similar to those reported by Serpone *et al.*¹⁰⁵ The unit cell of the crystals were obtained and found to correspond to $a = 8.31 \text{ \AA}$, $b = 10.69 \text{ \AA}$ and $c = 10.38 \text{ \AA}$, with angles of 90° , 94° and 90° . The unit cell shows a good agreement to the structure already reported so the full structure was not obtained. Therefore when an excess of TiCl_4 is reacted with TiCl_4 it can be concluded that a Cl bridged dimer is formed.

3.4 CONCLUSION

This chapter has looked into the reactions of TiCl_4 with ester groups. The ester group is a good equivalent to the more complicated glycerol group observed at one end of the soya oil molecule. Therefore this chapter has given information on how soya oil will react with TiCl_4 when used in industry. Glycerol tribenzoate was also studied to ensure the information gathered could be compared to the glycerol end of the oil.

This chapter has shown that the diester binds coordinatively to the titanium centre forming an octahedral complex with none of the chlorine atoms having been lost. It showed that the R group on the malonate was not important and therefore, long chained hydrocarbons as seen in soya oil, could be present and the same chemistry would be observed. This was key as working with C₁₈ chains provides many difficulties with purification and solubility. The reaction with glycerol tribenzoate confirmed that the diester is a good equivalent to the glycerol end as the bonding observed was similar. There were two types of bonding in the glycerol tribenzoate due to the three ketone groups on the molecule. However, even in the binuclear titanium centre no chlorine atoms were lost from either titanium centre.

All compounds synthesised in this chapter (except the acacH which does not relate to the glycerol) show coordination of the ester groups to the titanium centre without the loss of chlorine atoms. This shows that in the right conditions the reaction could be reversible releasing TiCl₄ back into the mixture. This is key for the industrial purification of TiCl₄ as the amount of TiCl₄ is in large excess to the VOCl₃. Therefore, in synthesising novel compounds this chapter has provided a mechanism to understand how the soya oil can react with the TiCl₄, coordinate to it and not be broken down. In the following chapter the reaction of the same esters with VOCl₃ will be studied to investigate what differences can be observed at a molecular level.

3.5 EXPERIMENTAL

All reactions were carried out under argon obtained from BOC in anhydrous solvents using standard Schlenk techniques. The solvents were dried using a stills system. Anhydrous TiCl_4 and malonate starting materials were purchased from Sigma Aldrich; all were used without further purification

^1H and $^{13}\text{C}\{^1\text{H}\}$ NMR spectra were obtained on a Bruker AV-600 Mz spectrometer, operating at 295 K and 600.13 MHz (^1H). Signals are reported relative to SiMe_4 ($\delta = 0.00$ ppm) and the following abbreviations are used s (singlet), d (doublet), t (triplet), q (quartet), m (multiplet), b (broad). Deuterated CDCl_3 was obtained from GOSS Scientific and was dried and degassed over 3 Å molecular sieves.

3.5.1 *Synthesis of tetrachloro(diethyl malonate)-titanium(IV) [1]*

Diethyl malonate (0.5 cm^3 , 3.3 mmol) was added dropwise to 1 cm^3 of TiCl_4 (9.1 mmol) in 50 cm^3 of hexane and stirred under nitrogen for 2 h. An excess of TiCl_4 was used as excess TiCl_4 is facile to remove from the reaction after completion. A yellow precipitate was immediately formed and the reaction was stirred for a further 2 h to ensure a complete reaction. The yellow precipitate was filtered and washed three times with 20 cm^3 hexane and dried *in vacuo* to afford complex [1] in good yield (0.9 g, 78%). Some of the product was re-dissolved in 5 cm^3 of dichloromethane and layered with 15 cm^3 of hexane. Crystals immediately began forming and after 12 h a number of large crystals were formed. ^1H NMR (CDCl_3): δ 4.76

(b, 4H, -CH₂), δ 4.05 (s, 2H, -CH₂), δ 1.47 (t, 6H, -CH₃, J = 7.08 Hz). ¹³C {¹H} NMR (CDCl₃): δ 14.0 (-CH₃), 37.7 (-CH₂), 68.0 (-OCH₂), 173.4 (C=O). Analysis calculated for TiCl₄C₇O₄H₁₂: C, 24.03; H, 3.46. Found: C, 23.81; H, 3.45.

3.5.2 Synthesis of tetrachloro(bis isopropyl malonate)-titanium(IV) [2]

The same synthetic procedure was followed as for complex [1] and yellow crystals were again formed from a dichloromethane solution layered with hexane. A good yield was isolated (0.8g, 63%). The molecular structure of [2] was determined by X-ray crystallography. ¹H NMR (CDCl₃): δ 5.46 (b, 2H, -CH), δ 3.95 (b, 2H, -CH₂), δ 1.47 (d, 12H, -CH₃, J = 6.20 Hz). ¹³C {¹H} NMR (CDCl₃): δ 21.7 (-CH₃), 38.0 (-CH₂), 54.8 (-OCH₂), 172 (C = O). Analysis calculated for TiCl₄C₉O₄H₁₆: C, 28.60; H, 4.27. Found: C, 26.03; H, 3.45.

3.5.3 Synthesis of bis t-Bu Malonate-titanium(IV) chloride

Bis-tBu malonate (0.5cm³, 2.2 mmol) was added dropwise to 2 cm³ of TiCl₄ (18.2 mmol) in 50 cm³ of hexane and stirred under nitrogen for 2 h. A yellow precipitate formed immediately, and the reaction stirred for 2 h to ensure a complete reaction. The yellow precipitate was filtered off and washed 3 times with 10 cm³ hexane and dried *in vacuo*, to give a good yield (3.01g, 75%). As the solid did not dissolve in dichloromethane, hexane or any other suitable solvent, no NMR data could be recorded. A crystal suitable for X-ray analysis could not be grown.

3.5.4 *Synthesis of tetrachloro(dibenzyl malonate)-titanium(IV) [3]*

The same synthetic procedure was followed as for complex [1] and yellow crystals were again formed from a solution layered with hexane. Again, a good yield was recovered (1.2g, 77%). The molecular structure of [3] was determined by X-ray crystallography. ^1H NMR (CDCl_3): δ 7.5 (m, 10H, Ph), δ 5.5 (b, 4H, $-\text{CH}_2$), δ 4.0 (b, 2H, $-\text{CH}_2$). ^{13}C $\{^1\text{H}\}$ NMR (CDCl_3) 38.0 ($-\text{CH}_2$), 73.0 ($-\text{OCH}_2$), 129-130 (-Ph). Analysis calculated for $\text{TiCl}_4\text{C}_{15}\text{O}_4\text{H}_{12}$: C, 43.08; H, 3.40. Found: C, 43.24; H, 3.40.

3.5.5 *Synthesis of tetrachloro(diethyl succinate)-titanium(IV) [4]*

Diethyl succinate (0.5cm^3 , 3.3 mmol) was added dropwise to 2cm^3 of TiCl_4 (18.2 mmol) in 50cm^3 of hexane and stirred under nitrogen for 2 h. A yellow precipitate formed immediately, the reaction was stirred for 2 h to ensure a complete reaction. The yellow precipitate was filtered off and washed three times with 10cm^3 hexane and dried *in vacuo*, to afford complex [4] in a good yield (0.9 g, 75%). The product was re-dissolved in 5cm^3 dichloromethane and layered with 10cm^3 hexane. Small crystals formed overnight and were large enough for the crystal structure to be obtained. ^1H NMR (CDCl_3): δ 4.61 (q, 4H, $-\text{CH}_2$, $J=14.3\text{ Hz}$), δ 3.08 (s, 4H, $-\text{CH}_2$), δ 1.46 (t, 6H, $-\text{CH}_3$, $J=14\text{ Hz}$). ^{13}C $\{^1\text{H}\}$ NMR (CDCl_3): δ 14.1 ($-\text{CH}_3$), 29.2 ($-\text{CH}_2\text{CH}_2$), 66.2 ($-\text{OCH}_2$), 179 (C = O). Analysis calculated for $\text{TiCl}_4\text{C}_8\text{O}_4\text{H}_{14}$: C, 26.4; H, 3.88. Found: C, 26.41; H, 3.40.

3.5.6 Synthesis of glycerol tribenzoate $TiCl_4$ [5]

Glycerol Tribenzoate (0.5 g, 1.2 mmol) was added gradually to 2 cm³ of $TiCl_4$ (18.2 mmol) in 50 cm³ of hexane and stirred under nitrogen for 2 h. A yellow product was formed, filtered with hexane and dried *in vacuo* to afford [5] in a good yield (1.6g 75%). Recrystallisation was attempted by layering dichloromethane with hexane but the solid crashed out of solution rapidly affording no suitable crystals. Crystallisation was then attempted by dissolving the yellow solid in a minimum amount of dichloromethane and cooling to -10 °C. After 1 month X-ray suitable crystals were grown. ¹H NMR ($CDCl_3$): δ 8.27 (d, 2H, *o*-CH, $J=7.7$ Hz), 8.17 (d, 4H, *o*-CH, $J=7.7$ Hz), 7.69(t, 1H, *p*-CH)(7.7 Hz), 7.65 (t, 1H, *p*-CH, $J=7.7$ Hz), 7.53 (t, 1H, *m*-CH, $J=7.7$ Hz), 7.50(t, 1H, *m*-CH, $J=7.7$ Hz), 5.82 (quin, 1H - OCH, $J=5.1$ Hz), 4.98(dd, 2H, -CH₂, $J = 4.8$ Hz, 12.3Hz), 4.75(dd, 2H, -C H₂, $J=4.8$ Hz, 12.3 Hz). ¹³C {¹H} NMR ($CDCl_3$): 63.54 (CH₂), 72.23(CH), 129 (*o*-CH), 131 (*p*-CH), 135 (*m*-CH), 168 (C = O). Analysis calculated for $Ti_4Cl_{16}C_{48}O_{12}H_{46}$: C, 36.64; H, 2.95. Found: C, 37.62; H, 2.98.

The crystal structure was determined using single crystal X-ray diffraction.

3.5.7 Synthesis of tetrachloro(acac)-titanium(IV) [6]

AcacH (0.5cm³, 4.87 mmol) was added dropwise to 2 cm³ of $TiCl_4$ (18.2 mmol) in 40 cm³ of hexane and stirred under nitrogen for 2 h. An orange precipitate formed immediately, and the reaction stirred for 2 h to ensure a complete reaction. The yellow precipitate was filtered off and washed three times with 10 cm³ hexane and dried *in*

vacuo, to afford the complex [TiCl₃(acac)] in a good yield (0.8g, 65%). Some of the product was re-dissolved in 3 cm³ dichloromethane and layered with 10 cm³ hexane. Large crystals formed overnight and were analysed using single X-ray Crystallography. ¹H NMR (CDCl₃): δ 6.00 (s, 1H, CH), δ 2.17 (s, 6H, CH₃). ¹³C {¹H} NMR (CDCl₃): δ 187 (-C=O), δ 109 (CH), δ 25 (CH₃).

REACTIONS OF VANADIUM CHLORIDES WITH DIESTERS

4.1 VANADIUM OXYCHLORIDE COMPLEXES

In the previous chapter the mechanism for the reaction of TiCl_4 with ketones and esters were established. This chapter investigates how VOCl_3 reacts differently with the esters and ketones, and studies how this could explain a mechanism for the removal of VOCl_3 from TiCl_4 in the industrial plant to make TiO_2 .

With the exception of the $[\text{TiCl}_2(\text{acac})_2]$ and the $[\text{TiCl}_3\text{acac}]$ reaction, all the TiCl_4 reactions proceeded to form coordinated complexes without the loss of any chlorine atoms. This work was initiated to investigate differences between the two, if VOCl_3 were to form similar products it would give us no information on the difference in reactivity.,

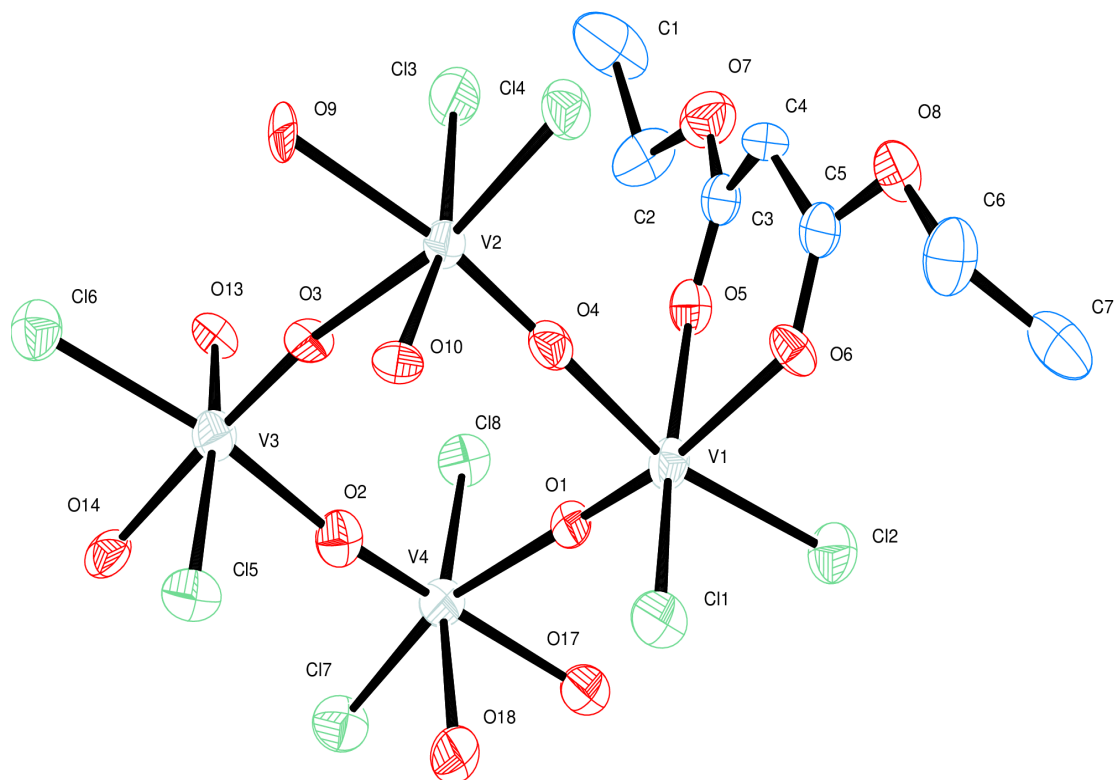
The titanium chloride complexes formed interesting coordination complexes with malonates and other diesters giving highly moisture sensitive but clean products. The VOCl_3 complexes are much more difficult to isolate and tend to form oily products. The differences between vanadium and titanium will be exploited in this investigation.

4.1.1 Reaction of VOCl_3 with diethyl malonate [7]

The reaction to yield complex [7] was carried out in a similar way to the reactions with TiCl_4 but using an excess of VOCl_3 . The product [7] was a dark red/purple precipitate which formed an oil during the 2 hours of the experiment. The analysis was therefore carried out quickly and the crystals were formed by layering a dichloromethane solution of the oil with hexane. The crystals did not form quickly and cleanly as in the case of the titanium crystals, however, they grew over the course of a few weeks and were suitable for single crystal X-ray crystallography.

The ^1H NMR of [7] showed shifts of around 0.2 ppm for all three of the peaks in the spectrum, this indicates coordination of the ligand to vanadium as previously observed for titanium. The peaks were broader than for the titanium complex because vanadium (IV) is paramagnetic. The integrals of the peaks show that there has been no loss of protons during the experiment. However, as the ^1H NMR can only give us information about the organic species it does not elucidate the coordination geometry around the vanadium centre.

The crystal structure was obtained for compound [7], however after comparing the solved structure to the Cambridge structural database (CSD) it was found that the structure had already been reported. The structure of [7] was tetrameric with four vanadium centres and four malonate ligands. The unit cell obtained for [7] was different to that reported in the previous study and therefore the full structure was obtained.



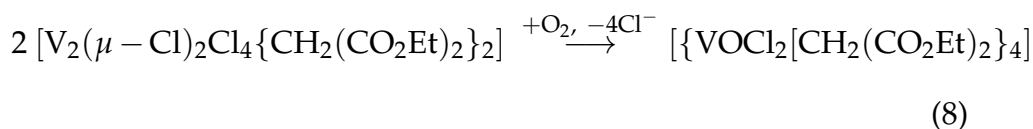
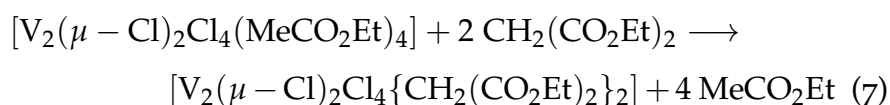
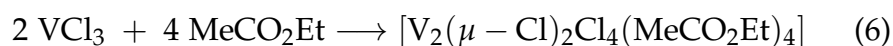
Crystal System	triclinic	
Space group	P-1	
Unit cell dimensions	$a = 9.9955(3)\text{\AA}$	$\alpha = 71.868(2)^\circ$
	$126\ b = 13.9772(3)\text{\AA}$	$\beta = 76.307(2)^\circ$
	$129\ c = 14.4644(4)\text{\AA}$	$\gamma = 77.073(2)^\circ$

Figure 47: Crystal structure of [7], one malonate ligand is shown for clarity, O17 and O18 are part of a malonate as are O13, O14, O9 and O10.

Table 12: Selected bond lengths Å and angles (°) for compound [7]

O(4)-V(1)	2.021(11)	C(3)-O(5)	1.222(19)
O(1)-V(1)	1.622(10)	C(5)-O(6)	1.248(19)
O(6)-V(1)	2.157(11)	C(3)-C(4)	1.44(2)
O(5)-V(1)	2.097(11)	C(4)-C(5)	1.49(2)
Cl(1)-V(1)	2.311(5)	O(4)-V(2)	1.645(11)
Cl(2)-V(1)	2.313(5)	O(1)-V(4)	2.029(10)
<hr/>			
O(5)-C(3)-C(4)	126.5(16)	O(4)-V(1)-O(6)	79.5(4)
C(3)-C(4)-C(5)	117.7(16)	O(5)-V(1)-O(6)	80.3(4)
O(6)-C(5)-C(4)	122.9(16)	O(1)-V(1)-Cl(1)	97.5(4)
V(2)-O(4)-V(1)	174.8(7)	O(4)-V(1)-Cl(1)	90.7(3)
V(1)-O(1)-V(4)	172.1(6)	O(5)-V(1)-Cl(1)	167.3(4)
C(3)-O(5)-V(1)	132.3(12)	O(6)-V(1)-Cl(1)	87.7(3)
C(5)-O(6)-V(1)	132.0(11)	O(1)-V(1)-Cl(2)	99.9(4)
O(1)-V(1)-O(4)	93.8(5)	O(4)-V(1)-Cl(2)	165.0(3)
O(1)-V(1)-O(5)	94.0(5)	O(5)-V(1)-Cl(2)	89.9(3)
O(4)-V(1)-O(5)	83.1(4)	O(6)-V(1)-Cl(2)	86.3(3)
O(1)-V(1)-O(6)	171.6(5)	Cl(1)-V(1)-Cl(2)	93.49(19)

The structure was originally obtained by Sobota *et al.*¹⁰⁶ The compound was synthesised as described in equations 6, 7 and 8. As the equations show the compound was formed by reaction of $[V_2(\mu - Cl)_2Cl_4\{CH_2(CO_2Et)_2\}_2]$ with oxygen. The compound reported by Sobota *et al* resulted due to an accidental addition of oxygen to the crystallisation flask. The compound matches exactly what was seen for the reaction of $VOCl_3$ with diethyl malonate. However, in the reaction reported here the oxygen bridges most likely derive from the $V=O$ bond in the $VOCl_3$ starting material and not from oxygen in the air.



The crystal structure of compound [7] shows the formation of a tetrameric molecule with four bridging oxygens and four vanadium atoms. Each vanadium centre has lost a Cl atom (from $VOCl_3$) and the octahedral and the coordination sphere is filled with a further V-O bond. Therefore, each vanadium has 4 V-O bonds which have lengths of 2.021(11) Å, 1.622(10) Å, 2.157(11) Å and 2.097(11) Å. The two longer bond lengths at 2.157 Å and 2.097 Å are the dative bonds to the malonate ligand which are similar to

the bond lengths observed for the TiCl_4 malonate complexes [1-3]. The other two V-O bond lengths represent the bridging oxygen atoms, which show that the oxygen atom does not sit equidistant between the two vanadium atoms. One bond length is a little shorter but corresponds to the malonate dative bonds observed. The other is closer to the free V=O bond length reported at 1.595\AA ¹⁰⁷ for VOCl_3 . This shows that the original V=O bond in the VOCl_3 is not broken and datively bonds to the other vanadium atom via lone pairs of electrons on the oxygen.

The interesting part of the structure for this project is the fact that a Cl atom is lost when reacted with the malonate which is not the case for TiCl_4 complex. This is likely to be due to the electron deficient nature of the vanadium centre being very oxophilic. The dative V-O bond at $2.021(11)\text{\AA}$ is shorter than the V-Cl bonds at $2.311(5)\text{\AA}$. This shows how the coordination sphere of the oxygen is important in these reactions, and until the oxygen is bound to two other elements it will be reactive when subjected to an electron poor metal centre.

4.1.2 Reaction of VOCl_3 with bis-isopropyl malonate [8]

Bis-isopropyl malonate was reacted with an excess of VOCl_3 to understand what effect a different R-group would have on the resulting complex. A dark red precipitate was formed in a dark solution, the solid was washed with hexane to remove unreacted VOCl_3 . After washing three times as before, the final washing was still red which indicated that the product is likely to be partially soluble in hexane. The red solid [8] was dried *in vacuo*. ^1H NMR

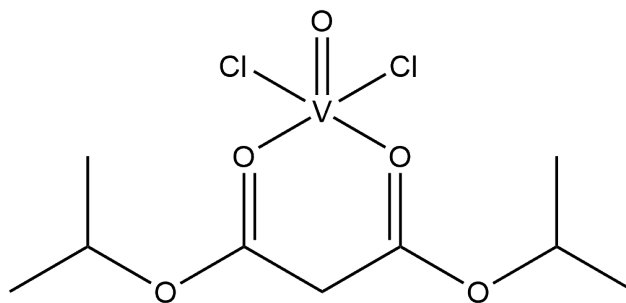


Figure 48: Diagram to show the possible structure of complex [8]

and $^{13}\text{C}\{^1\text{H}\}$ NMR of [8] were recorded in deuterated chloroform and a solution of [8] in dichloromethane was layered with hexane in an attempt to form crystals. Crystals suitable for single X-ray diffraction could not be isolated in this case.

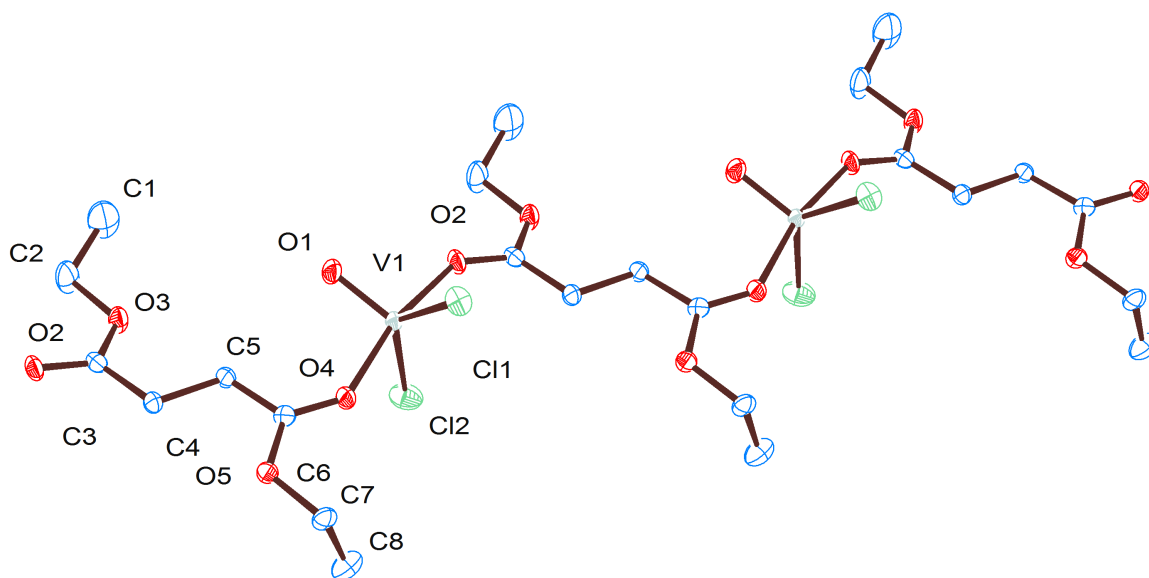
The ^1H NMR of [8] showed a large amount of broadening due to the presence of the vanadium metal and a small shift in the peaks at 5 and 3.4 ppm. These shifts observed were small, and were much less than observed with the TiCl_4 analogue compound [2]. Therefore, it is unclear whether coordination has occurred in this instance. The $^{13}\text{C}\{^1\text{H}\}$ NMR of [8] showed no peak shifts from the starting materials suggesting in this case that no coordination had occurred. A colour change was observed during the reaction suggesting that some sort of reaction did in fact take place. It is likely that the product formed was unstable and decomposed before the NMR could be recorded. It is likely that in this case a similar product to complex 7 was observed as shown in Figure 48. It is likely it could not be formed due to the malonate but did not form the tetramer, it is the difficulty in forming the tetramer that was likely to be the reason the crystal could not be analysed.

4.1.3 Reaction of VOCl_3 with di-ethyl succinate [9]

Diethyl succinate was reacted with VOCl_3 as the extra bridging carbon present in the ligand provides an interesting difference to the malonate. In the case of the titanium, reaction with the succinate was the same as with the malonate, therefore the same reaction with VOCl_3 was studied to see if any difference could be observed. An excess of VOCl_3 was reacted with diethyl succinate and a red product was observed immediately but in this case no precipitate was formed. After removing the solvent *in vacuo* for one hour a red liquid product was isolated. After two weeks at room temperature green crystals [9] had formed, which could be analysed by single crystal X-ray diffraction.

The ^1H and $^{13}\text{C}\{^1\text{H}\}$ of NMR [9] showed small shifts in the positions of the peaks in comparison to the free ligand, but not large shifts as previously observed for the titanium compound. There is obvious broadening of all the peaks and so from the NMR it is difficult to be sure of the coordination but a small shift of approximately 0.1 ppm can be observed. It is not the case that some of the starting material is unreacted as there is clearly only one broad peak for each of the protons.

The molecular structure for compound [9] was determined as shown in Figure 49, along with selected bond distances and angles in Table 13. The structure of [9] is different to another compound isolated in this project. The diethyl succinate acts as a bidentate ligand as seen previously in the case of the other malonates in



Crystal System	monoclinic	
Space group	$P2_1/c$	
Unit cell dimensions	$a = 15.3393(8) \text{ \AA}$	$\alpha = 90^\circ$
	$b = 9.7939(5) \text{ \AA}$	$\beta = 94.664(5)^\circ$
	$c = 8.6842(5) \text{ \AA}$	$\gamma = 90^\circ$

Figure 49: Crystal structure of [9]

Table 13: Selected bond lengths Å and angles (°) for compound [9]

V1-Cl1	2.2855(6)	O2-C3	1.228(2)
V1-Cl2	2.2776(6)	O4-C6	1.237(2)
V1-O1	1.5784(14)	C6-C5	1.492(3)
V1-O4	2.0370(13)	C3-C4	1.487(3)
V1-O2	2.0484(13)	C5-C4	1.529(3)
Cl2-V1-Cl1	131.61(3)	C6-O4-V1	134.71(12)
O1-V1-Cl1	113.25(7)	C3-O2-V1	142.20(13)
O1-V1-Cl2	115.12(7)	O4-C6-O5	121.14(17)
O4-V1-Cl1	87.07(4)	C5-C6-O5	115.30(16)
O4-V1-Cl2	86.73(5)	C5-C6-O4	123.56(17)
O4-V1-O1	98.62(7)	C4-C3-O3	114.73(17)
O2-V1-Cl1	90.51(4)	C4-C3-O2	124.26(17)
O2-V1-Cl2	85.89(4)	C4-C5-C6	115.21(15)
O2-V1-O1	93.39(7)	C5-C4-C3	113.59(16)
O2-V1-O4	167.72(6)		

compounds [1-3,7], but in [9] it binds to two different vanadium centres. The vanadium forms two bonds to ester groups from two different malonate ligands, thus forming a polymer chain. This polymer chain is classed as a one dimensional coordination polymer.

Coordination polymers are metal-ligand complexes that extend indefinitely into one, two or three dimensions via covalent metal-ligand bonding.¹⁰⁸ Coordination polymers are also known as metal organic coordination networks or metal organic frameworks (MOFs). They are thought to have properties suitable for many applications in the same way as zeolites do. There is a great deal of research into using MOFs in catalysis and other applications,^{109 110} and as such is one of the highest activity areas of research currently in chemistry.^{111 112 113}

Due to the extended nature of the research this section will focus on vanadium based coordination polymers. The majority of vanadium containing coordination polymers are in the form of clusters and contain extra metals such as tin¹¹⁴ or silver.¹¹⁵ The first non-cluster vanadium coordination polymer was synthesised by Zhang, *et al*¹¹⁶ with the report of $[\text{VO}(\text{dod})_2]\text{X}_2$ ($\text{X}=\text{Cl}, \text{Br}$; $\text{dod} = 1,4\text{-diazoniabicyclo}[2,2,2]\text{octane-1,4-diacetate}$). The compound forms a 2-dimensional polymer with the vanadium bound to the oxygen in the acetate and the rest of the ligand bridging to the next vanadium. Every four units the polymer forms a square, which makes the polymer into a 2-dimensional lattice.

There have been two reported 1-dimensional coordination polymers containing vanadium, both contain dinuclear vanadium. The first one contains O,O,N-dichelating ligands¹¹⁷ and the second with N,N chelating ligands to stabilise with O bidentate ligands forming the bridge.¹¹⁸ These compounds are similar to the one observed in this thesis, however, they are more stable as they do not have any V-Cl bonds which react when in contact with air.

This thesis reports the first mononuclear vanadium 1-dimensional coordination polymer to be isolated as a single crystal and the structure probed by X-ray diffraction. The vanadium centre in [9] is similar to a $[\text{VOCl}_2(\text{acac})]$ structure described later in this chapter. However, a different arrangement of the ligands is adapted in the second compound. In both compounds a distorted trigonal bipyramidal coordination geometry is adopted but in $[\text{VOCl}_2(\text{acac})]$ the ketone oxygens are *cis* to each other as they come from the same ligand. In compound [9], the ketones are *trans* to each other which causes the formation of the polymer chain. The O-V-O angle in [9] is $167.72(6)^\circ$, and hence distorted from 180° due to polymer formation. Derivation using single crystal X-ray crystallography indicates that the chain is infinite. To discover the actual chain length more complexed polymer techniques would have to be used which are not facile with moisture sensitive materials.

The V-O bond length to the succinate ligand in [9] is on average 2.04 \AA , which represents a dative coordinative bond as seen in the other structures presented in this thesis, and is longer

than the expected terminal V-O bond length of 1.5784(1). It is likely this compound forms this polymer because of the two bridging carbon atoms between the ester groups. When there is one bridging carbon, as in the case of malonate, it coordinates in a chelating fashion with the acac, where both of the ketones lie on the same side of the chain. Whereas with two bridging carbon atoms they can rotate and therefore lie on opposite sides due to steric effects. In the case of the titanium complex, these were overcome and the bidentate ligand bound to a single titanium atom. As shown with the diethyl malonate the vanadium centres are not as stable as monomers and it is this instability which leads to the formation of the more complex polymeric structure.

4.1.4 Reaction of VOCl_3 with glycerol tribenzoate [10]

Glycerol tribenzoate forms a useful link between the esters studied in this chapter and with the soya oil used in industry. Due to this, the reaction of VOCl_3 with glycerol tribenzoate was investigated. An excess of VOCl_3 was used in the reaction to mimic industrial conditions and to aid separation of the experimental products. The reaction was carried out as before at room temperature and stirred for two hours. When the glycerol tribenzoate was added to VOCl_3 (in hexane) the solution darkened to red from orange but the precipitate (glycerol tribenzoate) didn't change colour. The product was washed and dried *in vacuo* and the ^1H NMR of which indicated that the glycerol tribenzoate had not reacted with VOCl_3 , as no shifts were observed and there was not any broadening of the peaks.

As no reaction was observed at room temperature, the reaction was repeated in toluene and refluxed for 15 hours. A red brown solution was observed with formation of a brown precipitate. The brown precipitate was washed with hexane and dried *in vacuo*, yielding a brown oily product [10]. Compound [10] was analysed via ^1H and ^{13}C $\{^1\text{H}\}$ NMR spectroscopy. The ^1H NMR of [10] showed five broad peaks, suggesting that the vanadium is coordinated to the ligand as it has caused paramagnetic broadening, which is most likely due to the presence of V^{4+} . The peaks at 7.50 and 8.05 ppm relate to the protons on the benzyl groups. The integral for the two peaks is 25 which is higher than the expected 15 for a simple adduct of the VOCl_3 with the ligand, which alludes to increased complexity. The peaks at 4.8 and 5.75 ppm correspond well with the peaks observed for the TiCl_4 -glycerol tribenzoate product compound [5]. This suggests that a similar product may have formed with the ketones bound to the vanadium centre. It is likely that there are two ketones bound to each vanadium centre as previously observed and identified as the loss of a Cl atom. However, this could not be confirmed by X-ray crystallography as a single crystal could not be grown.

In the ^1H NMR of [10] there is one further broad peak at 3.9 ppm. This peak has an integral of two and explains why the integral at around 7 ppm was markedly high as it accounts for a further product. This product is methyl benzoate as the peak at 3.9 ppm is a match to the literature value of 3.91 ppm.¹¹⁹ If the methyl benzoate product is separated from glycerol tribenzoate, ethylene glycol dibenzoate is formed. From the literature, peaks observed in

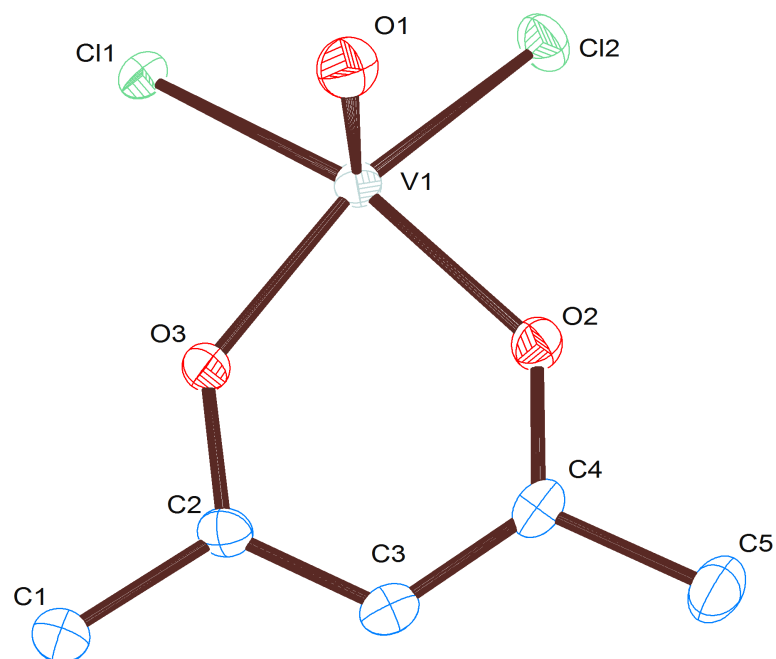
the proton NMR for the ethane protons occur at 4.67 ppm,¹²⁰ which are present in the spectra of [10]. However, due to the broadness of peaks in this spectra a more exact analysis can not be made.

4.1.5 *The reaction of VOCl₃ acacH [11]*

As described earlier for the [TiCl₄(acac)] complex, acac is a well used ligand in inorganic chemistry. Indeed, [VO(acac)₂] is a well known compound¹²¹ that has been used as a precursor for the deposition of thin films.¹²² However, the reaction of VOCl₃ with acacH has not previously been studied, therefore it was carried out to complete the understanding of the different reactions of TiCl₄ and VOCl₃ with diesters and diketones.

Excess VOCl₃ was reacted with acacH and stirred for 2 hours in a nitrogen environment. A dark precipitate in a dark black solution formed immediately but the reaction was allowed to stir for 2 hours to ensure a full reaction. The precipitate was filtered and washed to give a dark purple powder and the ¹H and ¹³C {¹H} NMR were investigated. The product [11] was redissolved in dichloromethane and layered with hexane. After one week small dark black crystals were observed which were suitable for single crystal X-ray crystallography. The crystal structure of [11] is shown in Figure 50 along with selected bond lengths and angles in Table 14.

The ¹H NMR of [11] showed a shift of 0.3 ppm for the peak at around 2.2 ppm from the starting material acacH. AcacH shows



Crystal System	orthorhombic	
Space group	$P2_12_12_1$	
Unit cell dimensions	$a = 8.3503(3) \text{ \AA}$	$\alpha = 90^\circ$
	$b = 13.5046(4) \text{ \AA}$	$\beta = 90^\circ$
	$c = 15.2041(5) \text{ \AA}$	$\gamma = 90^\circ$

Figure 50: Crystal structure of [11]

Table 14: Selected bond lengths Å and angles (°) for compound [11]

V1-Cl1	2.2880(8)	O3-C2	1.290(4)
V1-Cl2	2.2275(9)	O2-C4	1.283(4)
V1-O2	1.918(2)	C2-C3	1.398(4)
V-O3	1.903(2)	C4-C3	1.383(4)
V1-O1	1.569(2)		
<hr/>			
Cl2-V1-Cl1	93.45(3)	O-V1-O2	101.11(10)
O2-V1-Cl1	158.65(7)	O1-V1-O3	100.11(10)
O2-V1-Cl2	88.12(7)	C4-O2-V1	133.0(2)
O3-V1-Cl1	86.65(7)	C2-O3-V1	134.21(19)
O3-V1-Cl2	159.64(7)	C3-C2-O3	121.9(3)
O3-V1-O2	84.62(9)	C3-C4-O2	123.7(3)
O1-V1-Cl1	99.58(9)	C4-C3-C2	121.0(3)
O1-V1-Cl2	99.94(9)		

two further peaks at 3.5 ppm and 5.4 ppm. These peaks represent the hydrogens bonded to the bridging carbon in the acac ligand. When acacH is not coordinated one of the hydrogens can dissociate which changes the shift of the other to give the peak at 5.4 ppm. This is a useful tool in determining coordination as in this structure there is only one further peak at 6.1 ppm. This is clear evidence that one proton from the acacH has been lost indicating coordination to the vanadium centre.

The ^{13}C $\{^1\text{H}\}$ NMR of **[11]** showed one large shift from 55 ppm to 104 ppm. This is for the bridging carbon and demonstrates the formation of a delocalised ring in the acac system when bonded to the metal centre. This again is a clear indication that VOCl_3 is bonded to the acac ligand.

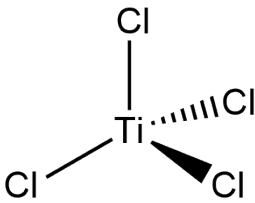
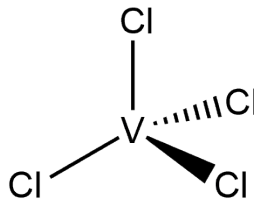
The structure of compound **[11]** shows the acac bound to the vanadium centre *via* the ketone oxygens. The V-O bond lengths were 1.918(2) Å and 1.903(2) Å, smaller than the dative V-O bond lengths observed for the vanadium malonate complex [7] which were on average 2.1 Å. This is caused by the increased electron density given from the ketone oxygen. A proton from C(3) is lost in the reaction and a delocalised system is created between O(3),C(2),C(3),C(4) and O(2) and bond lengths in the ring confirm this. This results in the ligand having a negative charge, which is stabilised by the reaction with VOCl_3 . Resulting in a stronger bond to the vanadium centre than previously seen for the malonate complexes.

Compound **[11]** is five coordinate, which is common for vanadium species and is particularly common when a V=O bond is present forming a square based pyramidal structure. This is also seen for [VO(acac)₂]¹²³ where the compound is five coordinate with the four acac oxygen atoms adopting an almost square planar position with the double bond perpendicular. The bond distances for [VO(acac)₂] show the same V=O bond distance and slightly longer V-O acac bonds than are found in compound **[11]**. This is due to the chlorine atoms having a larger electron density which causes them to sit further from the vanadium centre. This means the oxygen atoms can sit closer to the vanadium compared to when there are four oxygen atoms all packing tightly to the vanadium centre.

4.2 VANADIUM TETRACHLORIDE COMPLEXES

VCl₄ as mentioned in the introduction is the only monomeric transition metal chloride species that exists at room temperature other than TiCl₄. It is not believed that there is any VCl₄ in the industrial process as the formation of VCl₄ requires an oxygen free environment. During the chlorination oxygen is present from the metal oxide mixture. However, it is interesting to consider VCl₄ as the exact amount formed has not yet been confirmed and may provide further information about the metal chlorides.

Table 15: Table to compare properties of TiCl_4 and VCl_4

	TiCl_4	VCl_4
Structure		
Molecular Mass	189.70 g/mol	192.57 g/mol
Boiling point	136 °C	154 °C
Melting point	-24 °C	-28 °C
Density	1.726 g/cm ³	1.816 g/cm ³

This section investigates the reactions of the VCl_4 with the same diester groups to investigate whether the VCl_4 would react with the oil, should it be formed. The properties of VCl_4 and TiCl_4 are very similar, (as shown in Table 15). The table shows how the structure, molecular mass, density, boiling and melting points are very similar. The only chemical difference is the number of d-electrons. Titanium has 4-d e^- therefore the oxidation state can not be increased beyond 4+ whereas, vanadium has 5-d e^- electrons, so vanadium can be 5⁺ as in the case of VOCl_3

4.2.1 Reaction of VCl_4 with di-ethyl malonate [12]

As crystals had been formed with the previous metal chlorides and the diethyl malonate ligand (compounds [1] and [7]) it was the clear starting point for the next set of experiments. Diethyl

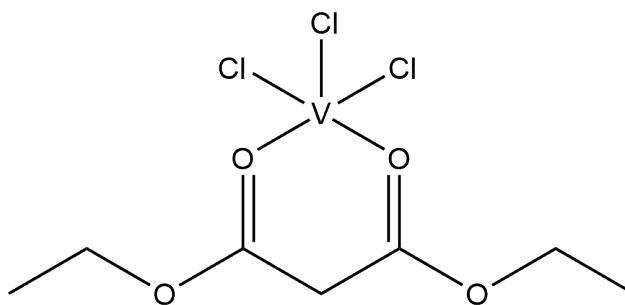


Figure 51: Diagram to show the possible structure of the intermediate complex [12]

malonate was reacted with excess VCl_4 in hexane for two hours. A light red precipitate in a darker red solution was formed. The precipitate was washed and dried to give compound [12]. A solution of compound [12] in dichloromethane was layered with hexane and slowly over the course of a week multiple small crystals were formed.

These crystals were analysed by single crystal X-ray crystallography and showed that the flask had been exposed to air during crystallisation. The crystals formed here were identical to the VOCl_3 malonate complex [7], this proved that oxygen leaked into the flask at some point during the crystallisation. This is consistent with work carried out by Sobota *et al*¹⁰⁶ and therefore, it can be assumed that the product formed is the same as product [2] in their paper.

The pathway for this reaction is likely to be through the intermediate shown in Figure 51. This intermediate was not isolated as it is likely to be very air sensitive and unstable as shown for other vanadium compounds.

The ^1H NMR of compound [12] displayed only two peaks, one at 4.35 ppm and the other at 1.35 ppm. The peak at 1.35 ppm clearly represents the CH_3 and is shifted by approximately 0.25 ppm as observed for compound [7]. The other peak represents the CH_2 next to the oxygen which is shifted by 0.35 ppm again as observed for compound [7]. When this spectra is compared to that of compound 7 it is noticeable that the middle proton of the malonate is not observed. The proton is not observed as the spectrum is broad due to the paramagnetic broadening. The ^{13}C $\{^1\text{H}\}$ NMR describes the same pattern with the same Carbon not being observed. It is therefore difficult to draw any solid conclusions from this experiment.

4.2.2 Reaction of VCl_4 with di-ethyl succinate [13]

Excess VCl_4 was reacted with diethyl succinate to give a red solution in which no precipitation was observed. The solution was dried *in vacuo* to yield an oily liquid product. This product solidified over the course of a week, and it was hoped that parts would be crystalline for single crystal analysis, however, this proved not to be the case. The product was analysed via ^1H NMR and ^{13}C $\{^1\text{H}\}$ NMR.

The ^1H NMR for compound [13] displayed large shifts as observed for the titanium-diethyl-succinate complex [4]. This was in contrast to the shifts seen for the VOCl_3 diethyl succinate complex [9]. A diagram to show the location of the carbon atoms on which the protons in questions are bonded to is shown in Figure 52 Initially it was believed that the CH_2 next to the oxygen

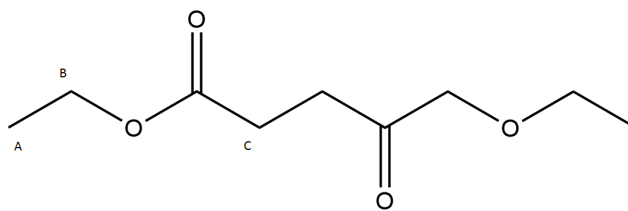


Figure 52: Diagram to show positions of protons ABC for reference in the NMR study

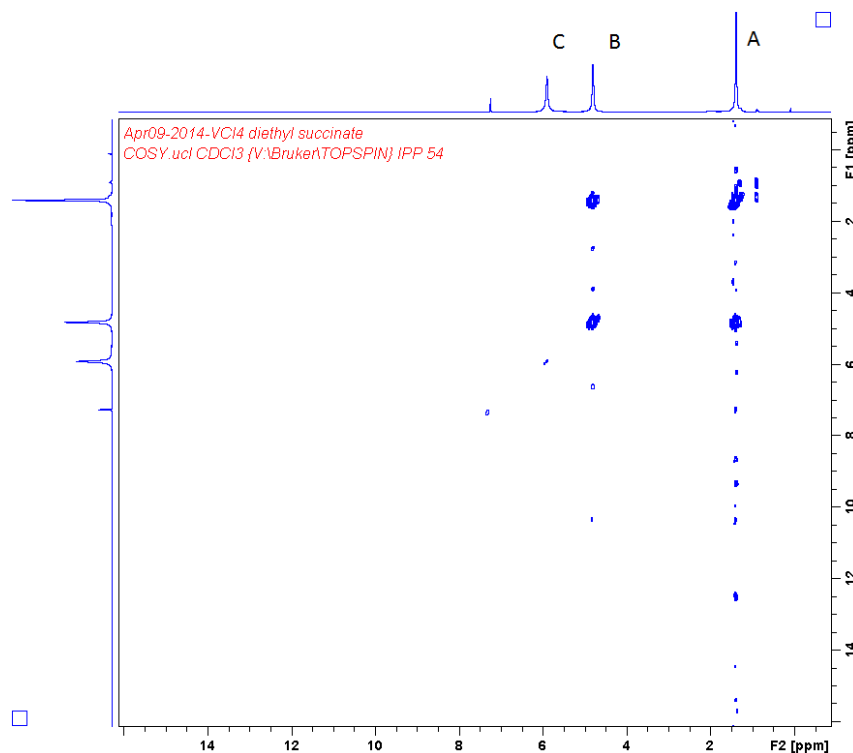


Figure 53: COSY NMR of compound[13]

(B) had shifted by 1.1 ppm and the bridging CH₂ (C) by 2.1 ppm. However after analysing the peaks the shifts did not look the same a previous complexes.

Compound [13] was then analysed by COSY NMR as shown in figure 53. This demonstrated that both peaks are shifted by very different amounts. Peak (B) is in fact only shifted by 0.5 ppm which represents a similar shift to compound [12]. Peak (C) however, is shifted by 2.8 ppm. This is a very large shift and it is difficult to

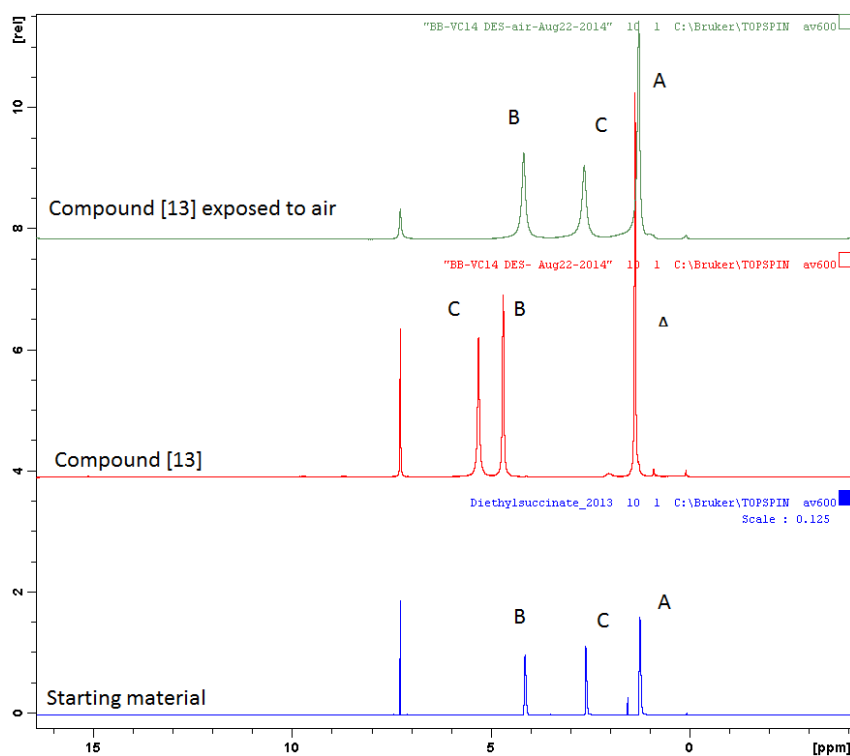


Figure 54: ^1H NMR of compound [13] shown before and after exposure to air and compared to the starting material

understand how such a large shift could occur. Many theories were established including the breakdown of the structure or the addition of a chlorine atom across the bridge between the ketones, however, none could be proven using the available analytical techniques.

As shown earlier if the product is exposed to air it dissociates from the metal chloride and returns to the starting material. If the compound had reacted and changed structure this clearly would not be possible. Therefore, as before the compound was exposed to air and then analysed by ^1H NMR again. This is shown in figure 54. This shows that although there is broadening the peaks are in the same position and therefore the succinate ligand has not been changed over the course of the reaction. The complex must have been formed in a similar way to the previous compounds but a

crystal to prove how the electron density on the bridging carbons was so high could not be formed.

4.2.3 Reaction of VCl_4 with glycerol tribenzoate

An excess of VCl_4 was added to glycerol tribenzoate to yield a light brown solid in a red solution. The red solution was removed and the light brown solid washed and dried *in vacuo*. This yielded an off white product which was analysed by NMR. It was seen to be the starting glycerol tribenzoate, so no reaction was observed.

The 1H NMR for this compound did not display any shifts or changes from the starting glycerol tribenzoate spectrum. Therefore, from the NMR and the appearance of the light coloured solid it can be seen that no reaction has taken place. The reaction was repeated at high temperature and by reflux in toluene but no reaction occurred. The reactivity of the VCl_4 with the previous two ligands was slower than for $TiCl_4$ and $VOCl_3$, therefore, it is not surprising that no reaction has been observed for the glycerol tribenzoate. There is steric hindrance effects which are responsible for reducing the opportunity for stabilising the metal chloride.

As mentioned previously the glycerol tribenzoate ligand is important for relating the reactivity back to soya oil. The $TiCl_4$ complex [5] showed the binding of the $TiCl_4$ with the glycerol tribenzoate without the loss of any chlorine atoms from the metal centre. The $VOCl_3$ product could not be fully understood, as a crystal could not be grown. However, from looking at the NMR, complexation via the loss of a chlorine is likely from comparing to

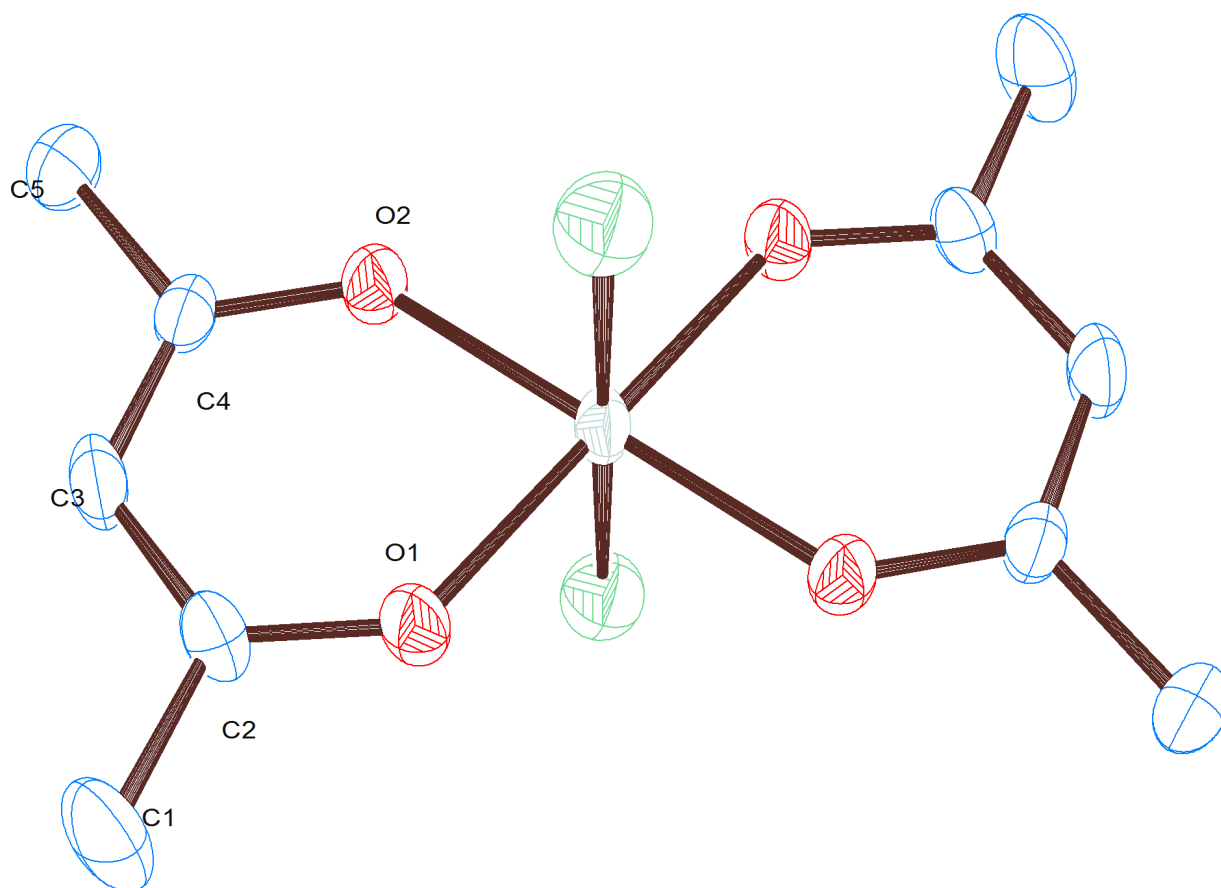
complex [7]. This VCl_4 reaction showed no change from the starting ligand, therefore, the understanding of the reactivity with the soya oil is well established.

4.2.4 Reaction of VCl_4 with *acacH* [14]

The *acacH* ligand provided a chance to compare the VCl_4 complexation to the other metal chlorides after crystallising previous compounds proved difficult. The *acac* ligand is a strong ligand which due to the delocalisation of electrons could form a stronger complex with the VCl_4 leading to crystallisation.

An excess of VCl_4 was reacted with *acacH* in hexane for 2 hours. Immediately a blue solution was formed with a blue precipitate, the experiment was run for 2 hours to ensure a full reaction. The precipitate was washed and dried *in vacuo*, this was then re-dissolved in dichloromethane and layered with hexane. After 24 hours the solution afforded green crystals which were suitable for single X-ray crystallography.

The 1H NMR spectrum for compound [14] is very similar to that of compound [11]. It shows two peaks one for the terminal methyl group which has shifted by 0.3 ppm upon coordination with the metal centre. The other peak represents the middle proton in the *acac* ligand which appears at 6.1 ppm. This is a clear indication that the complex has formed with the loss of the *acacH* proton. The ^{13}C $\{^1H\}$ NMR also confirms that the complex formed with 3 carbon peaks visible at 193 ppm for the quaternary ketone carbon, at 105



Crystal System	triclinic
Space group	$P-1$
Unit cell dimensions	$a = 7.3291(10) \text{ \AA}$ $\alpha = 93.585^\circ$ $b = 7.5808(8) \text{ \AA}$ $\beta = 115.873(12)^\circ$ $c = 7.9522(8) \text{ \AA}$ $\gamma = 117.719(12)^\circ$

Figure 55: Crystal structure of [12]

Table 16: Selected bond lengths (Å) and angles (°) for compound [14]

V1-Cl1	2.3178(12)	O1-C2	1.266(4)
V1-Cl1 ¹	2.3178(12)	O2-C4	1.280(3)
V1-O2	1.8971(19)	C2-C3	1.395(4)
V1-O1	1.898(2)	C4-C3	1.381(4)

Cl1 ¹ -V1-Cl1	180.0	O-V1-O2	87.06(9)
O2-V1-Cl1	89.83(8)	O1-V1-Cl1	90.19(8)
O2-V1-Cl1 ¹	90.17(8)	C4-O2-V1	132.53(18)
C4-C3-C2	123.3(3)	C3-C4-O2	122.1(3)

ppm for the middle carbon and at 26 ppm for the terminal methyl group.

Compound [14] was analysed by single crystal X-ray crystallography and the structure is shown in Figure 55 along with selected bonds and angles in Table 16. The structure shows a vanadium central atom with two chlorine atoms and two acac groups attached. The two chlorine atoms are observed *trans* to each other as are the acac groups. The acac acts as a -1 charged ligand as do the chlorine atoms leaving the vanadium 4+ as in the VCl_4 .

The structure around the vanadium centre is almost a perfect octahedral apart from slightly smaller angles between the oxygen acac atoms and the vanadium (87.06(9) Å). The vanadium chlorine bond length at 2.3178(12) Å is a little longer than the V-Cl bonds observed in compound [11] at 2.2880(8) Å. The V-O bond is on average 1.898 Å and is very similar to that of compound [11] where the bond length is 1.903(2) Å.

The different structures observed for the 3 acac complexes [6], [11] and [14] show the reactivity of the three metal chlorides. $TiCl_4$ forms a complex with the loss of one chlorine and the addition of one acac ligand in compound [6]. $VOCl_3$ follows the same pathway and forms a complex with the loss of one chlorine and the addition of one acac ligand. The VCl_4 in this compound [15] displays the loss of two chlorines and the addition of two acac units. It is well known that the metals are most stable as oxides. Therefore, it is not surprising that the VCl_4 is stabilised by more V-O bonds. It can be

deduced that VCl_4 requires the addition of a further acac ligand to stabilise the complex, whereas complexes [6] and [11] are stable with one acac ligand.

4.3 CONCLUSION

This chapter has described the synthesis of vanadium compounds with diesters, acacH and glycerol tribenzoate. A novel route to synthesise compound [7] was found and the new compound [9] was synthesised providing a very interesting polymeric structure. As well as a new acac compound [11] was also synthesised.

In the previous chapter it was shown that the diesters and glycerol tribenzoate could coordinate to the titanium metal centre without the loss of any chlorine atoms. This showed that in moisture free conditions in the presence of a large excess of $TiCl_4$ the reaction could be reversible. The vanadium compounds synthesised in this chapter all show the loss of one chlorine atom to stabilise the compound. This loss of chlorine means that the reaction can not be easily seen as reversible in any conditions, as the reaction would release $VOCl_2$ not $VOCl_3$. In the industrial process $VOCl_2$ has a far greater boiling point and can be removed by the cyclone. It has been believed by Huntsman pigments for some time that the vanadium is removed as $VOCl_2$. Through forming single crystals of molecular structures this work has elucidated a mechanism for the formation of $VOCl_2$.

These structures combined with those of titanium in the previous chapter suggest how the glycerol end of the oil could be responsible for the separation of VOCl_3 from TiCl_4 . The glycerol initially reacts with the excess TiCl_4 to form a coordination compound. This coordination compound is then broken down again, and releases TiCl_4 back into the gas phase, and the glycerol then reacts with VOCl_3 and reduces the vanadium to VOCl_2 . This is a solid at operating temperatures and demonstrates how soya oil can separate vanadium from titanium.

The majority of this thesis has focused on TiCl_4 and VOCl_3 , however, as VCl_4 is very similar to the two liquids it was worth investigating. Crystallisation of the VCl_4 products proved difficult which was likely to be due to the instability of the product. Compounds [12] and [13] showed coordination to the VCl_4 but it was slower than for the other metal chlorides. The lack of reactivity was typified with the attempted formation of this compound, where no reaction was observed. The colour change was due to a charge transfer complex with the benzene groups not a coordination compound.

4.4 EXPERIMENTAL

All reactions were carried out under argon obtained from BOC in anhydrous solvents using standard Schlenk techniques. The solvents were dried using a stills system. Anhydrous VOCl_3 , VCl_4 and malonate starting materials were purchased from Sigma Aldrich; all were used without further purification

^1H and $^{13}\text{C}\{^1\text{H}\}$ NMR spectra were obtained on a Bruker AV-600 Mz spectrometer, operating at 295 K and 600.13 MHz (^1H). Signals are reported relative to SiMe_4 ($\delta = 0.00$ ppm) and the following abbreviations are used s (singlet), d (doublet), t (triplet), q (quartet), m (multiplet), b (broad). Deuterated CDCl_3 was obtained from GOSS Scientific and was dried and degassed over 3 Å molecular sieves.

4.4.1 Reaction of VOCl_3 with ethyl malonate [7]

Diethyl malonate (0.5 cm^3 , 3.3 mmol) was added dropwise to 2 cm^3 of VOCl_3 (21.1 mmol) in 50 cm^3 of hexane and stirred under nitrogen for 2 h. An excess of VOCl_3 was used as excess VOCl_3 is facile to remove from the reaction after completion. A very dark precipitate was formed in a dark red solution. The dark precipitate was filtered and washed 3 times with 20 cm^3 hexane and dried *in vacuo* to afford complex [7] in good yield (0.9g, 78%). Some of the product was re-dissolved in 5 cm^3 dichloromethane and layered with 15 cm^3 hexane. Small crystals formed after approximately a week which were large enough for a crystal structure to be obtained. ^1H NMR (CDCl_3): δ 4.18 (q, 4H, $-\text{CH}_2$, $J=7.25$ Hz), δ 3.35 (s, 2H, $-\text{CH}_2$), δ 1.27 (t, 6H, $-\text{CH}_3$ $J=7.25$ Hz). ^{13}C $\{^1\text{H}\}$ NMR (CDCl_3): δ 14.2 (CH_3), 55.9 (CH_2), 63.6 (CH_2CH_3), 163 ($\text{C}=\text{O}$).

4.4.2 Reaction of VOCl_3 with bis-isopropyl malonate [8]

Bis-isopropyl malonate (0.5 cm^3 , 2.7 mmol) was added dropwise to 2 cm^3 of VOCl_3 (21.1 mmol) in 40 cm^3 of hexane and stirred under nitrogen for 2 h. A dark red precipitate [8] was formed in

a dark solution, the precipitate was filtered and washed 3 times with 20 cm³ hexane, the final washing was coloured red suggesting the product is partially soluble in hexane. The sample was dried *in vacuo*. ¹H NMR (CDCl₃): δ 5.14 (b, -CH), δ 3.37 (b, -CH₂), δ 1.30 (b, -CH₃) ¹³C {¹H} NMR (CDCl₃): δ 21.5 (CH₃), 54 (CH₂), 73 (CH), 129 (C=O)

4.4.3 Reaction of VOCl₃ with di-ethyl succinate [9]

Di-ethyl succinate (0.5 cm³, 3.3 mmol) was added dropwise to 2 cm³ of VOCl₃ (21.1 mmol) in 40 cm³ of hexane and stirred under nitrogen for 2 h. A dark red solution was formed immediately but no precipitate observed. Drying *in vacuo* of the solution was attempted and all of the solvent and VOCl₃ was removed however a liquid product was observed. This liquid product was left to one side, after 2 weeks crystals suitable for single crystal X-ray analysis were formed. ¹H NMR (CDCl₃): δ 4.12 (b, 4H, -CH₂CH₃), δ 2.59 (b, 4H, -CH₂CH₂), δ 1.21 (b, 6H, -CH₃) ¹³C {¹H} NMR (CDCl₃): δ 14.3 (CH₃), 29.2 (CH₂CH₂), 60.9 (CH₂CH₃), 173 (C=O)

4.4.4 Reaction of VOCl₃ with glycerol tribenzoate [10]

Glycerol tribenzoate (0.5 g, 1.2 mmol) was added dropwise to 2 cm³ of VOCl₃ (21.1 mmol) in 30 cm³ of hexane and stirred under nitrogen for 2 h. A white precipitate was observed in an orange red solution, this was filtered and washed with hexane 3 times. ¹H and ¹³C NMR were recorded in CDCl₃. From the NMR it was clear no reaction had taken place as no peaks had shifted and therefore, the spectra are not analysed here. The reaction was repeated in toluene

and refluxed for 15 hours, this gave a red-brown solution and a brown precipitate. This precipitate was washed and dried *in vacuo* and ^1H and ^{13}C NMR were observed. No crystals suitable for single crystal X-ray analysis could be grown from this sample

^1H NMR (CDCl_3): δ 8.05 (broad, 9H, (*o*-CH)), 7.5 (broad, 16H, *p*-CH and *m*-CH) 5.7 (broad, 1H -OCH), 4.8 (broad, 4H, -CH₂), 3.85 (broad, 2H, (O-CH₃)). ^{13}C $\{^1\text{H}\}$ NMR (CDCl_3): 63.30 (CH₂), 71.32 (CH), 128 (*o*-CH), 130 (*p*-CH), 134 (*m*-CH), 166 (C=O).

4.4.5 Reaction of VOCl_3 with *acacH* [11]

AcacH (0.5 cm³, 4.87 mmol) was added dropwise to 2 cm³ of VOCl_3 (21.1 mmol) in 30 cm³ of hexane and stirred under nitrogen for 2 h. A dark precipitate formed immediately in a dark black solution. The precipitate was filtered and washed with hexane and dried *in vacuo*. This afforded complex [11] in a good yield, and crystals suitable for single crystal X-ray diffraction were grown by layering a solution of dichloromethane with hexane. Large green crystals formed over the course of 2 days and were analysed.

^1H NMR (CDCl_3): δ 6.13 (s, 1H, CH), δ 2.39 (s, 6H, CH₃). ^{13}C $\{^1\text{H}\}$ NMR (CDCl_3): δ 193 (-C=O), δ 105 (CH), δ 26 (CH₃).

4.4.6 Reaction of VCl_4 with *di-ethyl malonate*[12]

Diethyl malonate (0.5 cm³, 3.3 mmol) was added dropwise to 2 cm³ of VCl_4 (18.9 mmol) in 50 cm³ of hexane and stirred under nitrogen for 2 h. A light red precipitate was formed in a red solution. The light precipitate was filtered and washed 3 times with 20 cm³ hexane and dried *in vacuo* to afford complex [12].

Some of the product was re-dissolved in 5 cm³ dichloromethane and layered with 15 cm³ hexane. Small crystals formed over approximately a week however, none were suitable for single crystal X-ray crystallography. ¹H NMR (CDCl₃): δ 4.35 (b, -CH₂), δ 1.35 (b, -CH₃). ¹³C {¹H} NMR (CDCl₃): δ 14.2 (CH₃), 63.6 (CH₂CH₃), 163 (C=O).

4.4.7 Reaction of VCl₄ with di-ethyl succinate [13]

Di-ethyl succinate (0.5 cm³, 3.3 mmol) was added dropwise to 2 cm³ of VOCl₃ (21.1 mmol) in 40 cm³ of hexane and stirred under nitrogen for 2 h. A dark red solution is formed immediately but no precipitate observed. Drying *in vacuo* of the solution was attempted and all of the solvent and VOCl₃ was removed however a liquid product was observed. This product was left to one side as other experiments were attempted, after 1 week precipitate was observed in the reaction vessel. It was initially thought the solid may contain crystals however, they were not suitable for single X-ray crystallography. ¹H NMR (CDCl₃): δ 5.30 (b, 4H, -CH₂CH₂), δ 4.65 (b, 4H, -CH₂CH₃), δ 1.36 (b, 6H, -CH₃) ¹³C {¹H} NMR (CDCl₃): δ 15.3 (CH₃), 40.8 (CH₂CH₂), 65.4 (CH₂CH₃), 185 (C=O) The solid precipitate was then exposed to air, this solid was then analysed by ¹H and ¹³C {¹H} NMR. ¹H NMR (CDCl₃): δ 4.2 (b, 4H, -CH₂CH₃), δ 2.2 (b, 4H, -CH₂CH₂), δ 1.25 (b, 6H, -CH₃) ¹³C {¹H} NMR (CDCl₃): δ 14.2 (CH₃), 29.2 (CH₂CH₂), 60.9 (CH₂CH₃), 173 (C=O)

4.4.8 Reaction of VCl_4 with glycerol tribenzoate

Glycerol tribenzoate (0.5 g, 1.2 mmol) was added dropwise to 2 cm³ of $VOCl_3$ (21.1 mmol) in 30 cm³ of hexane and stirred under nitrogen for 2 h. A light brown precipitate in a red solution was observed, this was filtered and washed with hexane 3 times. The product was dried *in vacuo* and the residue was an 'off' white powder, this was analysed by ¹H NMR and found to be starting material with slight broadening due to VCl_4 .

4.4.9 Reaction of VCl_4 with acacH[14]

AcacH (0.5 cm³, 4.87 mmol) was added dropwise to 2 cm³ of $VOCl_3$ (21.1 mmol) in 30 cm³ of hexane and stirred under nitrogen for 2 h. A blue solution with a blue precipitate was observed immediately. The precipitate was filtered and washed with hexane and dried *in vacuo*. This afforded complex [14] in good yield, the solid was dissolved in dichloromethane and layered with hexane, this afforded high quality green crystals suitable for single crystal X-ray crystallography.

¹H NMR ($CDCl_3$): δ 6.13 (s, 1H, CH), δ 2.39 (s, 6H, CH_3). ¹³C {¹H} NMR ($CDCl_3$): δ 193 (-C = O), δ 105 (CH), δ 26 (CH_3).

DESIGN OF UV-VIS FLOW CELL

A major challenge in studying an industrial problem in the laboratory is creating similar conditions to the large scale industrial plant. As described in Chapter 1, the plant is a large facility where the pressures and temperatures get very high. Safety at the plant is obtained by ensuring that all the walls of the containers are very thick and monitoring the plant in real time for any cracks. In the laboratory it is not possible to safely handle the large volume of TiCl_4 at temperatures and pressures equivalent to the plant.

The removal of vanadium in the process occurs through the addition of soya oil to the $\text{TiCl}_4/\text{VOCl}_3$ mix at approximately 130°C . This mixture is distilled and the vanadium content does not distil across with the TiCl_4 . When this project was established the biggest problem was vanadium slip, which is where some of the vanadium did get distilled over and turns the pigment yellow (since vanadium oxide is yellow), and hence discolours the white TiO_2 .

UV-vis spectroscopy is a technique that can be used to monitor chemical species in the gas phase. With modern advances the UV-vis spectrometer and light source are now small enough to be transportable and fitted onto an existing system with reasonable

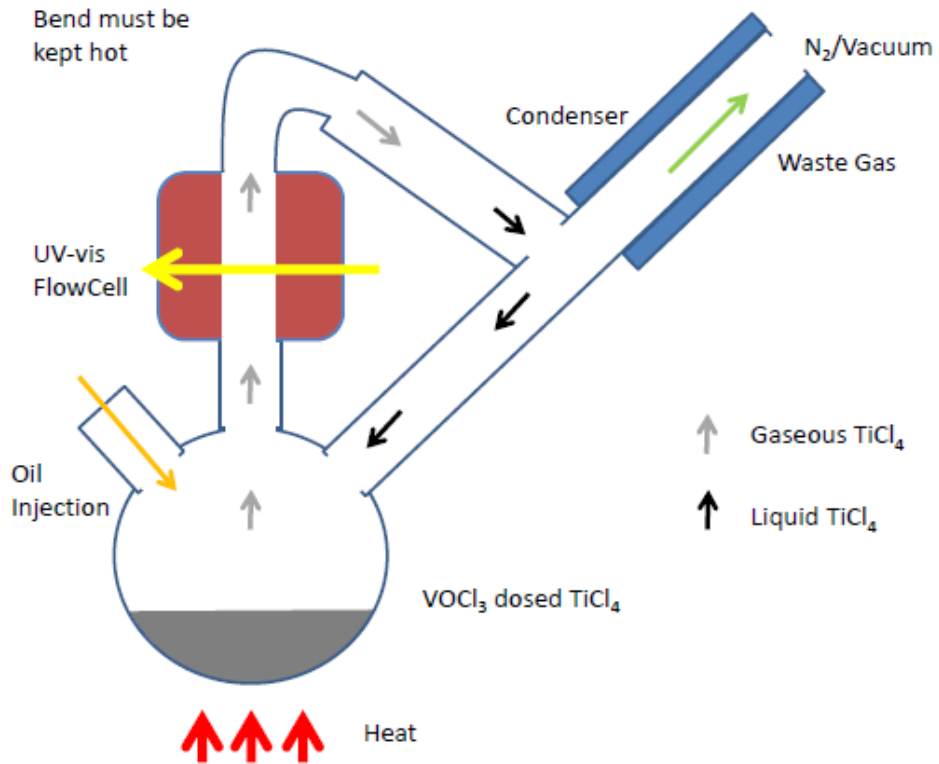


Figure 56: Schematic of the original design of UV-vis flow cell



Figure 57: UV-vis cell as received from Mettler Toledo

ease. Huntsman Pigments have a UV-vis spectrometer that is used to monitor chlorine slip. Chlorine slip is where too much un-reacted chlorine leaves the chlorinator, which can reduce the efficiency of the rest of the process. After visiting the plant, the UV-vis flow cell was designed and manufactured by Mettler Toledo.

The flow cell was originally designed as shown in Figure 56. The flow set up worked by heating TiCl_4 to its boiling point, it then passes through the UV-vis flow cell and condenses back into the round bottomed flask. The UV-vis cell manufactured by Mettler Toledo is shown in Figure 57. The UV-vis spectrum of the gas is taken every second during the experiment. The idea is that when the system is running, oil is added and any change in the spectrum is observed. It was hoped that as the oil was added the peak in the UV-vis would decrease. The UV-vis spectra for TiCl_4 and VOCl_3 have been previously recorded and are shown in Figure 58.¹²⁴ The spectra show that by using UV-vis, TiCl_4 and VOCl_3 can be separately analysed. It should therefore be possible to observe even trace amounts of VOCl_3 during the experiment as UV-vis is a very sensitive technique.

The key properties of the custom made cell are; the fibre-optic attachments from the UV-vis spectrometer along with quartz windows, the two inch long 4 mm holes in the body, where two resistive heaters can be inserted to allow the cell to be heated up to 180 °C. There is also a screw attachment into the body in which

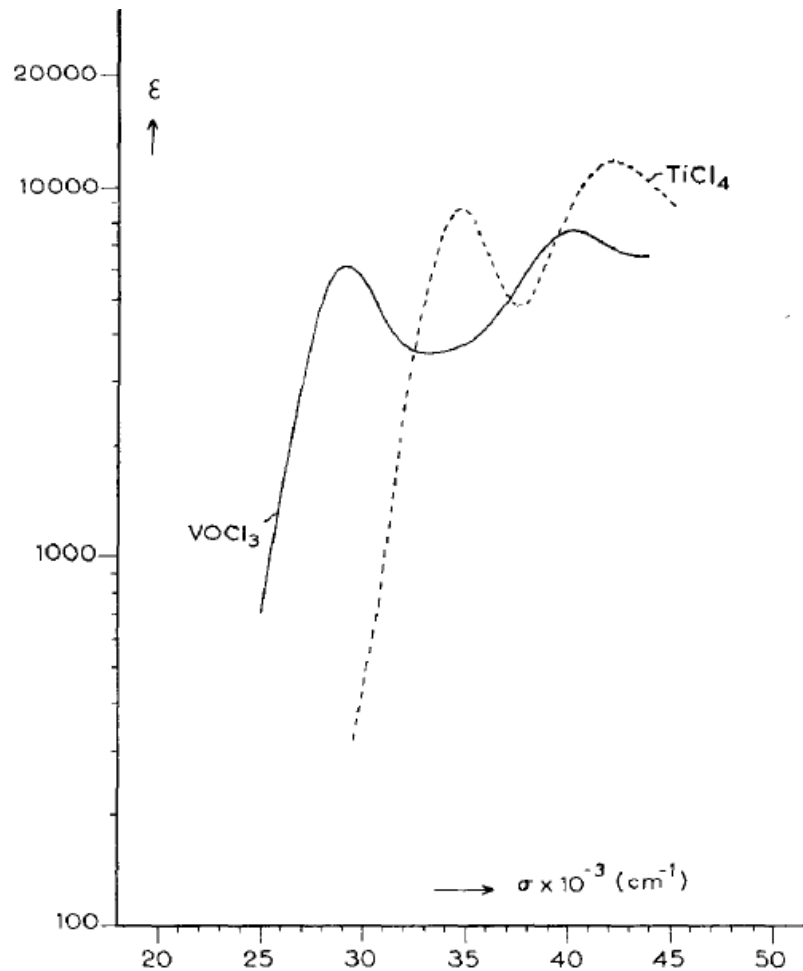


Figure 58: UV-vis spectra of TiCl₄ and VOCl₃¹²⁴

a thermocouple is inserted to monitor and therefore maintain a constant temperature.

The UV-vis spectra were recorded using an ocean optic 600 receiver, using a UV source containing deuterium and halogen bulbs thus giving a full ranging spectrum. The spectra was analysed by ocean optics' SPECTRASUITE[®] software. Spectra were recorded every 20 ms and 100 spectra were averaged for each data point. The receiver analyses the light that reaches it and measures the difference in intensity from the light when there is no absorbance. The π electrons in the molecules absorb the energy to

excite the electrons into higher orbitals, this absorbance then relates to the band structure of the material. The gas cell is 2 cm in length which is long for a UV cuvette, which are usually 1 cm. However, the length is appropriate for a gas, due to the low concentration. When absorbance goes over 99.9% the spectrum is saturated and no data can be accurately collected. Preliminary results recorded from the flow cell are shown in Figure 59. This shows how VOCl_3 and TiCl_4 can be observed separately by different peaks, it also shows the saturation of the peaks at low wavenumber ($< 250 \text{ cm}^{-1}$).

This absorbance limit proved to be a major obstacle in data acquisition. The flow cell system was pre-heated to 150°C , the round bottomed flask was then slowly heated up to the boiling point of TiCl_4 at 136°C . Before the TiCl_4 had boiled, the absorption limit was reached, this happened on every run of the experiment. When this issue was investigated it was believed that the problem was due to the cold nitrogen, which was used to force the TiCl_4 around the cell. This cold nitrogen gas cooled the whole system and caused TiO_2 to be deposited on the flow cell windows. This absorbed the UV light strongly, as a TiO_2 solid film is very absorbant and any light that did pass through was refracted away from the fibre-optic detector.

After further consultation with Huntsman Pigments it became clear that either the nitrogen had to be heated or not used as a driving force. Heating the nitrogen created a host of further problems due to the complexation of heating a gas stream so a

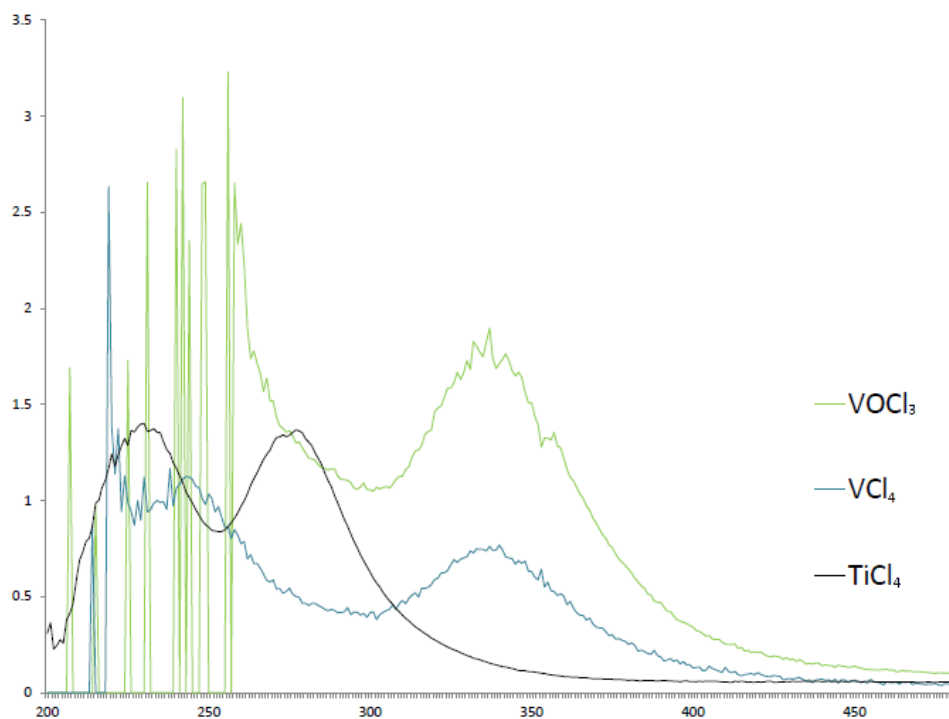


Figure 59: UV-vis spectra of TiCl₄ and VOCl₃ and VCl₄ recorded using the UV-vis flow cell

solution without a gas driving force was required. The new set up included using a Soxhlet extractor and is shown in Figure 61.

A Soxhlet adaptor is used in organic chemistry to separate a solid mixture. It is generally used when the desired product is partially soluble in a solvent and the impurity is not soluble in the solvent. It helps the extraction process by passing the warm solvent over the solid mixture many times as shown in Figure 60. Passing the solvent over many times means that even if the solid is only partially soluble it can be removed without using a huge excess of solvent.

In the flow cell set up the Soxhlet is not used for its traditional use, it is used to control the directionality of the flow of the TiCl₄

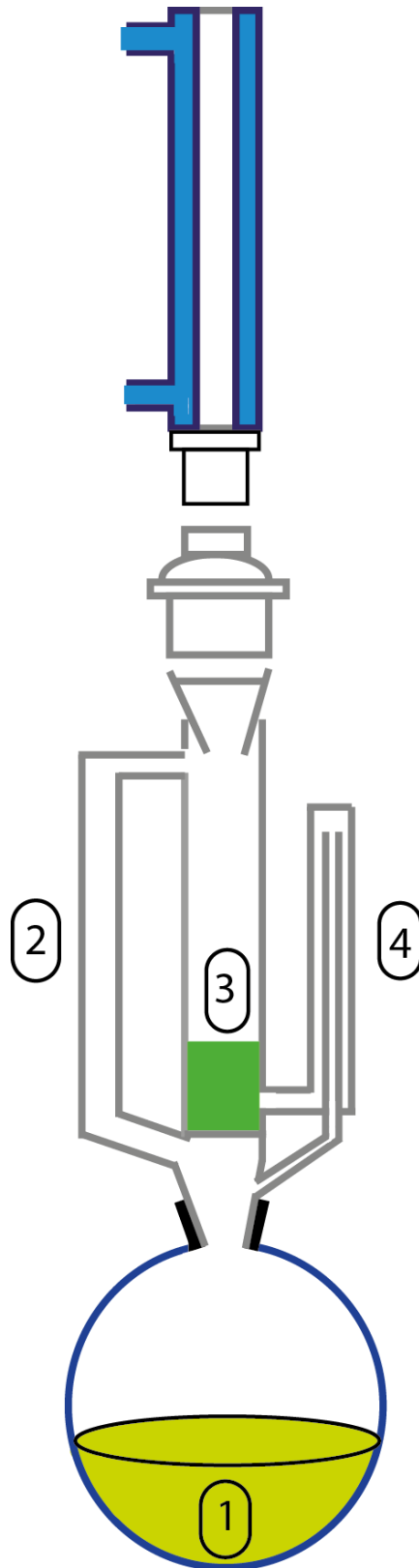


Figure 60: Diagram to show the mechanism of a Soxhlet extractor. The solid of which the product is to be extracted from is placed in the Soxhlet at position (3). The solvent is evaporated from position (1) through (2), to (3) where it dissolves the product, the siphon (4) is then filled and once full deposits back into the round bottomed flask (1)

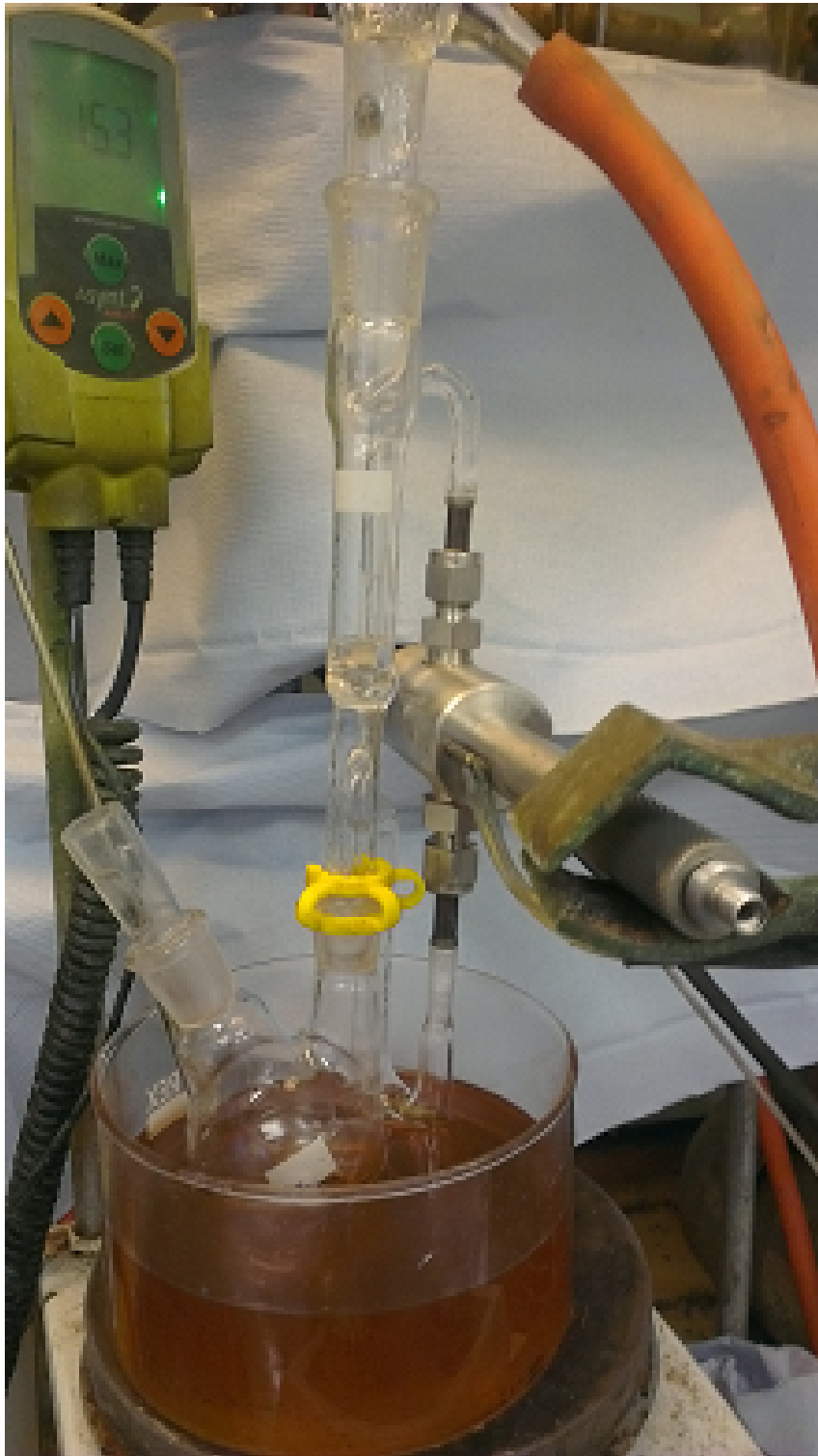


Figure 61: Photo to show the UV-vis flow cell set up with the Soxhlet extractor attached.

through the system. The Soxhlet is adapted as shown in Figure 62. This adaptation forces the gaseous TiCl_4 through the flow cell and then into the Soxhlet, then back into the flask when the siphon is activated without the need for a nitrogen flow. This greatly reduces the heat loss of the system during the reaction. These adaptations reduced the build up of solid but not sufficiently to record useful results. It was hoped the vanadium peak shown in the spectra would decrease over the experiment as the oil was added, however, the experiment never continued long enough to record this data.

The whole set up contains two metal-glass joints which makes the system extremely fragile. Due to this the glassware broke several times during the development. This has resulted in this aspect of the project to be incomplete at this stage. My colleague Ben Blackburn is continuing this research. He has developed another flow cell which does not involve the use of UV-vis but follows the same reaction. The analysis is carried out using NMR instead of UV-vis. He has shown that the oil reacts with TiCl_4 resulting in the breakdown of the alkene end of the oil and a C_3 fragment with 3 Cl atoms attached. When the VOCl_3 reacts with the soya oil this fragment is not formed, this is due to the VOCl_3 reacting much quicker and more violently, hence no fragment is formed. This demonstrates in the plant how VOCl_3 is not carried over in the plant as the reaction proceeds favourably to the TiCl_4 .

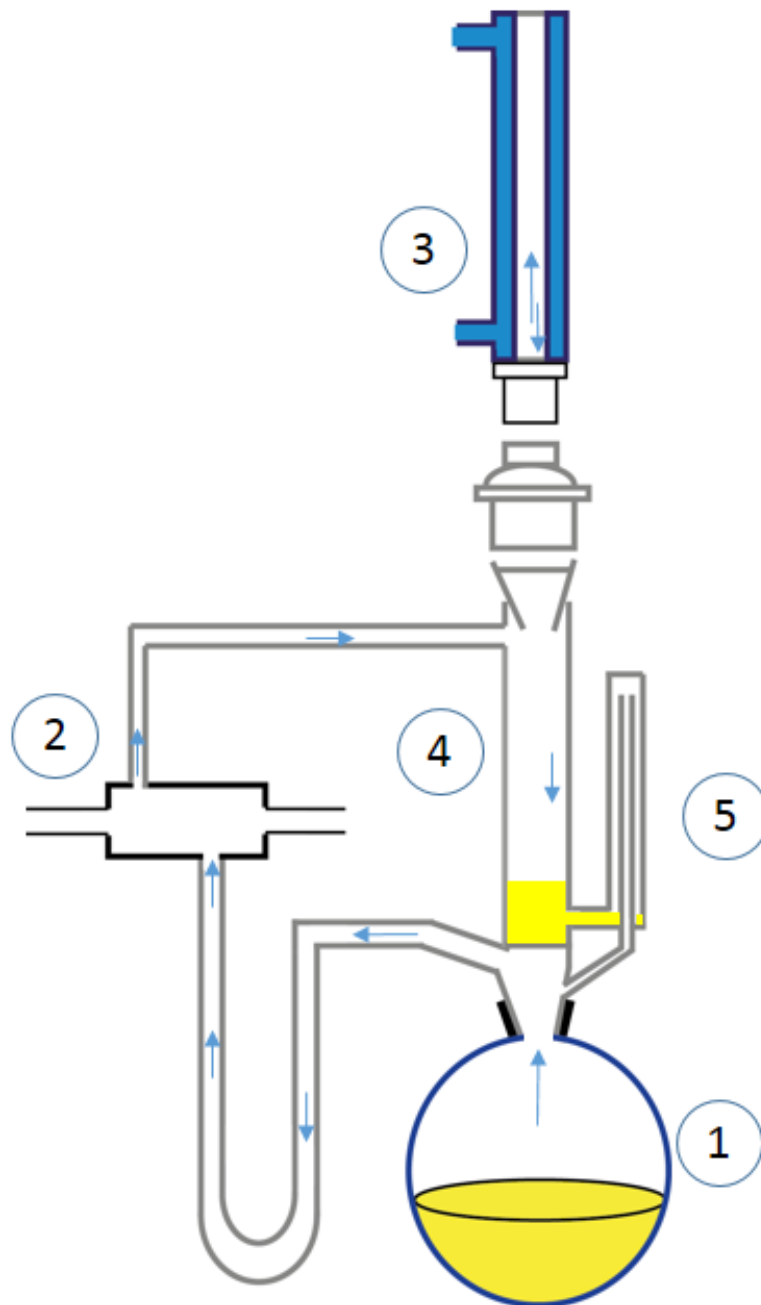


Figure 62: Diagram to show the mechanism of the adapted Soxhlet extractor. (1) The TiCl_4 is evaporated, (2) the hot gaseous mixture passes through the UV-vis cell, (3) the TiCl_4 is condensed, (4) the TiCl_4 collects in the Soxhlet, (5) the siphon activates when the Soxhlet is full releasing the liquid back into the reaction flask

CONCLUSIONS

The aim of this thesis was to compare the reactivity of TiCl_4 and VOCl_3 . The focus was on the reactions with soya oil, as it is known to separate VOCl_3 from TiCl_4 in the chloride process. The chloride process is well established in industry, however, understanding of the chemistry behind the removal is not well known in the literature. This thesis has provided a new hypothesis for the separation of VOCl_3 from TiCl_4 using soya oil

Chapter 2 investigated the direct reaction of both TiCl_4 and VOCl_3 with soya oil. It was anticipated that by studying the reaction using NMR a greater understanding of the process could be garnered. It was originally thought VCl_4 would play a role in the industrial process, however, after the NMR analysis of the reaction of VCl_4 and soya oil it was found to not be the case. The NMR experiment showed no reaction with VCl_4 , therefore, if VCl_4 was present in the chlorination process it would not be removed by the soya oil and would be present in the final product.

The direct reaction of VOCl_3 and TiCl_4 with soya oil was carried out but did not provide evidence of the separation that occurs in the chlorine process. In fact the NMR analysis showed a greater reaction of TiCl_4 with soya oil than VOCl_3 . The reaction of

the metal chlorides with 2,3-octene provided the first evidence of a preferential reaction with VOCl_3 over TiCl_4 . During all of these reactions only the organic product was isolated to be analysed. To understand the process better a greater understanding of the metal chloride product was needed.

To further understand the metal chloride product a new analytical technique was required. The most detailed technique for looking into a metal structure is through single crystal X-ray diffraction. To form crystals of the products the starting ligand must be simplified from the soya oil. The chosen ligand for the initial experiments was diethyl-malonate. This accounted for the glycerol end of the oil. The alkene end was also studied but simple products could not be formed and whilst some interesting features were observed they are not included in this thesis as the work is incomplete and makes up part of a colleagues thesis.

Chapter 3 described the reactions of TiCl_4 with diesters. This demonstrated that diesters bind to the titanium centre as a bidentate ligand without the loss of any chlorine atoms. Therefore the ligand can be described as a dative ligand as in this case it does not donate electron density to the metal centre. The reaction with the acac formed a different product with the acac forming a delocalised system with the loss of a chlorine atom and subsequent dimerisation. This difference in reactivity explained how the soya oil could coordinate with the TiCl_4 in plant conditions and then reverse the reaction to leave TiCl_4 . The final reaction used glycerol tribenzoate to react with the TiCl_4 . This showed the same dative

coordination as the ester and provided evidence that the soya oil could be simplified to an ester.

Chapter 4 investigated the reaction of diester with VOCl_3 . This chapter described the difference in coordination observed with the vanadium centre as opposed to the titanium centre. All the vanadium reactions were characterised by the loss of a chlorine atom. This demonstrates that in plant conditions the reaction could not be seen as reversible with respect to the VOCl_3 , which gives a mechanism for the removal of VOCl_3 from TiCl_4 using soya oil.

In chapter 5 an *in situ* approach was taken to further understand the reaction to provide kinetics describing the reduction of VOCl_3 . This part of the project encountered many problems mainly due to the highly air sensitive nature of the metal chlorides and the complexity of the design. A simpler design has been used by a colleague which has shown the rate of the reaction of the oil with the VOCl_3 is far greater than with the TiCl_4 and that the product has a high boiling point.

The aim of this thesis was to discover how VOCl_3 is removed from TiCl_4 using soya oil in the chlorine process. This thesis has shown that the reaction of the metal chlorides with the ester end provides the difference and that in high TiCl_4 conditions the coordination of TiCl_4 with the ester can be said to be reversible. This is not the case for the VOCl_3 with the ester. It is likely that the alkene also plays a part in the removal as preliminary experiments

with stilbene have displayed reaction times of 1000X faster with the VOCl_3 compared with TiCl_4 .

To continue this work further the focus should be away from the ester end as this thesis has now provided the evidence for it's part in the process. The stilbene chemistry should be studied with the help of organic chemists to understand what part the alkene plays. This work also needs to be applied to the industrial site though lab reactions which closer mimic the actual conditions in the plant.

BIBLIOGRAPHY

- [1] H J Kakkonen, J Pursiainen, T A Pakkanen, and M Ahlgren. TiCl_4 , diester complexes : relationships between the crystal structures and properties of Ziegler-Natta catalysts. *Journal of Organometallic Chemistry*, 453:175–184, 1993. (Cited on pages 13, 57, 58, 63, 64, 70, and 83.)
- [2] C L Boyd. Purification of crude titanium tetrachloride patent no. US3253885, January 1966. URL <http://www.google.com/patents?hl=en&lr=&vid=USPAT4070252&id=UWMxAAAAEBAJ&oi=fnd&dq=purification+of+crude+titanium+tetrachloride&printsec=abstract>. (Cited on pages 14 and 36.)
- [3] http://www.cbis-group.net/titaniumdioxide_dw_mx.dwt accessed 15/02/2012. URL http://www.cbis-group.net/titaniumdioxide_dw_mx.dwt. (Cited on pages 15 and 16.)
- [4] X Chen and S S Mao. Titanium dioxide nanomaterials: synthesis, properties, modifications, and applications. *Chemical Reviews*, 107(7):2891–959, July 2007. ISSN 0009-2665. doi: 10.1021/cr0500535. URL <http://www.ncbi.nlm.nih.gov/pubmed/17590053>. (Cited on page 15.)
- [5] A Kafizas, C W Dunnill, and I P Parkin. Combinatorial atmospheric pressure chemical vapour deposition (cAPCVD) of niobium doped anatase; effect of niobium on the conductivity and photocatalytic activity. *Journal of Materials Chemistry*, 20(38):8336, 2010. ISSN 0959-9428. doi: 10.1039/c0jm01244k. URL <http://xlink.rsc.org/?DOI=c0jm01244k>. (Cited on page 15.)
- [6] A Fujishima, T N Rao, and D A Tryk. Titanium dioxide photocatalysis. *Journal of Photochemistry and Photobiology C*, 1(1):1–21, June 2000. ISSN 13895567. doi: 10.1016/S1389-5567(00)00002-2. URL <http://linkinghub.elsevier.com/retrieve/pii/S1389556700000022>. (Cited on page 15.)
- [7] A Fujishima and K Honda. TiO_2 photoelectrochemistry and photocatalysis. *Nature*, 213(1998):8656, 1972. URL <https://electrochem.org/dl/ma/203/pdfs/2729.pdf>. (Cited on page 15.)

- [8] A Fujishima, X Zhang, and D Tryk. TiO₂ photocatalysis and related surface phenomena. *Surface Science Reports*, 63(12):515–582, December 2008. ISSN 01675729. doi: 10.1016/j.surfrep.2008.10.001. URL <http://dx.doi.org/10.1016/j.surfrep.2008.10.001>. (Cited on page 16.)
- [9] K Hashimoto, H Irie, and A Fujishima. TiO₂ Photocatalysis: A Historical Overview and Future Prospects. *Japanese Journal of Applied Physics*, 44(12):8269–8285, December 2005. ISSN 0021-4922. doi: 10.1143/JJAP.44.8269. URL <http://jjap.jsap.jp/link?JJAP/44/8269/>. (Cited on page 16.)
- [10] J Herrmann. Heterogeneous photocatalysis : fundamentals and applications to the removal of various types of aqueous pollutants. *Catalysis Today*, 53:115–129, 1999. (Cited on page 16.)
- [11] S U M Khan, M Al-Shahry, and W B Ingler. Efficient photochemical water splitting by a chemically modified n-TiO₂. *Science (New York, N.Y.)*, 297(5590):2243–5, September 2002. ISSN 1095-9203. doi: 10.1126/science.1075035. URL <http://www.ncbi.nlm.nih.gov/pubmed/12351783>. (Cited on page 16.)
- [12] Y Paz, Z Luo, L Rabenberg, and A Heller. Photooxidative self-cleaning transparent titanium dioxide films on glass. *Journal of Materials Research*, 10(11):2842–2848, March 2011. ISSN 0884-2914. doi: 10.1557/JMR.1995.2842. URL http://www.journals.cambridge.org/abstract_S0884291400080067. (Cited on page 16.)
- [13] A J Huh and Y J Kwon. "Nanoantibiotics": A new paradigm for treating infectious diseases using nanomaterials in the antibiotics resistant era. *Journal of Controlled Release*, 156(2): 145–128, July 2011. ISSN 1873-4995. doi: 10.1016/j.jconrel.2011.07.002. URL <http://dx.doi.org/10.1016/j.jconrel.2011.07.002>. (Cited on page 16.)
- [14] H M Yates, M G Nolan, D W Sheel, and M E Pemble. of nitrogen doping on the development of visible light-induced photocatalytic activity in thin TiO₂ films grown on glass by chemical vapour deposition. *Journal of Photochemistry and Photobiology Photobiology A: Chemistry*, 179:213–223, 2006. doi: 10.1016/j.jphotochem.2005.08.018. URL <http://www.sciencedirect.com/science/article/pii/S1010603005004107>. (Cited on page 16.)
- [15] T Yoshida and K Terada. Electrochemical Self Assembly of Nanoporous ZnO Eosin Y Thin Films and Their

- Sensitized Photoelectrochemical Performance. *Advanced Materials*, 2(3):1214–1217, 2000. URL [http://onlinelibrary.wiley.com/doi/10.1002/1521-4095\(200008\)12:16%3C1214::AID-ADMA1214%3E3.0.CO;2-Z/full](http://onlinelibrary.wiley.com/doi/10.1002/1521-4095(200008)12:16%3C1214::AID-ADMA1214%3E3.0.CO;2-Z/full). (Cited on pages 16 and 17.)
- [16] Y Cong, J Zhang, F Chen, and M Anpo. Synthesis and characterization of nitrogen-doped TiO₂ nanophotocatalyst with high visible light activity. *The Journal of Physical Chemistry C*, (111):6976–6982, 2007. URL <http://pubs.acs.org/doi/abs/10.1021/jp0685030>. (Cited on page 16.)
- [17] C W Dunnill, Z Ansari, and A Kafizas. Visible light photocatalysts, N doped TiO₂ by sol gel, enhanced with surface bound silver nanoparticle islands. *Journal of Materials Chemistry*, (21):11854–11861, 2011. URL <http://pubs.rsc.org/en/content/articlehtml/2011/jm/c1jm11557j>. (Cited on page 16.)
- [18] L R Sheppard, T Bak, and J Nowotny. Electrical properties of niobium-doped titanium dioxide. 1. Defect disorder. *The journal of physical chemistry. B*, 110(45):22447–54, November 2006. ISSN 1520-6106. doi: 10.1021/jp0637025. URL <http://www.ncbi.nlm.nih.gov/pubmed/17091986>. (Cited on page 17.)
- [19] T Hitosugi, Y Furubayashi, A Ueda, K Itabashi, K Inaba, Y Hirose, G Kinoda, Y Yamamoto, T Shimada, and T Hasegawa. Ta-doped Anatase TiO₂ Epitaxial Film as Transparent Conducting Oxide. *Japanese Journal of Applied Physics*, 44(No. 34):L1063–L1065, August 2005. ISSN 0021-4922. doi: 10.1143/JJAP.44.L1063. URL <http://jjap.ipap.jp/link?JJAP/44/L1063/>. (Cited on page 17.)
- [20] L Zhou. Continuous Process for Producing Titanium Tetrachloride Using On-Line Patent No. US 0129278, 2010. (Cited on page 17.)
- [21] H B Clark. Purifying Crude TiCl₄ Vapor Patent No. 3,533,733, 1970. (Cited on page 19.)
- [22] H K Pulker, G Paesold, and E Ritter. Refractive indices of TiO₂ films produced by reactive evaporation of various titanium-oxygen phases. *Applied Optics*, 15(12):2986–91, December 1976. ISSN 0003-6935. URL <http://www.ncbi.nlm.nih.gov/pubmed/20168379>. (Cited on page 19.)
- [23] J Fontanella, R L Johnston, J H Colwell, and C Andeen. Temperature and pressure variation of the refractive index of diamond. *Applied Optics*, 16(11):2949–51, November

1977. ISSN 0003-6935. URL <http://www.ncbi.nlm.nih.gov/pubmed/20174273>. (Cited on page 19.)
- [24] R Erdogan. *A Quantum Chemical Study of Water and Ammonia Adsorption Mechanisms on Titanium Dioxide Surfaces*. PhD thesis, Middle East Technical University, 2010. (Cited on page 19.)
- [25] J J Powell, C C Ainley, R S Harvey, I M Mason, and R P Thompson. Characterisation of inorganic microparticles in pigment cells of human gut associated lymphoid tissue. *Gut*, 38(3):390–5, March 1996. ISSN 0017-5749. URL <http://www.pubmedcentral.nih.gov/articlerender.fcgi?artid=1383068&tool=pmcentrez&rendertype=abstract>. (Cited on page 19.)
- [26] T Thongkanluang, P Limsuwan, and P Rakkwamsuk. Preparation and Application of High Near-Infrared Reflective Green Pigment for Ceramic Tile Roofs. *International Journal of Applied Ceramic Technology*, 1458:no–no, December 2010. ISSN 1546542X. doi: 10.1111/j.1744-7402.2010.02599.x. URL <http://doi.wiley.com/10.1111/j.1744-7402.2010.02599.x>. (Cited on page 20.)
- [27] L E McNeil. Multiple scattering from rutile TiO₂ particles. *Acta materialia*, 48:4571–4576, 2000. URL <http://www.sciencedirect.com/science/article/pii/S1359645400002433>. (Cited on page 20.)
- [28] P M Hext, J A Tomenson, and P Thompson. Titanium dioxide: inhalation toxicology and epidemiology. *The Annals of Occupational hygiene*, 49(6):461–72, August 2005. ISSN 0003-4878. doi: 10.1093/annhyg/mei012. URL <http://www.ncbi.nlm.nih.gov/pubmed/15790613>. (Cited on page 20.)
- [29] H W Bichter. Process for making Titanium white patent no. US1,947,226, February 1934. URL <http://www.google.com/patents?hl=en&lr=&vid=USPAT1947226&id=wCVLAAAEEBAJ&oi=fnd&dq=Process+for+making+titanium+white&printsec=abstract>. (Cited on page 20.)
- [30] M Gueguin and F Cardarelli. Chemistry and Mineralogy of Titania-Rich Slags. Part 1-hemo-Ilmenite, Sulphate and upgraded Titania Slags. *Mineral Processing and Extractive Metallurgy Review*, 28(1):1–58, 2007. URL <http://www.tandfonline.com/doi/abs/10.1080/08827500600564242>. (Cited on page 20.)
- [31] L C Anand and A B Deshpande. Polymerization of Styrene with VOCl₃-Aluminum Alkyls. *Journal of Polymer*,

- 5(984):2079–2089, 1967. URL <http://onlinelibrary.wiley.com/doi/10.1002/pol.1967.150050824/abstract>. (Cited on pages 20 and 32.)
- [32] K. K. Sahu. An overview on the production of pigment grade titania from titania-rich slag. *Waste Management & Research*, 24(1):74–79, February 2006. ISSN 0734-242X. doi: 10.1177/0734242X06061016. URL <http://wmr.sagepub.com/cgi/doi/10.1177/0734242X06061016>. (Cited on page 21.)
- [33] W Zhang, Z Zhu, and C Y Cheng. A literature review of titanium metallurgical processes. *Hydrometallurgy*, 108(3-4):177–188, July 2011. ISSN 0304386X. doi: 10.1016/j.hydromet.2011.04.005. URL <http://linkinghub.elsevier.com/retrieve/pii/S0304386X11000922>. (Cited on pages 22 and 29.)
- [34] C A L Becker and J P Dahl. A CNDO-MO calculation of TiCl_4 . *Theoretica Chimica Acta*, 14(1):26–38, 1969. URL <http://www.springerlink.com/index/n65122031t858627.pdf>. (Cited on page 26.)
- [35] J P Dahl and H Johansen. Electronic structures of tetrahedral CrO_4 , VO_4 and TiCl_4 . *Theoretica Chimica Acta*, 11(1):26–30, 1968. (Cited on page 26.)
- [36] N N Greenwood and A Earnshaw. *Chemistry of the Elements*, volume 3. Elsevier, 1984. URL <http://www.lavoisier.fr/livre/notice.asp?id=0LAW0XA22XA0WJ>. (Cited on page 26.)
- [37] I Suzuki and Y Yamamoto. Mediation of the Reactivity of the Strong Lewis Acid TiCl_4 by Complexation with XPhs. *Journal of Organic Chemistry*, 58(6):4783–4784, 1993. (Cited on page 27.)
- [38] G N Lewis. Introductory address: valence and the electron. *Transactions of the Faraday Society*, pages 452–458, 1923. URL <http://pubs.rsc.org/en/content/articlepdf/1923/tf/tf9231900452>. (Cited on page 27.)
- [39] L T Suren, P J McKarns, B S Haggerty, G. Yap, A L Rheingold, and C H Winter. Adducts of titanium tetrachloride with organosulfur compounds. Crystal and molecular structures of $\text{TiCl}_4(\text{C}_4\text{H}_8\text{S})_2$ and $(\text{TiCl}_4)_2(\text{CH}_3\text{SSCH}_3)$. *Polyhedron*, 17(1):1–9, 1998. URL <http://www.sciencedirect.com/science/article/pii/S0277538797003094>. (Cited on pages 27 and 28.)
- [40] D L Barnes and N W Eilerts. $4, 4'$ -Biphenolate complexes of titanium and zirconium. *Polyhedron*, 13(5):743–748, 1994. URL <http://www.sciencedirect.com/science/article/pii/S0277538700816782>. (Cited on page 27.)

- [41] T Thomas, D Pugh, I P Parkin, and C J Carmalt. Novel ion pairs obtained from the reaction of titanium(IV) halides with simple arsane ligands. *Acta Crystallographica. Section C, Crystal Structure Communications*, 67(Pt 4):m96–9, April 2011. ISSN 1600-5759. doi: 10.1107/S0108270111006639. URL <http://www.ncbi.nlm.nih.gov/pubmed/21467617>. (Cited on page 28.)
- [42] S Ogawa. Magnetic Transition in TiCl_3 . *Journal of Physical Society Japan*, 15:1901, 1960. (Cited on page 28.)
- [43] C Starr and F Bitter. The Magnetic Properties of the Iron Group Anhydrous Chlorides at Low Temperatures. I. Experimental. *Physical Review*, 373(1), 1940. URL http://prola.aps.org/abstract/PR/v58/i11/p977_1. (Cited on page 28.)
- [44] E J Arlman. Ziegler-natta catalysis:: IV. The stereospecificity in the polymerization of olefins and conjugated dienes in relation to the crystal structure of TiCl_3 ([α],[β]). *Journal of Catalysis*, 5(1):178–189, 1966. URL <http://www.sciencedirect.com/science/article/pii/S0021951766801379>. (Cited on page 28.)
- [45] D C Bradley and R C Mehrotra. Structural chemistry of the alkoxides. Part I. Amyloxides of silicon, titanium, and zirconium. *Journal of the Chemistry Society*, 1:2027–2032, 1952. URL <http://pubs.rsc.org/en/content/articlepdf/1952/jr/jr9520002027>. (Cited on page 28.)
- [46] O Saied, M Simard, and J D Wuest. Complexes of Strong Bidentate Lewis Acids Derived from 2, 7-Bis (1, 1-dimethylethyl) fluorene-1, 8-diol. *Inorganic Chemistry*, 37 (11):2620–2625, 1998. URL <http://pubs.acs.org/doi/abs/10.1021/ic9715411>. (Cited on page 28.)
- [47] J Vaugeois. Thermodynamic and Kinetic Effects of the Double Coordination of Carbonyl Groups by Bidentate Lewis Acids. *Journal of the American Chemical*, (8):13016, 1998. URL <http://pubs.acs.org/doi/abs/10.1021/ja982725x>. (Cited on page 28.)
- [48] SB Desu. Ultra-thin TiO_2 films by a novel method. *Materials Science and Engineering: B*, 13(4):299–303, 1992. URL <http://www.sciencedirect.com/science/article/pii/S0921510792901325>. (Cited on page 28.)
- [49] Y Zhu, L Zhang, and C Gao. The synthesis of nanosized TiO_2 powder using a sol-gel method with TiCl_4 as a precursor. *Journal of Materials Science*, 5:4049–4054, 2000. URL <http://>

www.springerlink.com/index/RN3627620864X737.pdf. (Cited on page 28.)

- [50] J Kim. Properties including step coverage of TiN thin films prepared by atomic layer deposition. *Applied Surface Science*, 210(3-4):231–239, April 2003. ISSN 01694332. doi: 10.1016/S0169-4332(03)00158-2. URL <http://linkinghub.elsevier.com/retrieve/pii/S0169433203001582>. (Cited on page 29.)
- [51] W Kroll. The production of ductile titanium. *Journal of The Electrochemical Society*, 78(1931):35, 1940. URL <http://link.aip.org/link/?TES0AV/78/35/1>. (Cited on page 29.)
- [52] K Ziegler. Polymerization Catalyst Containing Alkyl Aluminium Dihalide Patent no. US3,546,133, 1970. URL <http://www.google.com/patents?hl=en&lr=&vid=USPAT3546133&id=ir0kAAAAEBAJ&oi=fnd&dq=POLYMERIZATION+CATALYST+CONTAINING+ALKYL+ALUMINUM+DIHALIDE&printsec=abstract>. (Cited on page 29.)
- [53] G Natta, P Pino, and P Corradini. Crystalline High Polymers of -Olefins. *Journal of the American Chemical Society*, 2104(5):5–7, 1955. URL <http://pubs.acs.org/doi/abs/10.1021/ja01611a109>. (Cited on page 30.)
- [54] P Cossee. Ziegler-Natta catalysis I. Mechanism of polymerization of alpha-olefins with Ziegler-Natta catalysts. *Journal of Catalysis*, 3(1):80–88, February 1964. ISSN 00219517. doi: 10.1016/0021-9517(64)90095-8. URL [http://dx.doi.org/10.1016/0021-9517\(64\)90095-8](http://dx.doi.org/10.1016/0021-9517(64)90095-8). (Cited on page 30.)
- [55] J Huang. Ziegler-Natta catalysts for olefin polymerization: mechanistic insights from metallocene systems. *Progress in Polymer Science*, 20:459–526, 1995. URL <http://www.sciencedirect.com/science/article/pii/S0079670094000395>. (Cited on page 30.)
- [56] Y Doi, K Soga, and M Murata. Synthesis of propylene/methyl vinyl ketone diblock copolymers with isotactic-specific Ziegler-Natta catalysts. *Die Makromolekulare*, 793:789–793, 1983. URL <http://onlinelibrary.wiley.com/doi/10.1002/marc.1983.030041207/abstract>. (Cited on page 30.)
- [57] <http://cas.utpb.edu/media/images/1atom.gif> accessed 29/02/2012. (Cited on page 31.)
- [58] J Galy, R Enjalbert, G Jugie, and J Strahle. VOCl₃: Crystallization, crystal structure, and structural relationships A joint X-ray and ³⁵Cl-NQR investigation. *Journal*

- of *Solid State Chemistry*, 47(2):143–150, 1983. URL <http://www.sciencedirect.com/science/article/pii/S0022459683900038>. (Cited on page 31.)
- [59] D McFaddin and M Reinking. Characterization of vanadium-based olefin polymerization catalyst precursors by solid-state ^{51}V -nmr. *Journal of Polymer Science Part A*, 33(3):563–570, 1995. URL <http://onlinelibrary.wiley.com/doi/10.1002/pola.1995.080330323/abstract>. (Cited on page 32.)
- [60] G A Mortimer. Molecular-weight and molecular-weight distribution control in HDPE with VOCl_3 -Based Ziegler-Natta catalysts. *Journal of Applied Polymer Science*, 20(1):55–61, 1976. URL http://apps.webofknowledge.com/full_record.do?product=UA&search_mode=GeneralSearch&qid=9&SID=R25mhP1aJ4CHdJc48jK&page=1&doc=2. (Cited on page 32.)
- [61] C D Beard, R J Barrie, J Evans, G Reid, and M D Spicer. Synthesis and Properties of Complexes of Vanadium(V) Oxide Trichloride with Nitrogen- and Oxygen-Donor Ligands. *European Journal of Inorganic Chemistry*, 2006 (21):4391–4398, November 2006. ISSN 14341948. doi: 10.1002/ejic.200600513. URL <http://doi.wiley.com/10.1002/ejic.200600513>. (Cited on pages 32 and 33.)
- [62] J G Zhang, P Liu, J A Turner, C E Tracy, and D K Benson. Highly stable vanadium oxide cathodes prepared by plasma-enhanced chemical vapor deposition. *Journal of the Electrochemical Society*, 145(6):1889–1892, 1998. URL http://apps.webofknowledge.com/full_record.do?product=UA&search_mode=GeneralSearch&qid=11&SID=R25mhP1aJ4CHdJc48jK&page=1&doc=4. (Cited on page 32.)
- [63] F J Morin. Oxides which show a metal-to-insulator transition at the Neel temperature. *Physical Review Letters*, 3:2–4, 1959. URL https://noppa.tkk.fi/noppa/kurssi/ke-35.2100/luennot/KE-35_2100_mit-efekti.pdf. (Cited on page 32.)
- [64] J Nag and R F Haglund Jr. Synthesis of vanadium dioxide thin films and nanoparticles. *Journal of Physics: Condensed Matter*, 20(26):264016, July 2008. ISSN 0953-8984. doi: 10.1088/0953-8984/20/26/264016. URL <http://stacks.iop.org/0953-8984/20/i=26/a=264016?key=crossref.199e71b9b816ce7ab87d9809c3454843>. (Cited on page 33.)
- [65] T D Manning and I P Parkin. Vanadium(IV) oxide thin films on glass and silicon from the atmospheric pressure chemical

- vapour deposition reaction of VOCl_3 and water. *Polyhedron*, 23(18):3087–3095, December 2004. ISSN 02775387. doi: 10.1016/j.poly.2004.09.020. URL <http://linkinghub.elsevier.com/retrieve/pii/S0277538704003821>. (Cited on page 33.)
- [66] A W Grant Jr. Vanadium for high school students. *Journal of Chemical Education*, page 500, 1977. URL <http://pubs.acs.org/doi/pdf/10.1021/ed054p500>. (Cited on page 33.)
- [67] C Sun, J Chen, H Zhang, X Han, and Q Luo. Investigations on transfer of water and vanadium ions across Nafion membrane in an operating vanadium redox flow battery. *Journal of Power Sources*, 195(3):890–897, February 2010. ISSN 03787753. doi: 10.1016/j.jpowsour.2009.08.041. URL <http://linkinghub.elsevier.com/retrieve/pii/S0378775309014153>. (Cited on page 33.)
- [68] S Ahrland and B Noren. The stability of metal halide complexes in aqueous solution. *Acta Chemica Scandinavica*, 12: 1595–1604, 1958. URL http://actachemscand.dk/pdf/acta_vol_17_p1567-1583.pdf. (Cited on page 34.)
- [69] O B Lapina, B S Bal'zhinimaev, S Boghosian, K M Eriksen, and R Fehrmann. Progress on the mechanistic understanding of SO_2 oxidation catalysts. *Catalysis Today*, 51(3-4):469–479, July 1999. ISSN 09205861. doi: 10.1016/S0920-5861(99)00034-6. URL <http://linkinghub.elsevier.com/retrieve/pii/S0920586199000346>. (Cited on page 34.)
- [70] R J H Clark. *Comprehensive Inorganic Chemistry*. Pergamon Press, 1st edition, 1973. (Cited on page 34.)
- [71] J H Simons and M G Powell. Properties of vanadium tetrachloride. *Journal of the American Chemical Society*, 1846(4):9–11, 1945. URL <http://pubs.acs.org/doi/abs/10.1021/ja01217a026>. (Cited on page 34.)
- [72] R G Cavell and A R Sanger. Metal Complexes of Substituted Dithiophosphinic Acids. Reactions of TiCl_4 , VCl_4 , NbCl_4 , NbCl_5 , and TaCl_5 , with Difluorodithiophosphinic Acid. *Inorganic Chemistry*, 11(9):2016–2019, 1972. (Cited on pages 34 and 35.)
- [73] C Muro and V Fernandez. Reactions of VCl_3 , VCl_4 and TiX_4 ($\text{X} = \text{Cl}, \text{Br}$) with benzofuroxan and its 5-methyl-, 5-chloro- and 5-methoxy-derivatives. I. *Inorganica chimica acta*, 134:215–219, 1987. URL <http://www.sciencedirect.com/science/article/pii/S0020169300880834>. (Cited on pages 34 and 35.)

- [74] V Fernandez and C Muro. Die Reaktion von TiCl_4 , ZrCl_4 und VCl_4 mit Benzofuroxan. *Zeitschrift für anorganische und allgemaene chemie*, 212:209–212, 1980. URL <http://onlinelibrary.wiley.com/doi/10.1002/zaac.19804660126/abstract>. (Cited on pages 34 and 35.)
- [75] A Arquero and P Souza. Complexes of TiCl_4 , VCl_4 and SnX_4 (X= Cl or Br) with Schiff bases derived from 2 aminobenzimidazole. *Transition Metal Chemistry*, 426:424–426, 1985. URL <http://link.springer.com/article/10.1007/BF01096751>. (Cited on pages 34 and 35.)
- [76] F Lu. Vanadium(IV) tetrachloride catalyzed oxidative homo-coupling of aryl lithium under mild reaction condition. *Tetrahedron Letters*, 53(19):2444–2446, May 2012. ISSN 00404039. doi: 10.1016/j.tetlet.2012.03.011. URL <http://linkinghub.elsevier.com/retrieve/pii/S0040403912003899>. (Cited on page 34.)
- [77] J J Eisch, P O Fregene, and D C Doetschman. Vanadium(I) Chloride and Lithium Vanadium(I) Dihydride as Epimetallating Reagents for Unsaturated Organic Substrates: Constitution and Mode of Reaction. *European Journal of Organic Chemistry*, 2008(16):2825–2835, June 2008. ISSN 1434193X. doi: 10.1002/ejoc.200800104. URL <http://doi.wiley.com/10.1002/ejoc.200800104>. (Cited on page 34.)
- [78] T Thomas, C S Blackman, I P Parkin, and CIJ Carmalt. Atmospheric pressure chemical vapour deposition of vanadium arsenide thin films via the reaction of VCl_4 or VOCl_3 with tBuAsH_2 . *Thin Solid Films*, 537:171–175, June 2013. ISSN 00406090. doi: 10.1016/j.tsf.2013.04.144. URL <http://linkinghub.elsevier.com/retrieve/pii/S0040609013007815>. (Cited on page 34.)
- [79] A Kafizas, G Hyett, and I P Parkin. Combinatorial atmospheric pressure chemical vapour deposition (cAPCVD) of a mixed vanadium oxide and vanadium oxynitride thin film. *Journal of Materials Chemistry*, 19(10):1399, 2009. ISSN 0959-9428. doi: 10.1039/b817429f. URL <http://xlink.rsc.org/?DOI=b817429f>. (Cited on page 34.)
- [80] S Pothoczki and L Pusztai. Molecular liquid TiCl_4 and VCl_4 : Two substances, one structure? *Journal of Molecular Liquids*, 145(1):38–40, March 2009. ISSN 01677322. doi: 10.1016/j.molliq.2008.11.012. URL <http://linkinghub.elsevier.com/retrieve/pii/S0167732208002407>. (Cited on page 34.)

- [81] I Cuadrado and M Morán. Reactions of TiCl_4 , VCl_4 and VOCl_3 with tetraalkyldiphosphine disulphides. *Transition Metal Chemistry*, 333:329–333, 1981. URL <http://link.springer.com/article/10.1007/BF00623648>. (Cited on page 36.)
- [82] I Cuadrado and M Morán. Reactions of TiX_4 and VOCl_3 with P= S ligands. *Transition Metal Chemistry*, 3:96–103, 1984. URL <http://link.springer.com/article/10.1007/BF00618584>. (Cited on page 36.)
- [83] G Barth-Wehrenalp. Purification of Titanium Tetrachloride patent no. US2819148, 1958. (Cited on page 36.)
- [84] V Brudz. Purification of Titanium Tetrachloride from Concomitant Impurities patent no: US3729540, 1973. (Cited on page 36.)
- [85] K Sun, YY Ma, and AG Dong. Separation of impurity vanadium from TiCl_4 by means of adsorption. *Rare Metals*, 18(2):129–132, 1999. URL http://apps.webofknowledge.com/full_record.do?product=UA&search_mode=GeneralSearch&qid=3&SID=V1CL3liopcFcpHFAk9b&page=3&doc=28. (Cited on page 36.)
- [86] D C Lynch. Conversion of VOCl_3 to VOCl_2 in liquid TiCl_4 . *Metallurgical and Materials Transactions B*, 31(February): 1–5, 2002. URL <http://www.springerlink.com/index/9802813013510561.pdf>. (Cited on page 36.)
- [87] P Ehrlich and W Siebert. Über die Entfernung von VCl_4 und VOCl_3 aus TiCl_4 . *Zeitschrift für Anorganische und Allgemeine Chemie*, 302:275–283, 1959. (Cited on page 36.)
- [88] E L Hahn. Nuclear induction due to free Larmor precession. *Physical Review*, 77(2):297–299, 1950. URL http://prola.aps.org/abstract/PR/v77/i2/p297_2. (Cited on page 38.)
- [89] H Kondo. Proton nmr study of metal coordination to biotin derivatives. *Journal of Inorganic Biochemistry*, 21(2):93–102, June 1984. ISSN 01620134. doi: 10.1016/0162-0134(84)85042-4. URL <http://linkinghub.elsevier.com/retrieve/pii/0162013484850424>. (Cited on page 39.)
- [90] F Frank, T Roberts, J Snell, C Yates, and J Collins. Trimyristin from nutmeg. *Journal of Chemical Education*, 48(4):255, April 1971. ISSN 0021-9584. doi: 10.1021/ed048p255. URL <http://dx.doi.org/10.1021/ed048p255>. (Cited on pages 46 and 52.)

- [91] J Blumel, P Hofmann, and F Kohler. NMR Spectroscopy of Paramagnetic Complexes-inatural abundance ^2H NMR of paramagnetic sandwich compounds. *Magnetic Resonance in Chemistry*, 31:2–6, 1993. URL <http://onlinelibrary.wiley.com/doi/10.1002/anie.197009461/abstract>. (Cited on page 48.)
- [92] K E Schwarzshans. NMR Spectroscopy of Paramagnetic Complexes. *Angewandte Chemie International Edition in English*, 9(12):946–953, December 1970. ISSN 0570-0833. doi: 10.1002/anie.197009461. URL <http://doi.wiley.com/10.1002/anie.197009461>. (Cited on page 48.)
- [93] <http://science.csustan.edu/tutorial/nmr/>. (Cited on page 55.)
- [94] P Sobota, S Szafert, and T Lis. Reactions of TiCl_4 , with diesters. Crystal structures of $[\text{CH}_2(\text{CO}_2\text{Et})_2\text{Cl}_4\text{Ti}]$ and $[\text{C}_2\text{H}_4(\text{CO}_2\text{CH}_2\text{CH}_2\text{OPh})_2\text{Cl}_4\text{Ti}]$. *Journal of Organometallic Chemistry*, 443:85–91, 1993. (Cited on pages 57, 63, and 65.)
- [95] K Joseph, S S Deshpande, S Gopinathan, and C Gopinathan. Chelated Oxovanadium(V) Dichlorides and Related Compounds. *Indian Journal of Chemistry, Section A: Inorganic, Physical, Theoretical & Analytical*, 22(2):159–160, 1983. (Cited on pages 58 and 60.)
- [96] G Maier, U Seipp, and R Boese. Isolierung und kristallstrukturanalyse eines titantetrachlorid-komplexes eines 1,3-Diketons. *Tetrahedron Letters*, 28(39):4515–4516, 1987. (Cited on pages 58 and 59.)
- [97] G Maier. ^{13}C -NMR Spectroscopy. Titanium Tetrachloride Complexes of Diketone: Their Importance for Hydride Reductions and Their Solid-State NMR spectra. *Chemische ...*, pages 1427–1436, 1994. URL <http://scholar.google.com/scholar?hl=en&btnG=Search&q=intitle:SOLID-STATE+C-13-NMR+SPECTROSCOPY+.1.+TITANIUM+TETRACHLORIDE+COMPLEXES+OF+DIKETONES+-+THEIR+IMPORTANCE+FOR+HYDRIDE+REDUCTIONS+AND+THEIR+SOLID-STATE+NMR-SPECTRA#0>. (Cited on page 59.)
- [98] M Shao, Y Ho, and H Gau. Reactions of TiCl_4 or $\text{Ti}(\text{O}-i\text{-Pr})\text{Cl}_3$ with 2,4-Pentanedione. The Molecular Structures of $\text{TiCl}_3(\text{acac})(\text{THF})$ and $\text{Ti}(\text{O}-i\text{-Pr})\text{Cl}_2(\text{acac})(\text{THF})$. *Journal of the Chinese Chemical Society*, 47:901–906, 2000. (Cited on page 59.)
- [99] G Ferguson and C Glidewell. Enantiomeric disorder in racemic *cis*-dichlorobis(pentane-2,4-dionato)titanium(IV).

Acta Crystallographica Section C Crystal Structure Communications, 57(3):264–265, March 2001. ISSN 0108-2701. doi: 10.1107/S0108270100019181. URL <http://scripts.iucr.org/cgi-bin/paper?S0108270100019181>. (Cited on pages 60 and 91.)

- [100] Y Huang and D W Stephan. Synthesis and structure of titanium diolate complexes derived from CpTiCl_3 . *Canadian Journal of chemistry*, 962(5 19):956–962, 1995. URL <http://www.nrcresearchpress.com/doi/pdf/10.1139/v95-118>. (Cited on pages 69 and 70.)
- [101] C Krempner, M Köckerling, H Reinke, and K Weichert. Trisilane-1,3-diolato complexes of Ti and Zr: syntheses and X-ray crystal structures. *Inorganic chemistry*, 45(8):3203–11, April 2006. ISSN 0020-1669. doi: 10.1021/ic0514997. URL <http://www.ncbi.nlm.nih.gov/pubmed/16602776>. (Cited on page 69.)
- [102] O Buitrago, G Jiménez, and T Cuenca. Titanium and zirconium chloro, oxo and alkyl derivatives containing silyl-cyclopentadienyl ligands. Synthesis and characterisation. *Journal of Organometallic Chemistry*, 683(1):70–76, October 2003. ISSN 0022328X. doi: 10.1016/S0022-328X(03)00430-3. URL <http://linkinghub.elsevier.com/retrieve/pii/S0022328X03004303>. (Cited on page 73.)
- [103] Y T Wu, Y C Ho, and C C Lin. Stepwise Reactions of TiCl_4 and $\text{Ti}(\text{OiPr})\text{Cl}_3$ with 2-Propanol. *Inorganic Chemistry*, (35):5948–5952, 1996. URL <http://pubs.acs.org/doi/abs/10.1021/ic960147k>. (Cited on page 90.)
- [104] M Cox, R J H Clark, and H J Milledge. Structural Studies on Group IV Metal Acetylacetonates. 1966. URL <http://www.nature.com/nature/journal/v212/n5068/abs/2121357a0.html>. (Cited on page 91.)
- [105] N Serpone and P H Bird. On supposedly five-co-ordinate titanium (IV) complexes. The crystal and molecular structure of $\text{Cl}_3\text{Ti}(\text{C}_5\text{H}_7\text{O}_2)$. *Journal of the Chemical Society*, (1):217–218, 1972. URL <http://pubs.rsc.org/en/content/articlepdf/1972/c3/c39720000217>. (Cited on pages 91 and 93.)
- [106] P Sobota, J Ejfler, and S Szafert. Synthesis and characterization of new di- and tetra-meric vanadium intermediates of olefin polymerization catalysts. Crystal structures of. *Journal of the Chemical Society, Dalton Transactions*, 424(1):1727–1732, 1995. URL <http://pubs.rsc.org/en/content/articlehtml/1995/dt/dt9950001727>. (Cited on pages 104 and 120.)

- [107] R F Barrow, D A Long, and D J Millen. *Molecular Spectroscopy*. Royal Society of Chemistry, 1973. ISBN 085186516X. URL <http://books.google.com/books?id=rVG4ETgHBioC&pgis=1>. (Cited on page 105.)
- [108] C Janiak. Engineering coordination polymers towards applications. *Dalton Transactions*, (14):2781, 2003. ISSN 1477-9226. doi: 10.1039/b305705b. URL <http://xlink.rsc.org/?DOI=b305705b>. (Cited on page 110.)
- [109] O Roubeau. Triazole-based one-dimensional spin-crossover coordination polymers. *Chemistry (Weinheim an der Bergstrasse, Germany)*, 18(48):15230–44, November 2012. ISSN 1521-3765. doi: 10.1002/chem.201201647. URL <http://www.ncbi.nlm.nih.gov/pubmed/23129322>. (Cited on page 110.)
- [110] L Alaerts, E Séguin, H Poelman, F Thibault-Starzyk, P Jacobs, and D E De Vos. Probing the Lewis acidity and catalytic activity of the metal-organic framework [Cu₃(btc)₂] (BTC=benzene-1,3,5-tricarboxylate). *Chemistry (Weinheim an der Bergstrasse, Germany)*, 12(28):7353–63, September 2006. ISSN 0947-6539. doi: 10.1002/chem.200600220. URL <http://www.ncbi.nlm.nih.gov/pubmed/16881030>. (Cited on page 110.)
- [111] J Lee, O K Farha, J Roberts, K Scheidt, S T Nguyen, and J T Hupp. Metal-organic framework materials as catalysts. *Chemical Society reviews*, 38(5):1450–9, May 2009. ISSN 0306-0012. doi: 10.1039/b80708of. URL <http://www.ncbi.nlm.nih.gov/pubmed/19384447>. (Cited on page 110.)
- [112] K Tanaka and T Yoshimura. A novel coordination polymer gel based on succinic acid copper(ii) nitrate DABCO: metal ion and counterion specific organogelation. *New Journal of Chemistry*, 36(7):1439, 2012. ISSN 1144-0546. doi: 10.1039/c2nj40182g. URL <http://xlink.rsc.org/?DOI=c2nj40182g>. (Cited on page 110.)
- [113] S Kitagawa, R Kitaura, and S Noro. Functional porous coordination polymers. *Angewandte Chemie (International ed. in English)*, 43(18):2334–75, April 2004. ISSN 1433-7851. doi: 10.1002/anie.200300610. URL <http://www.ncbi.nlm.nih.gov/pubmed/15114565>. (Cited on page 110.)
- [114] M Abrantes, M S Balula, A Valente, F Al Paz, M Pillinger, C C. Romão, J Rocha, and I S Gonçalves. Structural and Catalytic Studies of a Trimethyltin Vanadate Coordination Polymer. *Journal of Inorganic and Organometallic Polymers and*

- Materials*, 17(1):215–222, January 2007. ISSN 1574-1443. doi: 10.1007/s10904-006-9080-5. URL <http://link.springer.com/10.1007/s10904-006-9080-5>. (Cited on page 110.)
- [115] M Meisel and D Wulff-Molder. New Vanadium Phosphonate Clusters and Coordination Polymers. *Phosphorus, Sulfur, and Silicon and the Related Elements*, 144(1):231–234, January 1999. ISSN 1042-6507. doi: 10.1080/10426509908546224. URL <http://www.tandfonline.com/doi/abs/10.1080/10426509908546224>. (Cited on page 110.)
- [116] X Zhang, M Tong, H K Lee, and X Chen. The First Noncluster Vanadium(IV) Coordination Polymers: Solvothermal Syntheses, Crystal Structure, and Ion Exchange. *Journal of Solid State Chemistry*, 160(1):118–122, August 2001. ISSN 00224596. doi: 10.1006/jssc.2001.9202. URL <http://linkinghub.elsevier.com/retrieve/pii/S0022459601992023>. (Cited on page 110.)
- [117] H Hosseini-Monfared, N Asghari-Lalami, A Pazio, K Wozniak, and C Janiak. Dinuclear vanadium, copper, manganese and titanium complexes containing O,O,N-dichelating ligands: Synthesis, crystal structure and catalytic activity. *Inorganica Chimica Acta*, 406:241–250, September 2013. ISSN 00201693. doi: 10.1016/j.ica.2013.04.044. URL <http://linkinghub.elsevier.com/retrieve/pii/S0020169313002430>. (Cited on page 111.)
- [118] M Yuan, E Wang, Y Lu, S Wang, and Y Li. A novel chain like binuclear vanadium (V) coordination polymer containing mixed ligands: hydrothermal synthesis and crystal structure of [(VO₂[2,2-bipy])₂(tp)]. *Inorganica chimica acta*, 344(v):0–4, 2003. URL <http://www.sciencedirect.com/science/article/pii/S0020169302012604>. (Cited on page 111.)
- [119] X Wu and A E V Gorden. 2-Quinoxalinol Salen Copper Complexes for Oxidation of Aryl Methylenes. *European Journal of Organic Chemistry*, 2009(4):503–509, February 2009. ISSN 1434193X. doi: 10.1002/ejoc.200800928. URL <http://doi.wiley.com/10.1002/ejoc.200800928>. (Cited on page 113.)
- [120] S K Silverman and C S Foote. Singlet oxygen and electron-transfer mechanisms in the dicyanoanthracene-sensitized photooxidation of 2, 3-diphenyl-1, 4-dioxene. *Journal of the American Chemical Society*, (1 10):7672–7675, 1991. URL <http://pubs.acs.org/doi/abs/10.1021/ja00020a032>. (Cited on page 114.)

- [121] F A Cotton, G E Lewis, and G N Mott. New trinuclear, oxo-centered, basic carboxylate compounds of transition metals. 3. Syntheses and x-ray studies of the trivanadium (III, III, III) and trivanadium (II, III, III). *Inorganic Chemistry*, (15 mL):3316–3321, 1982. URL <http://pubs.acs.org/doi/pdf/10.1021/ic00139a013>. (Cited on page 114.)
- [122] J Crane, M Warwick, R Smith, N Furlan, and R Binions. The Application of Electric Fields to Aerosol Assisted Chemical Vapor Deposition Reactions. *Journal of The Electrochemical Society*, 158(2):D62, 2011. ISSN 00134651. doi: 10.1149/1.3519870. URL <http://link.aip.org/link/JES0AN/v158/i2/pD62/s1&Agg=doi>. (Cited on page 114.)
- [123] R P Dodge, D H Templeton, and A Zalkin. Crystal Structure of Vanadyl Bisacetylacetonate. Geometry of Vanadium in Fivefold Coordination. *The Journal of Chemical Physics*, 35(1):55, 1961. ISSN 00219606. doi: 10.1063/1.1731933. URL <http://link.aip.org/link/JCPSA6/v35/i1/p55/s1&Agg=doi>. (Cited on page 118.)
- [124] C Dijkgraaf. Similarities in the electronic spectra of TiCl_4 and VOCl_3 . *Spectrochimica Acta*, 21(8):1419–1421, August 1965. ISSN 03711951. doi: 10.1016/0371-1951(65)80052-2. URL <http://linkinghub.elsevier.com/retrieve/pii/0371195165800522>. (Cited on pages 138 and 139.)